Assessment of Component Mode Synthesis Methods for the Selection of Substructure Modes and Application to the Dynamic Analysis of Car Axle

Submitted in partial fulfilment of the requirements

of the degree of

Master of Technology

by

Manasvi Saxena

Roll No.: 08310906

Supervisors:

Prof. Salil Kulkarni   **Prof. Manfred Zehn**

Department of Mechanical Engineering   Institute of Mechanics

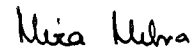INDIAN INSTITUTE OF TECHNOLOGY   TECHNICAL UNIVERSITY

BOMBAY   BERLIN

June 2011

Dissertation Approval

This dissertation entitled "Assessment of Component Mode Synthesis Methods for the Selection of Substructure Modes and Application to the Dynamic Analysis of Car Axle" by "Manasvi Saxena" is approved for the degree of Master of Technology.
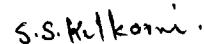
Prof. Mira Mitra

Dept. of Aero. Engg., IIT Bombay

(Internal Examiner)

Dr. N.K. Mukhopadhyay

(External Examiner)

Prof. Salil Kulkarni

Dept. of Mech. Engg., IIT Bombay

(Supervisor)

Prof. Sudarshan Kumar

Dept. of Aero. Engg., IIT Bombay

(Chairman)

Date: 12/07/2011
Place: IIT Bombay

Declaration

I, Manasvi Saxena, Roll No. 08310906, understand that plagiarism is defined as any one or the combination of the following:

1. Uncredited verbatim copying of individual sentences, paragraphs or illustrations (such as graphs, diagrams, etc.) from any source, published or unpublished, including the internet.
2. Uncredited improper paraphrasing of pages or paragraphs (changing a few words or phrases, or rearranging the original sentence order).
3. Credited verbatim copying of a major portion of a paper (or thesis chapter) without clear delineation of who did or wrote what. (Source: IEEE, The Institute, Dec. 2004)

I have made sure that all the ideas, expressions, graphs, diagrams, etc., that are not a result of my work, are properly credited. Long phrases or sentences that had to be used verbatim from published literature have been clearly identified using quotation marks.

I affirm that no portion of my work can be considered as plagiarism and I take full responsibility if such a complaint occurs. I understand fully well that the guide of the seminar report may not be in a position to check for the possibility of such incidences of plagiarism in this body of work.

Manasvi Saxena
(Roll No.: 08310906)

Date: 12/07/2011

Abstract

This report discusses the formulation procedure of the two types of model order reduction methods of Component mode synthesis, i) Fixed Interface method and ii) Free Interface method. The importance of various types of modes like normal modes, Constraint modes and Residual modes used in these methods in reducing the size of the system while still maintaining the accuracy of the results is studied. To make a comparison and therefore be able to make a judgment in choosing the best reduction technique, these methods are applied to study the dynamic analysis of simple problems of Fixed- Free beam and a cracked beam. Both of these methods are compared with regard to the degree of reduction attainable on the one hand and the accuracy that can be achieved on the other hand. Furthermore, these methods are rigorously assessed for the reduction in computational time achievable in completing an analysis in practical cases by applying them to the real structure of Car Axle.

The Fixed Interface method of Component Mode Synthesis is further reviewed in detail with the focus on the appropriate selection of the significant fixed interface normal modes for the reduction of interior dofs. For this purpose measures based on Effective Interface Mass (EIM) are discussed which determines the dynamically important modes required to be chosen for an accurate reduced representation. In this work, an extension of EIM is proposed for the appropriate selection of the coupled characteristic constraint (CC) modes for the reduction of junction degrees of freedom. It is also shown that EIM can be used to perform an interaction analysis between the interior and the junction coordinates of a substructure by determining the relative dynamic importance of the one with respect to another. This leads to appropriate reduction of the interface and junction dofs such that the accuracy of the final reduced is not at all compromised.

Contents

List of Figures

List of Tables

Nomenclature

M	Mass matrix of complete structure
K	Stiffness matrix of complete structure
x	Vector of displacement in physical dofs of complete structure
f	Vector of external forces of complete structure
m	Partition of mass matrix of a substructure
k	Partition of stiffness matrix of a substructure
I	Identity Matrix. Subscripts of I represents its size.
Φ	Matrix of mass normalized eigenvectors
Φ_c	Matrix of constraint modes
p	Vector of generalized coordinates of a substructure
$\bar{M}$	Generalized mass matrix of a substructure
$\bar{K}$	Generalized stiffness matrix of a substructure
$\bar{f}$	Vector of generalized forces of a substructure
$\bar{m}$	Partition of generalized mass matrix of a substructure
$\bar{k}$	Partition of generalized stiffness matrix of a substructure
S	Transformation matrix for coupling of substructures
q	Vector of generalized coordinates of reduced coupled structure
V	Combined set of kept normal mode shapes and static mode shapes
ω	Natural frequency
λ	Eigenvalue
β	Attachment mode shapes
P	Modal participation matrix
ψ	Coupled Characteristic Constraint modes
$\bar{\bar{M}}$	Effective Interface Mass

Z	Term by term square of modal participation factors
C	Compliance Matrix
c	Compliance coefficients
c^*	Non-dimensional compliance coefficients
E	Young's Modulus
R	Radius
D	Diameter
k^*	Material constant
ν	Poisson's ratio
a	Crack depth

Subscripts

i	Set of interior dofs
c	Set of coupling/interface dofs
n	Full set of all mass normalized eigenvectors
j	j^{th} Fixed Interface normal mode
l	l^{th} coupled CC mode
m	m^{th} coupling/interface dofs
cm	Combined matrices or vectors of all the substructures
q	Coupled and reduced structure
vel	Velocity
$disp$	Displacement
$accn$	Acceleration
A	Substructure A
B	Substructure B
k	Refers to kept mode shapes
$k\alpha$	Refers to kept mode shapes of αth substructure
$k\beta$	Refers to kept mode shapes of βth substructure

d	Refers to deleted mode shapes
r	Refers to rigid body mode shapes
f	Refers to flexible body mode shapes
eff	Refers to Effective Interface Mass
eff_vel	Refers to Effective Interface Mass velocity output
eff_disp	Refers to Effective Interface Mass displacement output
cr	Refers to crack
a	Refers to node of Substructure A at crack section
b	Refers to node of Substructure B at crack section
cra	Refers to node of Crack at section of Substructure A
crb	Refers to node of Crack at section of Substructure B

Superscripts

i	i^{th} substructure
α	α^{th} substructure
β	β^{th} substructure
T	Transformation of a matrix or a vector
^2	Term by term square

Chapter 1

Introduction and Background

1.1   Component Mode Synthesis

In the dynamic analysis of complex structures, evaluating the modal parameters and the response of the structure is required and can be accomplished by Finite Element Method (FEM) [1]. The Finite Element (FE) model of the complex structure will contain thousands of degrees of freedom (dofs) and therefore will require huge computational time and storage space in evaluating the modal parameters or response of the structure. Also the complex structure contains several substructures or parts which may be independently designed and fabricated by different organizations. Therefore, it is required to have enough flexibility in the independent design and analysis of these individual substructures and then reassembling them together to get the modal parameters of the complete model from that of the individual substructures. FEM doesn't provide such opportunity as it discretesizes the complete structure as a whole. These are the basic reasons which led to the development of a method called as Component Mode Synthesis (CMS) that provides a means for the reduction of the dofs of the FE model and thereby reduces the computational time in performing the dynamic analysis of the structures while still maintaining the good level of accuracy of the results.

1.1.1 Steps involved in CMS formulation

CMS involves five major steps (see for example [2]).
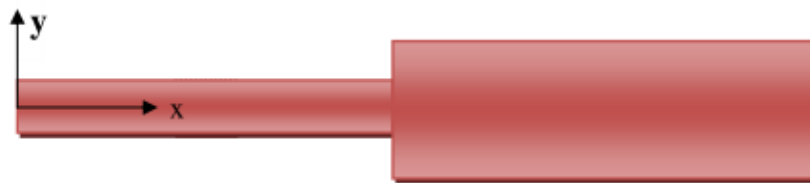
Figure 1.1: An example structure

(a) Substructuring:

Solving an eigenvalue problem of a square matrix of size n for all eigenvalues and eigenvectors takes $O(n^3)$ operations. This is very computationally costly for large structures. The basic idea of substructuring is to reduce this computational time by first dividing the structure into its individual substructures. Eigenvalue analysis is performed on each of these individual substructures and then the modal parameters of the complete structure are accurately determined from the modal parameters of the individual substructures. In this way instead of performing one large eigenvalue analysis for the complete structure (which is usually very computationally costly for large structures), one only need to perform several smaller eigenvalue analysis which takes much lesser time. Consider for example a structure shown in Figure 1.1, which can be divided into two substructures as shown in Figure 1.2. By dividing the structure into two substructures the number of operations required to obtain the modal parameters of the complete structure are $O(\left(\frac{n}{2}\right)^3 + \left(\frac{n}{2}\right)^3)$, i.e. $O(\frac{n^3}{4})$, and the computational time reduces by 75%.

c: Coupling or Interface degrees of freedom

i: Interior degrees of freedom
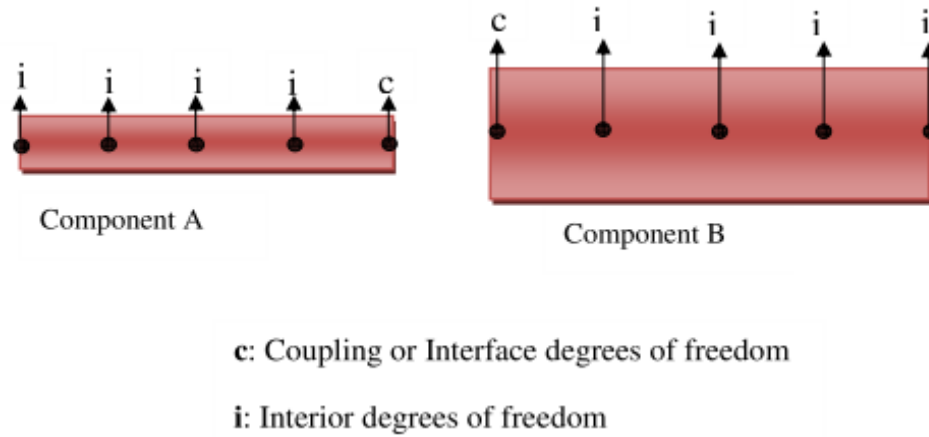
Figure 1.2: Partitioning the dofs.

(b) Partitioning the dofs:

The dofs of each of the substructure is partitioned into Interface and Interior dofs. Interface dofs of the substructure are those which share the connection between the two adjacent substructures. These are also called as boundary dofs or coupling dofs as they are used to couple the substructures together after the analysis of each of them has been performed. Interior dofs are those which are not a part of the set of Interface dofs. As shown

in Figure 1.2, the dofs representing connection between the two substructures are taken as coupling dofs (denoted as *'c'*) and rest all as Interior dofs (denoted as *'i'*).

(c) Analyses of substructures:

A discrete model for each of the substructures is obtained using Finite Element Method. At this stage the dofs of each of the substructures are reduced. CMS performs the reduction of dofs by transforming the physical dofs of each of the substructures into reduced coordinates with a special transformation matrix. The special transformation matrix which is used to transform the substructure's physical dofs into generalized coordinates consists of special set of dynamic and static modes. The dynamic modes are found out from the eigenvalue problem of each of the substructures by imposing certain boundary conditions at its interface dofs. Craig Bampton method or Fixed Interface method [**3**] is one of the most popular forms of CMS in which the dynamic modes are obtained with interface dofs as fixed. Many different variations of CMS methods like Free Interface Method [**4**] and Mixed Boundary method [**5**] were developed in which the dynamic modes are obtained with interface dofs as Free and Fixed-free respectively. All the dynamic modes obtained may not be significant in terms of their contribution to the dynamic response of the substructure within the frequency range of interest and therefore, only a particular set of significant modes is chosen. This process is called as Modal Truncation. Truncation of the model using only few significant modes, called as kept modes, is the key to model reduction and thereby huge reduction in the computational time. Those modes which are not chosen as kept modes are termed as deleted modes. So as to not to affect the accuracy of the results because of not considering completely the contribution of deleted modes, kept modes are augmented by a set of static modes. Depending on whether the Fixed or Free Interface method is selected, the static modes are the constraint modes or the residual attachment modes, respectively. The detailed derivation of the constraint modes and residual attachment modes are discussed in section 2.1.2 and 3.1.2 respectively. The combined set of substructure kept modes and the static modes forms the transformation matrix which is used to transform the substructure stiffness and mass matrices, and any external applied load from the physical coordinate system to a generalized coordinate system. The number of generalized coordinates is typically much lesser than the original number of physical dofs and size of the reduced system depends upon the number of the kept modes and the static modes. Furthermore, to be certain that the chosen dynamic modes completely represent the response of the substructure in the frequency

range of interest, it is important to have a proper measure on which the selection of dominant modes can be based. Various measures are discussed in section 1.1.2.

(d) Coupling of Substructures:

All the reduced models of the substructures are assembled or coupled together by enforcing displacement and force compatibility requirements to get a global reduced model of the complete structure.

(e) Global system response:

Once the global reduced model of the complete structure has been obtained, eigenvalue analysis and then the dynamic analysis is performed. The responses of the generalized coordinates hence obtained are transformed back by the same transformation matrix to get the responses of the physical dofs of the complete structure.

1.1.2 Measures for the selection of Substructure modes

There are many measures which are used by the structural dynamics community to determine the substructure's dominant modes that should be kept for any reduced representation.

(a) Thumb rule:

Thumb rule [**6**] though is fairly suppositional, but is commonly used by the engineers in quickly validating the reduced model. In thumb rule, all the substructure modes with the frequency less than 1.8 times the maximum frequency of interest of the complete structure are chosen. In some cases the thumb rule works well but in others the results could be highly misleading, as will be shown in section 6.1.2, therefore one cannot base decisions for the determination of dominant modes on this particular measure.

(b) Effective Mass Measure:

Effective Mass Measure [**7**] is also one of the widely used measures in the structural dynamics community which not only determines the important dynamic modes but also offers an advantage of being an absolute measure of dynamic importance. The advantage of an

absolute measure is that the dynamic importance of each mode shape can be computed with respect to an absolute reference, the value of which can be calculated based solely upon the partitions of FEM mass and stiffness matrices and is totally independent of any eigenvalue solution [8]. However, it has been shown also by Kammer et.al. [8] that Effective Mass measure ignores some of the very highly dominant modes and therefore, this method was generalized and a new method called as Effective Interface Mass (EIM) was derived.

(c) Effective Interface Mass Measure:

The main difference between the Effective Mass and Effective Interface Measure is that the former ranks the dynamic importance of modes based upon their contribution to the resultant forces at the substructure's fixed interface when the rigid body acceleration excitations are applied simultaneously at all the interface nodes and in turn along each of the directions, where as latter ranks the modes based upon their contributions to the forces individually at each of the interface dofs when the rigid body acceleration excitations are applied along each of the interface dofs in turn. This makes EIM a more proper measure for the determination of dominant modes to be chosen in the reduced representation [8]. Subsequently, EIM was extended and two more measures ranking the dynamic importance of modes based upon their contribution to modal velocity, or modal displacement at the substructure's fixed interface were derived by Kammer and Triller [9]. All these three measures based on EIM individually provides an effective means of selecting the dominant modes for accurately determining the acceleration, velocity or displacement response respectively in the frequency range of interest and allows a means for the proper reduction of the model. However, EIM can be effectively used to rank the dynamic importance for only those modes that are constrained by an interface such that there is no rigid body motion [10]. Therefore, if one relies on EIM to determine the dynamically important modes to be chosen in the reduced representation then performing reduction by Fixed Interface normal modes is more advantageous as compared to using Free Interface normal modes. This is because, Free–free elastic modes of an unconstrained substructure have zero contribution to EIM as the rigid body modes takes the complete mass and hence, one cannot determine the dynamically important Free-free modes to be chosen in the reduced representation using EIM. This makes the Mixed boundary method, which has a Fixed-free configuration, equally advantageous as Fixed Interface method with regard to be able to use proper measures like EIM for the selection of dominant modes. A generalization of Effective Mass for the selection of Free-

Free modes is proposed in [**10**], however if the acceleration output is of interest then at least modes from a much higher frequency region must be included in the reduced representation and therefore, further work must be performed to determine an acceptable level of dynamic completeness for Free Effective Mass that would produce a reduced model of acceptable size and accuracy. In the present work EIM measures will be studied only to rank the Fixed Interface normal modes obtained in the Craig-Brampton method.

1.1.3 Reduction of Interface dofs

In the Craig Brampton method, normal modes of the substructure are calculated by fixing all the interface dofs of the substructure and then only few of the dominant modes are selected based on a proper measure to transform the interior dofs of the substructure to these selected generalized coordinates. To allow for the coupling of the substructures at the interface while maintaining the displacement compatibility, these chosen dominant modes are augmented with Constraint modes (static modes). Constraint modes are found from the characteristic equation of the substructure. It represents the static deformation of a substructure due to successive unit displacement applied at the Interface dofs while keeping the remaining Interface dofs constrained and all Interior dofs free. These constraint modes provide a means of a statically complete coupling of the substructures by retaining all their interface dofs in the final transformed/reduced coordinate set. This makes the size of each of the final reduced substructures obtained by the Craig Brampton method as the sum of the number of selected generalized coordinates (from a measure like EIM) for the representation of the interior dofs, and the number of interface dofs. For very large assemblies of complex structures or in the cases where substructures are coupled with line or surface connections, the size of interface dofs is usually very large as compared to the number of chosen generalized coordinates and thus further effort is required for the reduction of these interface dofs.

Many methods have been proposed which allows a second level reduction of the interface dofs of each of the substructures by representing them in terms of some basis functions calculated in the second level eigenvalue analysis, after the first level eigenvalue analysis already done for the reduction of the interior dofs. The size of these basis functions is very less than the original number of interface dofs and therefore this second level eigenvalue analysis is justified.

(a) Wave Based Substructuring procedure:

Wave Based Substructuring procedure [**11**] is one of the recently developed methods in which the different basis functions [**12**] for reduction of the interface dofs of each of the substructures are calculated by first performing a modal analysis of the full Finite Element model of the complete structure only in the particular frequency range of interest, and then using the matrix partitions of the obtained mode shapes corresponding to the interface dofs of each of the substructures as their respective basis functions. The calculation of these basis functions from the full assembly model is justified in the scenario of modification analysis and optimization where these basis functions can be re-used for the assembly of modified substructures. However, it should be noted that an absolute measure for the calculation of dominant basis functions cannot be developed in WBS as these basis functions do not have the basic orthonormality properties of the Eigen vectors of the interface dofs, which is a key criteria for the expression of the absolute measure to be based solely upon the partitions of FEM mass and stiffness matrices.

(b) Interface Reduction by using Characteristic Constraint Modes

The basis functions for the reduction of interface dofs of each of the substructures can also be chosen as to be the Characteristic Constraint modes (CC) [**13**] which are obtained by performing a second level eigenvalue analysis on the partitions of the transformed stiffness and mass matrices of each of the substructures corresponding to the interface dofs. By using basis functions as CC modes, absolute measures like EIM can be used for the proper selection of the dominant CC modes so that the final reduced system, which contains selected Fixed Interface normal modes and CC modes for the representation of interior and interface dofs respectively, accurately represents all displacement, velocity and acceleration responses as compared to the full model FEM solution. However, since in the transformed set of equations for each of the substructures, the interface dofs and the Fixed interface normal modes are uncoupled in stiffness, CC modes for the unconstrained substructures will also have rigid body modes and that again precludes the use of EIM. Therefore these CC modes for a particular interface are instead obtained after the coupling of the first level reduced substructures and then performing an eigenvalue analysis on the partitions of stiffness and mass matrices corresponding to the particular interface keeping all other interfaces and generalized coordinates as fixed. So at the coupled substructure level irrespective of whether

the individual substructures are constrained or not, if the complete structure is constrained then eigenvalue analysis of the partition of stiffness and mass matrices corresponding to a particular interface will not give any rigid body modes and EIM can be effectively used. These modes obtained at the coupled substructure level are therefore termed as Coupled CC modes and are more advantageous for the reduction of the interface dofs as against to the use of CC modes.

1.1.4 Extension of EIM measure for selection of CC modes

In this work, EIM is extended to effectively rank the dynamic importance of the Coupled CC modes of a particular interface relative to the already selected generalized coordinates of all the substructures coupled to this interface at the coupled substructure level. Such an extension can also be found in [14] but they used EIM for ranking the dynamic importance of CC modes (instead of the Coupled CC modes) of a particular interface relative to the already selected generalized coordinates of only the substructure in which the interface is contained at the substructure level. As explained earlier, this could be applicable in only those cases where the all substructures of the system are constrained. Even the example problem that was used in [14] to show the extension of EIM for choosing CC modes assumes that both the substructures are constrained. In contrast to this, our approach uses Coupled CC modes in which EIM can be effectively used irrespective of whether the individual substructures are constrained or not.

1.1.5 Advantages of CMS

The Component Mode Synthesis has several advantages.

(a) Reduces computational effort and computer storage requirements.
(b) CMS allows the independent analysis of different substructures of a structure by different organizations, at different places and at different times. Once the modal parameters of each of the substructures are obtained, the modal parameters of the complete structure, only with in a particular frequency range of interest, can be determined from the modal parameters of the individual substructures. This feature is very important in the analysis of complex and large structures such as space station.
(c) CMS is very useful in the analysis of those structures which are symmetric about some axis and have alike parts on both sides of the symmetric plane like wings in aircrafts, doors,

and fenders in automobiles. Through CMS we need to analyze such similar parts only once as the same information can be used to model the other similar parts. Then depending on their locations in space and boundary/coupling conditions with the other non similar parts, they can be assembled together by enforcing various compatibility conditions. Hence the computational time and storage space requirements are reduced by avoiding repeated analysis of the alike parts.

(d) If a part of the structure is modified then usually its effect will be local and only to the substructures connected to it and therefore, only these parts need to be reanalyzed. CMS saves time and storage space by avoiding repeated analysis of those parts which have not been modified.

(e) By minimizing the number of dofs required to represent each substructure, the CMS approach reduces the amount of information to be exchanged and thereby simplifies the communication. Also, each organization is permitted to apply its own judgment for the reduction of the part of the structure in which it is dealing.

(f) Sometimes structure may contain parts in which it is too complex to determine their modal parameters by analytical or numerical techniques. In such cases these complex parts are independently modeled using experimental based methods whereas other less complex parts may be modeled with the same conventional numerical or analytical techniques. Thus, using CMS we can obtain the modal parameters of the global model from the modal parameters of each of the substructures, obtained from different modeling schemes.

1.1.6 Disadvantages of CMS

Component mode synthesis performs reduction by transforming the physical dofs into reduced coordinates using the normal and static modes of the system. Normal modes are obtained from the eigenvalue problem of the system and static modes are obtained from the characteristic equations of the system. Since, both these modes are linear; therefore, the reduced system obtained after transforming the system using these modes is also linear. Thus, the reduced model from CMS can be used to perform only linear analyses. An extensive research is going on in extending the use of CMS to problems having geometric and material nonlinearities. Interested readers can refer [15] for the model reduction of nonlinear structural systems using CMS and nonlinear normal modes; and [16], [17] for handling material nonlinearities.

1.2   Dissertation Objective and Outline

Motivated by the structural dynamic community's need for the development of appropriate reduced order models that can guarantee accurate solutions with in a particular frequency range of interest while keeping the computational cost to minimum, three distinctive objectives are identified and addressed in this research effort:

(a) To get an in-depth understanding of the formulation procedure of the Fixed and the Free interface method, and then apply it to simple academic problems so as to assess their ability for applying it to more complex real life problems. The methods are assessed with regard to the degree of reduction attainable on one hand and the level of accuracy achieved on the other hand.
(b) To rigorously assess both the methods for the reduction in computational time achievable in completing an analysis in practical cases by applying them to the real structure of Car Axle.
(c) To study measures based on EIM for the appropriate determination of dominant modes to be chosen for the reduction of the interior dofs. Propose an extension of EIM to effectively choose the dynamically important Coupled CC modes relative to the already selected generalized coordinates for the interior, so as to finally get a highly reduced system that can guarantee accurate solutions as compared to full model FEM.

The report is organized into series of chapters to provide the in detail study about the CMS.

Chapter 2 is devoted to provide the theoretical formulation of the Fixed Interface Method. The various deciding factors that affect the selection of substructure modes are discussed.

Chapter 3 describes Free Interface method in detail with the various deciding factors that affects selection of substructure modes in this method. Detailed derivation of the Residual flexibility for the constrained and unconstrained components is done.

Chapter 4 discusses about the theoretical formulation of the Effective Mass and Effective Interface measure for the selection of substructure modes. Extension of EIM for the cases when the required response is displacement or velocity is also described. A further extension of EIM is proposed for the reduction of Interface dofs.

Chapter 5 performs the numerical assessment of Fixed Interface and Free Interface methods. Two academic examples: i) A Fixed-Free beam problem and ii) A Cracked beam problem are used to assess the methods. These methods are also applied to perform the model reduction of a real structure of Car axle to study the reduction in computational time achievable by both these methods.

Chapter 6 performs the numerical assessment of the Thumb rule, Effective Mass, and Effective Interface measure for the selection of the substructure modes in the Fixed Interface method. An example Fixed-Free plate is used and the appropriateness of each of the particular measure is performed by comparing the displacement, velocity, and acceleration response obtained from the system, reduced by the Fixed Interface kept normal modes selected through each of these measures, to the full model FEM solution.

Chapter 7 presents the conclusions derived from the numerical assessment performed in Chapter 5 and Chapter 6. Scope of future work is clearly stated.

Chapter 2

Fixed Interface Method

2.1 Theoretical Formulation

In the Fixed Interface method, normal modes of the substructure are calculated by fixing all the interface dofs. The Fixed Interface method was first proposed by Hurty [18]. Hurty's approach required partitioning the interface dofs into rigid-body dofs and redundant interface dofs and then corresponding to each of these two sets of dofs rigid body modes and redundant constraint modes were obtained respectively. The Fixed Interface normal modes combined with rigid-body modes and redundant interface constraint modes were used to transform the system. Hurty's method was later simplified by Craig and Bampton [3] by treating all the interface dofs together. In Craig and Bampton method, constraint modes are obtained corresponding to all the interface dofs. Constraint modes (static modes) are augmented with these normal modes, so as to make the coupling of the substructures statically complete. These modes also maintain the continuity of displacements between the two adjacent substructures of a structure at the Interface dofs. This chapter presents the formulation procedure of Fixed Interface method as explicitly described by Craig [4].

To illustrate the method more clearly, a Fixed–free beam as shown in Figure 2.1 is taken. Before going through the formulation of Fixed Interface method, it is assumed that the complete structure has been discretesized into elements and the Finite Element model of the structure is at hand. Thus the mass, stiffness and the vector of external forces of structure is known and therefore, the equation of motion for a structure is given by,
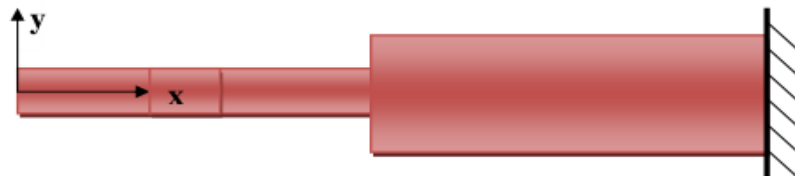
Figure 2.1: A Fixed-free beam

$$M\ddot{x} + Kx = f \tag{2.1}$$

where x is the vector of physical dofs, M is the mass matrix, K is the stiffness matrix and f is the vector of external forces. For simplicity, damping is not included. The structure is divided into n substructures and therefore the vector of physical dofs x is partitioned into physical dofs of each substructure, such that

$$x = \left[\{x^{(1)}\}\{x^{(2)}\}\{x^{(3)}\} \quad \dots \quad \{x^{(n)}\}\right]^{T} \tag{2.2}$$

where $x^{(i)}$ represents column vector of physical dofs of substructure 'i'. Similarly mass matrix, stiffness matrix and vectors of external forces are partitioned and obtained for each of the substructure, represented as $M^{(i)}$, $K^{(i)}$ and $f^{(i)}$ respectively. Further, the dofs of each of the substructure are partitioned into interior dofs (subscript i) and coupling dofs (subscript c). Therefore, the vectors of physical dofs for each substructure (from Eq. (2.2)) can be partitioned and represented as shown in Figure 2.2.

$$x^{(i)} = \begin{Bmatrix} x_i^{(i)} \\ x_c^{(i)} \end{Bmatrix} \tag{2.3}$$

Similarly, the mass $M^{(i)}$, stiffness $K^{(i)}$, and force $f^{(i)}$ that relate to each substructure are partitioned and represented as below.

$$M^{(i)} = \begin{bmatrix} m_{ii}^{(i)} & m_{ic}^{(i)} \\ m_{ci}^{(i)} & m_{cc}^{(i)} \end{bmatrix} \tag{2.4}$$

$$K^{(i)} = \begin{bmatrix} k_{ii}^{(i)} & k_{ic}^{(i)} \\ k_{ci}^{(i)} & k_{cc}^{(i)} \end{bmatrix} \tag{2.5}$$

$$f^{(i)} = \begin{Bmatrix} f_i^{(i)} \\ f_c^{(i)} \end{Bmatrix} \tag{2.6}$$

2.1.1 Fixed Interface normal modes

The equation of motion for each substructure (Eq. (2.7)) written in terms of partitions of interior and coupling dofs is given by Eq. (2.8).

$$M^{(i)}\ddot{x}^{(i)} + K^{(i)}x^{(i)} = f^{(i)} \tag{2.7}$$

$$\begin{bmatrix} m_{ii}^{(i)} & m_{ic}^{(i)} \\ m_{ci}^{(i)} & m_{cc}^{(i)} \end{bmatrix} \begin{Bmatrix} \ddot{x}_i^{(i)} \\ \ddot{x}_c^{(i)} \end{Bmatrix} + \begin{bmatrix} k_{ii}^{(i)} & k_{ic}^{(i)} \\ k_{ci}^{(i)} & k_{cc}^{(i)} \end{bmatrix} \begin{Bmatrix} x_i^{(i)} \\ x_c^{(i)} \end{Bmatrix} = \begin{Bmatrix} f_i^{(i)} \\ f_c^{(i)} \end{Bmatrix} \qquad (2.8)$$

Eq. (2.8) will be used to calculate the normal modes of the substructures by fixing all the coupling dofs. This is also explained Figure 2.2 for the example Fixed-free beam. First considering the Free vibration problem with the objective of calculating only the natural frequencies and mode shapes of the complete structure. For a Free vibration problem the external forces are set as zero, hence only the coupling forces $f_c^{(i)}$, originated because of separating the already connected substructures of a structure, acting between the substructures at their common interfaces will be present.
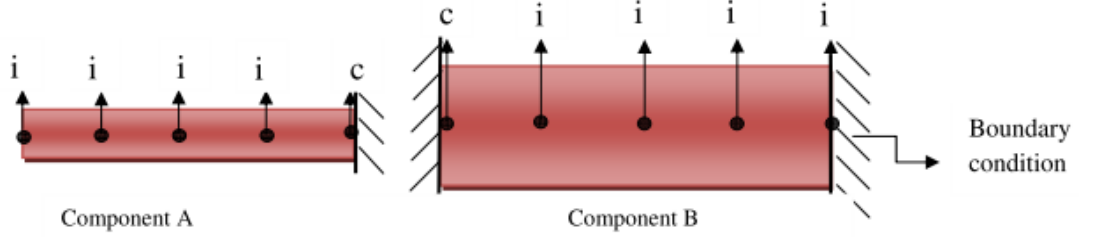
Figure 2.2: Boundary condition of substructures for calculation of Fixed Interface normal modes

Therefore the displacement boundary conditions and the force condition for the free vibration problem are given as below.

$$x_c^{(i)} = 0 \qquad (2.9)$$

$$f_i^{(i)} = 0 \qquad (2.10)$$

Applying the displacement boundary condition given by Eq. (2.9), the equation of motion for each of the substructures is given as below.

$$m_{ii}^{(i)} \ddot{x}_i^{(i)} + k_{ii}^{(i)} x_i^{(i)} = 0 \qquad (2.11)$$

Let Φ_n be the set of normal mode shapes found out by solving the eigenvalue problem formed from Eq. (2.11). As all these modes may not have a significant contribution in the dynamic response of the system within the frequency range of interest, we select few mode shapes

$\Phi_k \, (= \Phi_{ik})$, called as kept mode shapes from the complete set of normal mode shapes Φ_n, where k represents the selected set of mode numbers. Φ_k is mass normalized such that,

$$\Phi_k^T \, m_{ii}^{(i)} \, \Phi_k = I_{kk} \tag{2.12}$$

$$\Phi_k^T \, k_{ii}^{(i)} \, \Phi_k = \lambda_{kk} = diag(\omega_k^2) \tag{2.13}$$

where ω_k^2 is the eigenvalue corresponding to the kth kept mode shape. Using these kept modes the physical dofs $x^{(i)}$ can be therefore transformed into interior generalized coordinates p_k as below.

$$\begin{Bmatrix} x_i^{(i)} \\ x_c^{(i)} \end{Bmatrix} = \begin{bmatrix} \Phi_k \\ 0 \end{bmatrix} \begin{Bmatrix} p_k^{(i)} \end{Bmatrix} \tag{2.14}$$

It should be noted that as only few mode shapes Φ_k are selected, therefore the size of generalized coordinates p_k will be very less than the actual size of physical dofs and a reduced model is obtained. However, the selection of these kept mode shapes should be based on proper arguments, for the reduced representation to give accurate results within the frequency range of interest. The various deciding factors for the selection of modes depend not only on the application at hand but also on the particular results one is interested in. Few of these factors are assessed in section 2.1.4.

2.1.2 Constraint modes

Constraint modes $\{\Phi_c\}$ are found from the static equation of the substructure found after neglecting the inertia terms. It represents the static deformation of a structure due to successive unit displacement applied at the Interface dofs while keeping the remaining Interface dofs constrained and all Interior dofs free. As shown in Figure 2.3 these modes also ensure inter substructure compatibility of displacements. Constraint modes can be found from Eq. (2.8) by neglecting the dynamic terms as given below.

$$\begin{bmatrix} k_{ii}^{(i)} & k_{ic}^{(i)} \\ k_{ci}^{(i)} & k_{cc}^{(i)} \end{bmatrix} \begin{Bmatrix} x_i^{(i)} \\ x_c^{(i)} \end{Bmatrix} = \begin{Bmatrix} 0 \\ f_c^{(i)} \end{Bmatrix} \tag{2.15}$$

The upper partition of Eq. (2.15) defines the relation between the Interior and Interface dofs and is given as

$$x_i^{(i)} = (-k_{ii}^{(i)-1} k_{ic}^{(i)}) x_c^{(i)} \tag{2.16}$$

$$x_i^{(i)} = \Phi_c x_c^{(i)} \tag{2.17}$$

$$\Phi_c = (-k_{ii}^{(i)-1} k_{ic}^{(i)}) \tag{2.18}$$
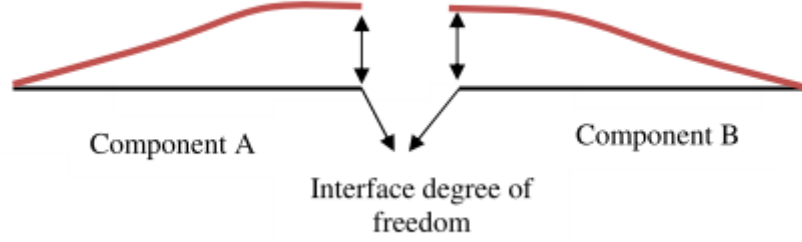
Figure 2.3: Representation of Constraint modes

where Φ_c are called as constrained modes. Using these constraint modes physical dofs $x^{(i)}$ can be transformed into interface physical dofs $x_c{}^{(i)}$ as below.

$$\begin{Bmatrix} x_i^{(i)} \\ x_c^{(i)} \end{Bmatrix} = \begin{bmatrix} \Phi_c \\ I \end{bmatrix} \begin{Bmatrix} x_c^{(i)} \end{Bmatrix} \tag{2.19}$$

2.1.3 Coordinate Transformation

The combined set of Fixed Interface normal modes and Constraint modes will define the transformation matrix that will be used to transform substructure's physical dofs into generalized coordinates. Hence, the coordinate transformation matrix for the entire substructure is defined from Eq. (2.14) and Eq. (2.19) as below. It should be noted from Eq. (2.20) that the final transformed coordinates of each of the substructure consists of generalized coordinates, and all the interface dofs in physical form. The presence of all the interface dofs in physical form will allow a statically complete coupling of the substructures together. The term "statically complete" means that the static deformation of the coupled reduced structure is exact as compared to that obtained from the full model FEM solution.

$$x^{(i)} = \begin{Bmatrix} x_i^{(i)} \\ x_c^{(i)} \end{Bmatrix} = \begin{bmatrix} \Phi_k & \Phi_c \\ 0 & I \end{bmatrix} \begin{Bmatrix} p_k^{(i)} \\ x_c^{(i)} \end{Bmatrix} \tag{2.20}$$

16

$$x^{(i)} = \left\{ \begin{matrix} x_i^{(i)} \\ x_c^{(i)} \end{matrix} \right\} = [V]\{p^{(i)}\} \tag{2.21}$$

Substituting the value of $x^{(i)}$ from Eq. (2.21) to Eq. (2.7), we get the new equation of the substructure in generalized coordinate system as follows.

$$M^{(i)}V\ddot{p}^{(i)} + K^{(i)}Vp^{(i)} = f^{(i)} \tag{2.22}$$

The properties of Φ_k, which is mass normnalized as given in Eq. (2.12) and Eq. (2.13), will be used to simplify the equations.

Premultiplying Eq. (2.22) by V^T we get

$$V^T M^{(i)} V \ddot{p}^{(i)} + V^T K^{(i)} V p^{(i)} = V^T f^{(i)} \tag{2.23}$$

$$\bar{M}^{(i)} \ddot{p}^{(i)} + \bar{K}^{(i)} p^{(i)} = \bar{f}^{(i)} \tag{2.24}$$

where $\bar{M}^{(i)}$, $\bar{K}^{(i)}$ and $\bar{f}^{(i)}$ represent the reduced mass, stiffness and force in the transformed generalized coordinates and the detailed expressions for each of these are given as below.

$$\bar{M}^{(i)} = V^T M^{(i)} V = \begin{bmatrix} \bar{m}_{kk}^{(i)} & \bar{m}_{kc}^{(i)} \\ \bar{m}_{ck}^{(i)} & \bar{m}_{cc}^{(i)} \end{bmatrix}$$

$$\bar{K}^{(i)} = V^T K^{(i)} V = \begin{bmatrix} \bar{k}_{kk}^{(i)} & \bar{k}_{kc}^{(i)} \\ \bar{k}_{ck}^{(i)} & \bar{k}_{cc}^{(i)} \end{bmatrix}$$

$$\bar{f}^{(i)} = V^T f^{(i)} = \left\{ \begin{matrix} \bar{f}_k^{(i)} \\ \bar{f}_c^{(i)} \end{matrix} \right\} \tag{2.25}$$

$$\bar{m}_{kk}^{(i)} = \Phi_k^T m_{ii}^{(i)} \Phi_k = I_{kk}$$

$$\bar{m}_{ck}^{(i)} = \bar{m}_{kc}^{T~(i)} = \Phi_k^T (m_{ii}^{(i)} \Phi_c + m_{ic}^{(i)})$$

$$\bar{m}_{cc}^{(i)} = m_{cc}^{(i)} + \left(\Phi_c^T m_{ii}^{(i)} + m_{ci}^{(i)} \right) \Phi_c + m_{ci}^{(i)} \Phi_c$$

$$\bar{k}_{kk}^{(i)} = \Phi_k^T k_{ii}^{(i)} \Phi_k = \lambda_{kk}$$

$$\bar{k}_{ck}^{(i)} = \bar{k}_{kc}^{T}{}^{(i)} = \Phi_k^T (k_{ii}^{(i)} \Phi_c) + \Phi_k^T k_{ic}^{(i)}$$

$$= \Phi_k^T (-k_{ic}^{(i)}) + \Phi_k^T k_{ic}^{(i)} = 0$$

$$\bar{k}_{cc}^{(i)} = k_{ci}^{(i)} \Phi_c + k_{cc}^{(i)}$$

$$\bar{f}_k^{(i)} = \Phi_k^T f_k^{(i)}$$

$$\bar{f}_c^{(i)} = \Phi_c^T f_k^{(i)} + f_c^{(i)}$$

Thus, all the substructures of the structure are transformed to the reduced generalized coordinates system. These reduced substructures will be coupled together to get the global reduced complete structure. Before understanding the coupling of these substructures, it is important to understand various deciding factors on which the selection of kept modes is based. If for a particular substructure, proper selection of mode shapes for the reduced representation is not done then the global reduced system cannot be guaranteed to give accurate results within the frequency range of interest.

2.1.4 Selection of Component modes

Various deciding factors which form the basis for the selection of component modes are listed as below.

(a) Frequency range of interest:

The frequency range of interest can be determined by the range in which the natural frequencies of the complete structure are required. In Fixed Interface method one actually determines the modal parameters of the complete structure from the Fixed Interface normal modes of each of its individual substructures. These Fixed Interface normal modes are obtained in an artificial sense (i.e. interface dofs are artificially fixed) and are not the real modes of each of the individual substructures. Therefore, one generally selects substructure's mode shapes from a wider frequency range (1.8 times) than the actual frequency range of interest of the complete structure. This is also called as thumb rule.

(b) Loads:

In case of Forced vibration problem, where loads acting on the substructures may be varying with time and also may have a spatial variation, the mode shapes in the reduced

representation should represent both the spatial and the temporal variation of the force. In other words, the mode shapes kept should represent the applied forces both statically and dynamically for their spatial and temporal variation respectively. For representing the temporal variation, the first step is to determine the forcing frequencies that are contained in the time varying forces. This can be determined from the well known Fourier Transforms. This also further gives a more clear idea about the frequency range of interest and depending on that one can select the modes as per thumb rule.

For the spatial variation of loads one can find out that the constraint modes corresponding to a particular dofs will completely represent the force acting along that dofs. This can also be readily verified from the expression of the generalized force vector in Eq. (2.25), which explicitly retains the forces at the coupling dofs in their physical form. So for the case of point loads acting along few dofs, one should consider those particular dofs also in the set of coupling dofs for the constraint modes to accurately project the forces, acting along these dofs, in the transformed generalized coordinates. However, if the loads acting on the substructure are body forces then by following the same reasoning, one would have to consider many dofs in the set of coupling dofs and this will drastically affect the size of reduced system. For such cases, kept mode shapes and constraint mode shapes are augmented with a special set of load dependent vectors[19], the size of which is also very low as compared to the size obtained by considering constraint modes corresponding to each dofs along which forces are applied. One can also follow the derivation in [20] to find out the physical force that is represented by a particular set of kept mode shapes, and if in case they are represented properly then there is no need to include additional load dependent Ritz vectors. The case of body forces is not considered in this work.

(c) Effective Mass Measures:

The dynamic mode shapes taken in to account by thumb rule, considering the frequency range of interest, will work for the cases when one is interested only in the displacement response of the system. This is because the displacement response is inversely proportional to the square of natural frequencies, so the contribution of higher modes keeps on decreasing. For higher derivatives of displacement, i.e. velocity and acceleration, many more modes are required to be chosen because the inertia of the system plays an important role in such cases. It will be shown in Chapter 6, that selecting modes from thumb rule will give

highly inaccurate results and therefore one need a proper measure which can determine the dynamically important modes for the cases of velocity and acceleration response. One of the most important measures is the Effective Mass measure which ranks the dynamic importance of the modes based on its contribution to the total structural mass of the substructure. So by keeping a particular set of modes which approximately represent, say 0.95%, the total structural mass of the system will give more accurate velocity and acceleration response. These measures are discussed in detail in Chapter 4.

2.1.5 Assembling of substructure equations

Once the model order reduction has been performed on every substructure of the structure as explained in section 2.1.3, these substructure equations need to be coupled together to find the global response of the complete structure.

Consider two substructures (α and β) sharing a common boundary or interface, which are to be assembled together. The combined set of generalized coordinates of both the substructures is defined as p_{cm}. This set can be ordered into normal kept coordinates and coupling coordinates, such that

$$p_{cm} = \begin{Bmatrix} p_k^{(\alpha)} \\ x_c^{(\alpha)} \\ p_k^{(\beta)} \\ x_c^{(\beta)} \end{Bmatrix} \tag{2.26}$$

Similarly, the property matrices of all the substructures are combined in a single set and the equation of motion for the overall system can be written as below.

$$M_{cm}\,\ddot{p}_{cm} + K_{cm}\,\ddot{p}_{cm} = f_{cm} \tag{2.27}$$

where,

$$M_{cm} = \begin{bmatrix} I_{kk}^{(\alpha)} & \bar{m}_{kc}^{(\alpha)} & 0 & 0 \\ \bar{m}_{ck}^{(\alpha)} & \bar{m}_{cc}^{(\alpha)} & 0 & 0 \\ 0 & 0 & I_{kk}^{(\beta)} & \bar{m}_{kc}^{(\beta)} \\ 0 & 0 & \bar{m}_{ck}^{(\beta)} & \bar{m}_{cc}^{(\beta)} \end{bmatrix} \tag{2.28}$$

$$K_{cm} = \begin{bmatrix} \bar{k}_{kk}^{(\alpha)} & 0 & 0 & 0 \\ 0 & \bar{k}_{cc}^{(\alpha)} & 0 & 0 \\ 0 & 0 & \bar{k}_{kk}^{(\beta)} & 0 \\ 0 & 0 & 0 & \bar{k}_{cc}^{(\beta)} \end{bmatrix} \qquad (2.29)$$

$$f_{cm} = \begin{Bmatrix} \bar{f}_k^{(\alpha)} \\ \bar{f}_c^{(\alpha)} \\ \bar{f}_k^{(\beta)} \\ \bar{f}_c^{(\beta)} \end{Bmatrix} \qquad (2.30)$$

These equations only represent the combined set of equations of all the substructures and are still uncoupled. We will couple them by invoking interface displacement and force compatibility between the substructures. As shown in Figure 2.2 the displacement compatibility equation can be written as

$$x_c^{(\alpha)} = x_c^{(\beta)} \qquad (2.31)$$

These equations can be coupled by transforming the coordinates p into a new set of coordinates q which have a common Interface coordinate. This is done as below

$$\begin{Bmatrix} p_k^{(\alpha)} \\ x_c^{(\alpha)} \\ p_k^{(\beta)} \\ x_c^{(\beta)} \end{Bmatrix} = \begin{bmatrix} I & 0 & 0 \\ 0 & 0 & I \\ 0 & I & 0 \\ 0 & 0 & I \end{bmatrix} \begin{Bmatrix} p_k^{(\alpha)} \\ p_k^{(\beta)} \\ x_c^{(\alpha)} \end{Bmatrix} \qquad (2.32)$$

Let,

$$S = \begin{bmatrix} I & 0 & 0 \\ 0 & 0 & I \\ 0 & I & 0 \\ 0 & 0 & I \end{bmatrix} \qquad (2.33)$$

$$q = \begin{Bmatrix} p_k^{(\alpha)} \\ p_k^{(\beta)} \\ x_c^{(\alpha)} \end{Bmatrix} \qquad (2.34)$$

Substituting the value of p from Eq. (2.32) into Eq. (2.27) and premultiplying both sides by S^T, we get as below.

$$S^T M_{cm} S \ddot{Q} + S^T K_{cm} S Q = S^T f_{cm} \tag{2.35}$$

$$M_q \ddot{Q} + K_q Q = f_q \tag{2.36}$$

where,

$$M_q = \begin{bmatrix} I_{kk}^{(\alpha)} & 0 & \bar{m}_{kc}^{(\alpha)} \\ 0 & I_{kk}^{(\beta)} & \bar{m}_{kc}^{(\beta)} \\ \bar{m}_{ck}^{(\alpha)} & \bar{m}_{ck}^{(\beta)} & \bar{m}_{cc}^{(\alpha)} + \bar{m}_{cc}^{(\beta)} \end{bmatrix} \tag{2.37}$$

$$K_q = \begin{bmatrix} \lambda_{kk}^{(\alpha)} & 0 & 0 \\ 0 & \lambda_{kk}^{(\beta)} & 0 \\ 0 & 0 & \bar{k}_{cc}^{(\alpha)} + \bar{k}_{cc}^{(\beta)} \end{bmatrix} \tag{2.38}$$

$$f_q = \begin{Bmatrix} \bar{f}_k^{(\alpha)} \\ \bar{f}_k^{(\beta)} \\ \bar{f}_c^{(\alpha)} + \bar{f}_c^{(\beta)} \end{Bmatrix} \tag{2.39}$$

After assembling all the substructures as described in section 2.1.5, the global response of the system can be calculated from the reduced system equation $\left[K_q - \omega_p^2 M_q\right]\Phi_p = 0$, having only kept and Interface generalized coordinates, where Φ_p is the pth global mode shape and ω_p^2 is the corresponding eigenvalue.

2.2 Concluding Remarks

The key to model reduction is selection of particular set of mode shapes or other vectors which completely represent the physics of the problem at hand. Inappropriate selection of mode shapes will drastically affect the accuracy of the results. In, Fixed Interface Method, constraint modes plays a very important role in making a statically complete coupling of the substructures and in accurately representing the forces acting at the coupling dofs. Normal modes take care of the time varying response of the structure.

Chapter 3

Free Interface Method

3.1   Theoretical Formulation

In this chapter the formulation procedure of Free Interface method is discussed. Goldman [**21**] proposed this method and later MacNeal [**22**] modified it and put forth a method which accounts for the static contribution of neglected or deleted modes. This is achieved by the concept of residual flexibility. Later, Rubin [**23**] went into considerable detail in the formulation of residual flexibility of individual unconstrained substructures which possesses rigid body modes. Craig and Chang [**4**] have explicitly described the complete formulation of the Free Interface method for constrained and unconstrained substructures, which is presented in the subsequent sections.

In general, the Free Interface method is more difficult to implement than the Fixed Interface method, but the former has two major advantages over the latter. First, in the cases where reduction techniques are used with the experimentally obtained modes, then the Free Interface method is preferred over the Fixed Interface method as the experimental mode shapes can be easily obtained for use in the Free Interface method as compared to Fixed Interface method. This is because for Fixed Interface method, the Fixed Interface normal modes of the substructure are required (by fixing the Interface dofs) which is practically infeasible, whereas in case of Free Interface method no such condition is required. Second, Free Interface method generally gives better results as compared to Fixed Interface method as will be shown in Chapter 5.

In Free Interface method, normal modes of the substructure are calculated by keeping all the Interface dofs as free. These normal modes are supplemented by attachment modes (static modes), so as to make the substructure statically complete. Free normal modes can also be supplemented by constraint mode shapes as static modes but in that case for substructures with rigid body motion, additional static mode shapes called inertia relief (IR) mode shapes must also be used [**22**].

3.1.1 Free Interface normal modes

The undamped equation of motion for each substructure is given below.

$$M^{(i)}\ddot{x}^{(i)} + K^{(i)}x^{(i)} = f^{(i)} \tag{3.1}$$

where, $x^{(i)}$ are the physical dofs of the substructure. Here 'i' refers to the substructure number and can be omitted from now onwards for simplicity. The physical dofs and all the system matrices are partitioned into Interior and Coupling dofs as described from Eq. (2.3) to Eq. (2.6). The Free interface normal modes of a substructure are calculated from the Eq. (3.1) by keeping all the Interface dofs as free or unconstrained, as shown in Figure 3.1. These are given by the solution of the following eigenvalue problem.

$$\left(K - \omega_j^2 M\right)(\Phi)_j = 0 \tag{3.2}$$
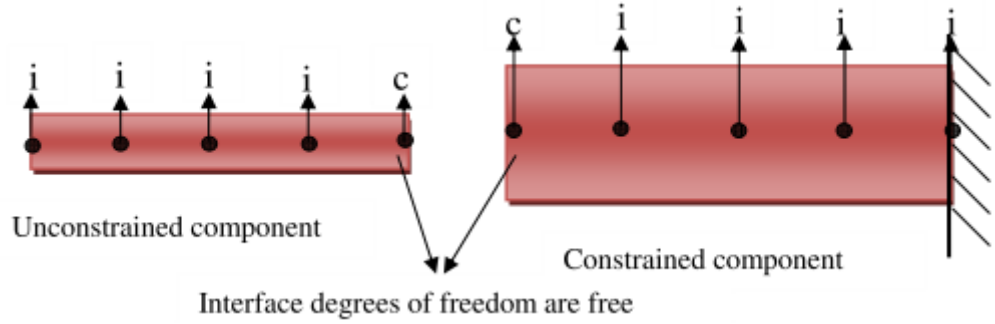
Figure 3.1: Boundary condition for calculation of Free Interface Normal modes

Let Φ_n be the set of normal mode shapes found out from Eq. (3.2) and Φ_k be the selected set of kept mode shapes from it. Φ_k is mass normalized as described in Eq. (2.12) and Eq. (2.13). Using these kept modes the physical dofs x can be therefore transformed into generalized coordinates p_k ($k < n$) as below, where k is the size of reduced generalized coordinates and n is the size of total physical dofs.

$$\{x\} = [\Phi_k]\{p_k\} \tag{3.3}$$

Neglecting some of the modes completely will affect the static completeness of the substructure and therefore, these Free Interface normal modes are augmented with additional static modes called as attachment modes. These attachments modes make the substructure

statically complete as the constraint modes does in the case of Fixed Interface method. The attachment modes are calculated from the Residual flexibility which is explained next.

3.1.2 Residual Flexibility

A detailed discussion of meaning and use of Residual flexibility and its role in substructure testing procedures is given in [**24**]. Residual flexibility is obtained from the flexibility matrix of the substructure, the formulation of which depends on whether the substructure under consideration is constrained or unconstrained. The derivation of flexibility and then the Residual flexibility for both the cases is explained in the following sections.

(a) Constrained Substructures:

$\Rightarrow$ *Flexibility Matrix*

Flexibility represents the static deformation of a system due to application of unit forces. When a unit static force is applied on a constrained substructure then the displacement can be obtained by the inverse of stiffness matrix, which is the flexibility matrix G as shown below.

$$K\, x = f \tag{3.4}$$

$$x = K^{-1} f \tag{3.5}$$

$$x = G\, f \tag{3.6}$$

Flexibility represents the total static deformation of the substructure but since some part of the total static deformation has already been taken into account by the Free Interface kept normal modes, only the static deformation due to the deleted modes need to be found out. The static contribution from the deleted modes is represented by the flexibility of the deleted modes or the residual modes and hence the word "Residual Flexibility" is derived. It should be noted that such a need of calculating static deformation of deleted modes didn't arise in the case of Fixed Interface method. This is because the constraint modes are completely independent of the Fixed Interface normal modes and even if a complete set of the Fixed interface normal modes of a substructure are chosen, further supplementing them with constraint modes is necessary to get the true deformation, which is not the case with the Free Interface method. Also, since the Fixed Interface normal modes of the substructure are not its true modes (unlike Free Interface normal modes), the static deformation which is taken into account by

the Fixed Interface kept modes doesn't represent any particular part of the total static deformation of the substructure, unlike the case for Free Interface modes. The derivation of Residual Flexibility is explained below.

⇒ *Residual Flexibility Matrix*

To get residual flexibility matrix we need to find out the static displacement due to deleted modes and therefore total static displacement should be divided into displacement due to kept modes and deleted modes. This is done by transforming the physical dofs into generalized coordinates by the complete modal matrix partitioned into kept modes and deleted modes as shown below.

$$x = [\Phi_n]\{p\} \tag{3.7}$$

$$x = [\Phi_k \quad \Phi_d]\begin{Bmatrix} p_k \\ p_d \end{Bmatrix} \tag{3.8}$$

$$x = \Phi_k\, p_k + \Phi_d\, p_d \tag{3.9}$$

where, Φ_k are the kept modes, Φ_d are the deleted modes, p_k are the kept generalized coordinates and p_d are the deleted generalized coordinates.

Substituting the value of x from Eq. (3.8) in Eq. (3.4) and multiplying both sides by transpose of modal matrix, we get

$$\begin{bmatrix} \Phi_k^T \\ \Phi_d^T \end{bmatrix} K \, [\Phi_k \quad \Phi_d] \begin{Bmatrix} p_k \\ p_d \end{Bmatrix} = \begin{bmatrix} \Phi_k^T \\ \Phi_d^T \end{bmatrix} f \tag{3.10}$$

As all modes are mass normalized, therefore $\Phi_k^T\, K\, \Phi_d = 0$ and Eq. (3.10) reduces to following.

$$\begin{bmatrix} [\Phi_k^T\, K\, \Phi_k]\, \{p_k\} \\ [\Phi_d^T\, K\, \Phi_d]\, \{p_d\} \end{bmatrix} = \begin{bmatrix} \Phi_k^T \\ \Phi_d^T \end{bmatrix} f \tag{3.11}$$

This gives the value of p_k and p_d as below.

$$p_k = {\lambda_{kk}}^{-1} \Phi_k^T\, f \tag{3.12}$$

$$p_d = {\lambda_{dd}}^{-1} \Phi_d^T\, f \tag{3.13}$$

26

where,

$$[\lambda_{kk}]^{-1} = (\Phi_k^T \ K \ \Phi_k)^{-1}$$

$$[\lambda_{dd}]^{-1} = (\Phi_d^T \ K \ \Phi_d)^{-1}$$

Now, multiplying both sides of Eq. (3.12) by Φ_k, we get

$$\Phi_k \ p_k = \ \Phi_k \ \lambda_{kk}^{-1} \Phi_k^T \ f \tag{3.14}$$

$$\Phi_k \ p_k = \ G_k \ f \tag{3.15}$$

where,

$$G_k = \ \Phi_k \ \lambda_{kk}^{-1} \Phi_k^T$$

From Eq. (3.6), Eq. (3.9) and Eq. (3.15),

$$G \ f = \ G_k \ f + \Phi_d \ p_d \tag{3.16}$$

Here $\Phi_d \ p_d$ refers to the static displacement of deleted modes and can be written as below.

$$x_d = \ \Phi_d \ p_d = (G - \ G_k)f \tag{3.17}$$

$$x_d = \ G_d f \tag{3.18}$$

Eq. (3.18) defines the static displacement due to deleted modes and term G_d is called the residual flexibility of the substructure. It should be noted that only kept modes are required to evaluate the residual flexibility as seen in Eq. (3.19) and therefore the deleted modes need not to be evaluated for calculating their static contribution.

$$G_d = \ G - \ \Phi_k \ \lambda_{kk}^{-1} \ \Phi_k^T \tag{3.19}$$

Also, from an explicit expression of G_d in Eq. (3.20) calculated using only the deleted modes, orthogonal properties of G_d can be obtained as in Eq. (3.21).

$$G_d = \Phi_d \ \lambda_{dd}^{-1} \ \Phi_d^T \tag{3.20}$$

$$\Phi_k^T \ K \ G_d = 0 \tag{3.21}$$

$$\Phi_k^T \, M \, G_d = 0$$

$\Rightarrow$ *Residual Attachment modes*

The Residual Attachment modes represent the static deformation due to deleted modes of the substructure and due to unit forces applied at the Interface dofs. These residual attachment modes are obtained in terms of the residual flexibility matrix G_d by applying unit force at each of the Interface dofs in turn, as given below.

$$\beta_d = \, G_d \, f$$
$$\beta_d = \left[G - \, \Phi_k \, \lambda_{kk}^{-1} \Phi_k^T \right] \begin{Bmatrix} 0_{ic} \\ I_{cc} \end{Bmatrix}$$

(3.22)

where f is the force vector representing unit forces at the coupling dofs and β_d are called as residual attachment modes. It should be noted that residual attachment modes are nothing but columns of the residual flexibility matrix corresponding to the coupling dofs. Also, the subscript 'd' in β_d represents the contribution from deleted modes, but its size is $(n \, x \, n_c)$ where n is the size of total dofs of the substructure and n_c is the size of coupling dofs of the substructure, corresponding to which residual attachment modes are obtained.

The above methodology to calculate the flexibility is applicable only when the stiffness matrix is not singular. For cases when the stiffness matrix is singular which shows the presence of rigid body motion additional steps would be required to remove the rigid body modes and are described in the subsequent sections.

(b) Unconstrained Substructures:

$\Rightarrow$ *Flexibility matrix*

Unconstrained substructure as shown in Figure 3.1, have singular stiffness matrix due to which it is not possible to determine the flexibility of the substructure with the procedure defined above for the constrained substructures (see (3.5)). However, if constraints are applied to restrain just the rigid body motion of the unconstrained substructure the stiffness matrix remains no longer singular, and therefore the constrained flexibility matrix of this unconstrained substructure can be obtained with the similar procedure as for the constrained substructures. Rigid body motion is removed while calculating the flexibility matrix of

unconstrained substructures. Residual flexibility, hence derived from this flexibility will also not contain the rigid body motion. Therefore, the rigid body motion is accounted by including the rigid body modes in the set of kept modes.

Unconstrained substructures will undergo both rigid and flexible body motion when force is applied on them. It can be interpreted that rigid body and flexible body motion are contributed by rigid body and flexible body modes respectively. The zero natural frequencies obtained on performing the eigenvalue analysis of unconstrained substructure physically signify that at this frequency there is no flexible or elastic motion of the substructure and hence eigenvectors corresponding to these zero natural frequencies represent rigid body modes. All other eigenvectors are flexible modes which contribute to the flexible body motion of the substructure.

To find the flexible body motion of the unconstrained substructure, the total displacement is first divided into rigid body and flexible body motion. This is done by transforming the physical dofs into generalized coordinates by the modal matrix partitioned into rigid body modes and flexible body modes, as shown below.

$$x = [\Phi_r \quad \Phi_f] \begin{Bmatrix} p_r \\ p_f \end{Bmatrix} \tag{3.23}$$

where, Φ_r are the rigid body modes, Φ_f are the flexible body modes, p_r are the rigid body coordinates, and p_f are the flexible body coordinates

Substituting x from Eq. (3.23) in the dynamic equation of the substructure and premultiplying by $[\Phi_r \quad \Phi_f]^T$, we get as below.

$$\begin{bmatrix} \Phi_r^T \\ \Phi_f^T \end{bmatrix} M [\Phi_r \quad \Phi_f] \begin{Bmatrix} \ddot{p}_r \\ \ddot{p}_f \end{Bmatrix} + \begin{bmatrix} \Phi_r^T \\ \Phi_f^T \end{bmatrix} K [\Phi_r \quad \Phi_f] \begin{Bmatrix} p_r \\ p_f \end{Bmatrix} = \begin{bmatrix} \Phi_r^T \\ \Phi_f^T \end{bmatrix} f \tag{3.24}$$

As all modes are mass normalized $\Phi_r^T M \Phi_f = 0$, $\Phi_r^T K \Phi_f = 0$, $\Phi_r^T M \Phi_r = I_{rr}$ where $r \neq f$. Eq. (3.24) reduces to following.

$$\ddot{p}_r = \Phi_r^T f \tag{3.25}$$

$$\ddot{p}_f + \lambda_{ff} p_f = \Phi_r^T f \tag{3.26}$$

where,

$$\lambda_{ff} = diag\ (\omega_f^2) = \Phi^T{}_f K\ \Phi_f$$

It should be noted that there is no stiffness term in Eq. (3.25) and the force f results only in the acceleration of rigid body coordinates $\ddot{p}_r$. This is the rigid body motion. In Eq. (3.26) there is a stiffness term and it signifies the flexible body motion of the substructure. From Eq. (3.25) and Eq. (3.26) we can conclude that a part of force f causes rigid body motion whereas other part causes flexible body motion. Thus,

$$f = f_f + f_{inertia} \tag{3.27}$$

where, f_f is flexible body force and $f_{inertia}$ is rigid body inertia force. As rigid body inertia force results only in the rigid body acceleration of the substructure,

$$f_{inertia} = M\ \ddot{x}_r = M\ \Phi_r \ddot{p}_r \tag{3.28}$$

Substituting the value of $\ddot{p}_r$ from Eq. (3.25) in Eq. (3.28) we get as below.

$$f_{inertia} = M\ \Phi_r \Phi_r^T f \tag{3.29}$$

Therefore flexible body force is defined from Eq. (3.27) as below.

$$f_f = f - f_{inertia} = (I - M\ \Phi_r \Phi_r^T)\ f = A\ f \tag{3.30}$$

where,

$$A = (I - M\ \Phi_r \Phi_r^T)$$

To evaluate the flexible body motion, we will first apply constraints on the substructure such that just the rigid body motion is restrained and then apply flexible body force f_f. This will give the same flexible body motion as would have obtained, relative to the rigid body motion, by applying the total force f to an unconstrained structure. Once the value of flexible body force is known from Eq. (3.30) we can calculate flexible body motion as below.

$$x_f = G_{constrained}\ f_f = G_{constrained}\ A\ f \tag{3.31}$$

where, $G_{constrained}$ is the constrained flexibility matrix of the unconstrained substructure obtained by putting zeros in rows and columns corresponding to the dofs at which statically determinate constraints are applied and inverse of flexible stiffness matrix in the rest as given below.

$$G_{constrained} = \begin{bmatrix} 0 & 0 \\ 0 & k_{ff}^{-1} \end{bmatrix} \tag{3.32}$$

where k_{ff} is the partition of the stiffness matrix K corresponding to the dofs other than those where statically determinate constraints are applied. It is important to recapitulate again that it is impossible to directly find out the flexibility matrix and hence the total deformation, which includes rigid body motion and flexible body motion of an unconstrained substructure, due to singularity of the stiffness matrix. However, we can find the flexible body motion x_f of the unconstrained substructure, and the rigid body motion is accounted by retaining the rigid body modes as the kept modes. Since the rigid body modes are exclusively kept, the flexible body motion should be mass orthogonal to the rigid body modes to avoid addition of any rigid body component twice. This condition is required because x_f still contains some component of the rigid body modes as it is not mass orthogonal to Φ_r. To make x_f mass orthogonal to rigid body modes, a new vector x_e is created in which the substructures of rigid body modes are removed as below.

$$x_e = x_f - \Phi_r c_r \tag{3.33}$$

$$x_e = G_{constrained} Af - \Phi_r c_r \tag{3.34}$$

where, c_r is such that,

$$\Phi_r^T M x_e = 0 \tag{3.35}$$

Substituting the value of x_e from Eq. (3.34) in Eq. (3.35) we get as below.

$$\Phi_r^T M (G_{constrained} A f - \Phi_r c_r) = 0 \tag{3.36}$$

$$c_r = \Phi_r^T M G_{constrained} Af \tag{3.37}$$

Substituting the value of c_r back into Eq. (3.34) we get the flexible body motion of an unconstrained substructure which is completely orthogonal to rigid body modes.

$$x = G_{constrained} \, A \, f - \Phi_r \Phi_r^T M \, G_{constrained} \, A \, f \qquad (3.38)$$

$$x = (I - \Phi_r \Phi_r^T M) \, G_{constrained} A \, f \qquad (3.39)$$

$$x = A^T G_{constrained} \, A \, f \qquad (3.40)$$

$$x = Gf \qquad (3.41)$$

$$G = A^T G_{constrained} \, A \qquad (3.42)$$

⇒ *Residual flexibility matrix*

Once the flexibility matrix is calculated for unconstrained structures the procedure for calculating residual flexibility matrix is same as described as for the constrained substructures and can be directly calculated from Eq. (3.19). It should be noted that while calculating the flexibility matrix of unconstrained substructures, the contribution of rigid body modes is completely removed. Therefore, the residual flexibility also doesn't contain any contribution of rigid body modes. Hence, the rigid body modes should always be included in the set of kept modes for their dynamic contribution. Thus rigid body modes are "must kept modes" for unconstrained substructures.

⇒ *Inertia relief Attachment modes*

Inertia relief attachment modes represent the static deformation of an unconstrained structure due to deleted modes and due to unit forces applied at interface dofs. Once the residual flexibility matrix is calculated for unconstrained substructures, the procedure for calculating Inertia relief attachment modes is same as described for constrained substructures from Eq. (3.22).

3.1.3 Coordinate Transformation

The transformation of the physical dofs to the generalized coordinates for a substructure can be done by the summation of both dynamic and static mode shapes as below.

$$\begin{bmatrix} x_i \\ x_c \end{bmatrix} = V \, p = [\Phi_k \;\; \beta_d] \begin{Bmatrix} p_k \\ p_d \end{Bmatrix} \qquad (3.43)$$

where Φ_k are the kept free interface normal modes which also include rigid body modes for the unconstrained substructures, β_d are the residual attachment modes defined in Eq. (3.22).

Substituting the value of x from Eq. (3.43) to Eq. (3.1) we get the new equation of the substructure in generalized coordinate system as follows.

$$MV\ddot{p} + KVp = f \tag{3.44}$$

Multiplying Eq. (3.44) by V^T we get

$$V^T MV\ddot{p} + V^T KVp = V^T f \tag{3.45}$$

$$\bar{M}\ddot{p} + \bar{K}\,p = \bar{f} \tag{3.46}$$

where,

$$\bar{M} = \begin{bmatrix} \Phi_k^T \\ \beta_d^T \end{bmatrix} M[\Phi_k \ \beta_d] = \begin{bmatrix} \bar{m}_{kk} & \bar{m}_{kd} \\ \bar{m}_{dk} & \bar{m}_{dd} \end{bmatrix}$$

$$\bar{K} = \begin{bmatrix} \Phi_k^T \\ \beta_d^T \end{bmatrix} K[\Phi_k \ \beta_d] = \begin{bmatrix} \bar{k}_{kk} & \bar{k}_{kd} \\ \bar{k}_{dk} & \bar{k}_{dd} \end{bmatrix}$$

$$\bar{f} = \begin{bmatrix} \Phi_k^T \\ \beta_d^T \end{bmatrix} f = \begin{Bmatrix} \bar{f}_k \\ \bar{f}_d \end{Bmatrix}$$

$$\bar{m}_{kk} = \Phi_k^T M\,\Phi_k = I_{kk}$$

$$\bar{m}_{dk} = \bar{m}_{kd}^T = \Phi_k^T M\beta_d = 0 \tag{3.47}$$

$$\bar{m}_{dd} = \beta_d^T M\beta_d$$

$$\bar{k}_{kk} = \Phi_k^T K\,\Phi_k = \lambda_{kk}$$

$$\bar{k}_{dk} = \bar{k}_{kd}^T = \Phi_k^T K\beta_d = 0$$

$$\bar{k}_{dd} = \beta_d^T K\beta_d = \beta_{cd} = \beta_{cd}^T$$

$$\bar{f}_k = \Phi_k^T f$$

$$\bar{f}_d = \beta_d^T f$$

The derived properties of G_d in Eq. (3.48) and orthogonal properties in Eq. (3.21), the expression $\bar{m}_{dk} = \bar{m}_{kd}^T = 0$, $\bar{k}_{dk} = \bar{k}_{kd}^T = 0$ and $\bar{k}_{dd} = \beta_{cd} = \beta_{cd}^T$ are obtained in Eq. (3.47). β_{cd} represents the partition of rows and columns of G_d corresponding to the coupling dofs.

$$
\begin{aligned}
G_d^T K G_d &= \Phi_d \lambda_{dd}^{-1} \Phi_d^T K \Phi_d \lambda_{dd}^{-1} \Phi_d^T \\
&= \Phi_d \lambda_{dd}^{-1} \lambda_{dd} \lambda_{dd}^{-1} \Phi_d^T \\
&= \Phi_d \lambda_{dd}^{-1} \Phi_d^T = G_d
\end{aligned}
\tag{3.48}
$$

3.1.4 Assembling of Substructure equations

After the physical dofs of each of the substructure are transformed into generalized coordinates, assembly of substructures is performed. Eq. (3.43) can be written in terms of its partitions corresponding to the interior and coupling dofs as below.

$$
\begin{bmatrix} x_i \\ x_c \end{bmatrix} = \begin{bmatrix} \Phi_{ik} & \beta_{id} \\ \Phi_{ck} & \beta_{cd} \end{bmatrix} \begin{Bmatrix} p_k \\ p_d \end{Bmatrix}
\tag{3.49}
$$

From the lower partition of Eq. (3.49) the generalized coordinates p_d corresponding to the coupling dofs can be written in terms of coupling physical dofs at the interface x_c as shown below. This will permit simple coupling between the adjacent substructures. It should be noted that β_{cd} is always a square matrix as it correspond to partition at connection dofs of residual attachment modes which are also obtained corresponding only to the connection dofs between the two adjacent substructures. Hence, the number of rows and columns are same as the number of connection dofs.

$$
p_d = -\beta_{cd}^{-1} \Phi_{ck} p_k + \beta_{cd}^{-1} x_c
\tag{3.50}
$$

From Eq. (3.49) a second transformation matrix can be written as follows.

$$
\begin{bmatrix} p_k \\ p_d \end{bmatrix} = \begin{bmatrix} \Phi_{ik} & \beta_{id} \\ -\beta_{cd}^{-1} \Phi_{ck} & \beta_{cd}^{-1} \end{bmatrix} \begin{Bmatrix} p_k \\ x_c \end{Bmatrix}
\tag{3.51}
$$

Using the above transformation Eq. (3.46) is again transformed. It should be noted that after this transformation, the final transformed coordinates are in the same form as for the case of Fixed Interface method in Eq. (2.20). This allows using the same coupling procedures as

already described in section 2.1.5. Detailed derivation of the generalized system and mass matrices after the second transformation is given in [**25**]. In the above transformation, the residual effects are included in all the stiffness and mass matrices. Also the coupling dofs appears in the final transformed coordinate set as in the case of Fixed Interface Method.

3.1.5 Neglection of residual effects in inertia terms

It should be noted that Eq. (3.46) gets decoupled into coordinates corresponding to kept and deleted modes and is written as below.

$$\bar{m}_{kk}\,\ddot{p}_k + \bar{k}_{kk}\,p_k = \, \Phi_k^T f \tag{3.52}$$

$$\bar{m}_{dd}\,\ddot{p}_d + \bar{k}_{dd}\,p_d = \, \beta_d^T f \tag{3.53}$$

At this stage an assumption is made in which the inertia term of the coordinates corresponding to deleted modes $\ddot{p}_d$ is neglected which gives another formulation as proposed by MacNeal [**22**]. In this formulation, the residual effects are considered only in stiffness. So this takes into account only pseudo static solution of p_d. Eq. (3.53) hence reduces to

$$\bar{k}_{dd}\,p_d = \, \beta_d^T f \tag{3.54}$$

The value of $\bar{k}_{dd}$ is substituted in Eq. (3.54) from Eq. (3.47) to get

$$\beta_{cd}^T\,p_d = \, \beta_d^T f \tag{3.55}$$

Considering that the forces act only on the coupling dofs then the following equation can be derived,

$$\beta_{cd}^T(p_d - f_c) = 0 \tag{3.56}$$

where f_c represents the partition of the force vector f at the coupling dofs. Since β_{cd}^T is non singular therefore following relation is achieved,

$$p_d = f_c \tag{3.57}$$

The above relation is used to simplify the transformation defined in Eq. (3.43) as below.

$$x = \Phi_k\, p_k + \beta_d\, f_c \tag{3.58}$$

An advantage of using the above transformation is that the coupling dofs do not appear in the final reduced system and therefore, the size of the reduced system is less as compared to the formulation in which residual effects are taken for both mass and stiffness. This gives higher degree of model order reduction. However, this is a less accurate representation as the effects of deleted modes is considered only in quasi-static sense. It should be noted that such a formulation where coupling dofs do not appear in the final transformed equations cannot be achieved in the Fixed Interface method because the mass is coupled between the kept coordinates and boundary coordinates ($\bar{m}_{ck} \neq 0$).

The process of assembling for this formulation is different. Consider two coupled substructures (α and β) having a common boundary or interface. For substructure α, dynamic equation for kept modes can be written from Eq. (3.52), when forces are acting only at the coupling dofs.

$$\ddot{p}_k^{(\alpha)} + \lambda_{kk}^{(\alpha)}\, p_k^{(\alpha)} = \Phi_{ck}^{T\,(\alpha)} f_c^{\,(\alpha)} \tag{3.59}$$

The equation for the transformation of the physical dofs to the generalized coordinates for a substructure in terms of both the kept modes and residual attachment modes can be written from Eq. (3.58) as below.

$$x^{(\alpha)} = \Phi_k^{(\alpha)}\, p_k^{(\alpha)} + \beta_d^{(\alpha)}\, f_c^{(\alpha)} \tag{3.60}$$

Similarly for substructure β these equations can be written as below.

$$\ddot{p}_k^{(\beta)} + \lambda_{kk}^{(\beta)} p_k^{(\beta)} = \Phi_{ck}^{T\,(\beta)} f_c^{\,(\beta)} \tag{3.61}$$

$$x^{(\beta)} = \Phi_k^{(\beta)}\, p_k^{(\beta)} + \beta_d^{(\beta)}\, f_c^{(\beta)} \tag{3.62}$$

As the displacements at the junction coordinates must be equal and sum of all the coupling forces must be zero, the coupling equations for the two substructures are as below.

$$x_c^{(\alpha)} = x_c^{(\beta)} \tag{3.63}$$

$$\Phi_{ck}^{(\alpha)} \, p_k^{(\alpha)} + \beta_{cd}^{(\alpha)} \, f_c^{\,(\alpha)} = \Phi_{ck}^{(\beta)} \, p_k^{(\beta)} + \beta_{cd}^{(\beta)} \, f_c^{\,(\beta)} \tag{3.64}$$

$$f_c^{\,(\alpha)} = - f_c^{\,(\beta)} \tag{3.65}$$

where it is assumed that any required coordinate transformations have been made so that the junction coordinates of both the substructures coincide, as given by the compatibility Eq. (3.63) and (3.65).

From Eq. (3.64) and (3.65) we get the following

$$f_c^{\,(\alpha)} = (\beta_{cd}^{(\alpha)} + \beta_{cd}^{(\beta)})^{-1} \, (\Phi_{ck}^{(\beta)} \, p_k^{(\beta)} - \Phi_{ck}^{(\alpha)} \, p_k^{(\alpha)}) \tag{3.66}$$

Eq. (3.66) is substituted in Eq. (3.59) to get

$$\ddot{p}_k^{(\alpha)} + \lambda_{kk}^{(\alpha)} \, p_k^{(\alpha)}$$
$$= \Phi_{ck}^{T\,(\alpha)} (\beta_{cd}^{(\alpha)} + \beta_{cd}^{(\beta)})^{-1} \, (\Phi_{ck}^{(\beta)} \, p_k^{(\beta)} \tag{3.67}$$
$$- \Phi_{ck}^{(\alpha)} \, p_k^{(\alpha)})$$

Similarly,

$$\ddot{p}_k^{(\beta)} + \lambda_{kk}^{(\beta)} \, p_k^{(\beta)}$$
$$= \Phi_{ck}^{T\,(\beta)} (\beta_{cd}^{(\alpha)} + \beta_{cd}^{(\beta)})^{-1} \, (\Phi_{ck}^{(\beta)} \, p_k^{(\beta)} \tag{3.68}$$
$$- \Phi_{ck}^{(\alpha)} \, p_k^{(\alpha)})$$

Eq. (3.67) and (3.68) are combined and after arranging its various terms we get the equation of the coupled structure as below.

$$\begin{Bmatrix} \ddot{p}_k^{(\alpha)} \\ \ddot{p}_k^{(\beta)} \end{Bmatrix} + \begin{bmatrix} K_k^{(\alpha\alpha)} & K_k^{(\alpha\beta)} \\ K_k^{(\beta\alpha)} & K_k^{(\beta\beta)} \end{bmatrix} \begin{Bmatrix} p_k^{(\alpha)} \\ p_k^{(\beta)} \end{Bmatrix} = 0 \tag{3.69}$$

where,

$$K_k^{(\alpha\alpha)} = \lambda_{kk}^{(\alpha)} + \Phi_{ck}^{T\,(\alpha)} \, d_k \, \Phi_{ck}^{(\alpha)} \tag{3.70}$$

$$K_k^{(\alpha\beta)} = K_k^{(\beta\alpha)^T} = -\Phi_{ck}^{T\,(\alpha)} \, d_k \, \Phi_{ck}^{(\beta)} \tag{3.71}$$

$$K_k^{(\beta\beta)} = \lambda_{kk}^{(\beta)} + \Phi_{ck}^{T\,(\beta)} \, d_k \, \Phi_{ck}^{(\beta)} \tag{3.72}$$

$$d_k = (\beta_{cd}^{(\alpha)} + \beta_{cd}^{(\beta)})^{-1} \tag{3.73}$$

As can be seen from the coupled equation of the substructures i.e. Eq. (3.69), coupling dofs doesn't appear at all and only the kept generalized coordinates of each of the substructures appear. But it can be noticed that the sparsity of the generalized stiffness matrix is completely lost in the above formulation, which is preserved in the formulation where residual effects were kept both in mass and stiffness as can be seen in Eq. (3.47). Rixen [26] recently developed a method called as Dual Craig-Bampton method which preserves the sparsity of the stiffness matrix and also the coupling dofs doesn't appear in the final set of transformed equations. After assembling all the substructures as described above, the global response of the system can be calculated from the reduced system equation in Eq. (3.69), having only kept generalized coordinates of each of the substructures.

3.1.6 Selection of Component modes

Various deciding factors which form the basis for the selection of component modes in the Free Interface Method are listed as below.

(a) Frequency range of interest:

In the Free Interface method the modal parameters of the complete structure are determined from the Free Interface normal modes of each of its individual substructures. These Free Interface normal modes are the true modes of each of the substructure and therefore one just have to select substructure's mode shapes only in the frequency range of interest of the complete structure. This is contrary to the case of Fixed Interface method.

(b) Loads:

As described in the case of Fixed Interface method, the mode shapes in the reduced representation should represent both the spatial and the temporal variation of the force. For representing the temporal variation, after determining the forcing frequencies contained in the

time varying forces and depending on that deciding the frequency range of interest, one just have to select substructure's mode shapes only in that frequency range of interest.

Like Fixed Interface method, in the Free Interface method after the second transformation, as described in Eq. (3.51), for the spatial variation of loads one can find out that the residual attachment modes corresponding to a particular dofs will completely represent the force acting along that dofs. So for the case of point loads acting along few dofs, one should consider those particular dofs also in the set of coupling dofs for the residual attachment modes to accurately project/retain the forces, acting along these dofs, in the transformed generalized coordinates. However, this will not work for the cases of body force as it will drastically affect the size of reduced system. Alternatively, one can also use another formulation of Free Interface method (considering the residual effects only in stiffness and neglecting in mass) as described in section 3.1.4, in which coupling dofs doesn't appear in the final set of transformed equations. But in such cases, any loading that is represented by the non retained modes will have no dynamic amplification and will produce only quasi-static response (no dynamic effects will be captured) [20]. Augmenting the kept modes with a special set of load dependent vectors [19] is the only option for the case of body forces.

(c) Effective Mass Measure:

As described before, for higher derivatives of displacement, i.e. velocity and acceleration, many more modes are required to be chosen because the inertia of the system plays an important role in such cases. Also, Free–free elastic modes of an unconstrained substructure (which are usually encountered by Free Interface method) have zero contribution to EIM as the rigid body modes takes the complete mass and hence, one cannot determine the dynamically important Free-free modes to be chosen in the reduced representation using EIM. A generalization of Effective Mass for the selection of Free-Free modes is proposed in[10]. However, if the acceleration output is of interest then at least modes from a much higher frequency region must be included in the reduced representation. Therefore, further work must be performed to determine an acceptable level of dynamic completeness for Free Effective Mass that would produce a reduced model of acceptable size and accuracy. In the present work EIM measures will be studied only to rank the Fixed Interface normal modes obtained in the Craig-Brampton method.

3.2   Concluding remarks

Free Interface method is more advantageous than Fixed Interface method especially for very complex structures which are modeled experimentally as the experimental mode shapes can be easily obtained for use in the Free Interface method as compared to Fixed Interface method. Residual flexibility matrix includes the contribution of deleted modes and its formulation procedure depends on whether the substructure is Constrained or Unconstrained. For Unconstrained substructures, evaluation of flexibility matrix requires pre removal of rigid body modes and hence these modes are always kept as a dynamic normal mode. A particular formulation of the Free Interface method in which interface or boundary dofs do not appear in the equations of motion of the substructure is presented. This formulation leads to higher degree of model order reduction as compared to the Fixed Interface method. However, this is a less accurate representation as the effects of deleted modes is considered only in quasi-static sense. EIM cannot be used to determine the dynamically important Free-free modes to be chosen in the reduced representation.

Chapter 4

Measures for the selection of Component modes

4.1 Theoretical Formulation

In this chapter, the formulation procedure of Effective Interface Mass (EIM) Measure [8] is introduced. EIM is a more generalized form of Effective Mass and has the advantages of not only appropriately determining the important dynamic modes but also being an absolute measure of dynamic importance. The advantage of an absolute measure is that the structure can be reduced by the most dynamically important modes which achieve a desired fraction of the total Effective Interface Mass (absolute reference) guaranteeing that the reduced representation of the structure will be accurate. The value of this absolute reference can be calculated based solely upon the partitions of FEM mass and stiffness matrices and is totally independent of any eigenvalue solution [8]. Though Effective Mass is also an absolute measure of dynamic importance it has been shown that it ignores some of the very highly dominant modes. Therefore EIM which is a more generalized form of Effective Mass was suggested by Kammer [8]. The drawback of EIM is that it can be effectively used to rank the dynamic importance for only those modes that are constrained by an interface such that there is no rigid body motion [10]. This is because Free–free elastic modes of an unconstrained substructure have zero contribution to Effective Interface Mass as the rigid body modes takes the complete mass and hence, one cannot determine the dynamically important Free-free modes to be chosen in the reduced representation using EIM. A generalization of Effective Mass for the selection of Free-Free modes is proposed in [10], however if the acceleration output is of interest then at least modes from a much higher frequency region must be included in the reduced representation. Further work must be performed to determine an acceptable level of dynamic completeness for Free Effective Mass that would produce a reduced model of acceptable size and accuracy. In the present work Effective Interface Mass measures will be studied only to rank the Fixed Interface normal modes obtained in the Craig-Brampton method. The formulation procedure of Effective Interface Mass is described in the following section and then the formulation procedure of Effective Mass is also described to clarify the reasons of the superiority of EIM over Effective Mass. Further, the extension of EIM for the reduction of interface dofs is proposed.

4.1.1 Effective Interface Mass

The formulation procedure of EIM is discussed in this section as explicitly described by [**8**]. To derive EIM, the substructure is first excited by applying rigid body acceleration excitations successively along each of the interface dofs in turn and due to this excitation the response of the interior generalized coordinates is obtained. Then these interface dofs are constrained to determine the reaction forces acting on them due to the earlier obtained response of the interior generalized coordinates. The dynamic importance of each of the Fixed Interface normal mode is determined by its contribution to these reaction forces at the interface dofs. So, first considering the transformed equation of each of the substructure in generalized coordinates as obtained in the Fixed Interface Method from Eq. (2.25). This is given as below,

$$
\begin{bmatrix} I_{nn} & \Phi_n^T \left(m_{ii}\,\Phi_c + m_{ic} \right) \\ \left(\Phi_n^T \left(m_{ii}\,\Phi_c + m_{ic} \right) \right)^T & m_{cc} + \Phi_c^T \left(m_{ii}\,\Phi_c + m_{ic} \right) + m_{ci}\,\Phi_c \end{bmatrix} \begin{Bmatrix} \ddot{p}_n \\ \ddot{x}_c \end{Bmatrix}
$$
$$
+ \begin{bmatrix} \lambda_{nn} & 0 \\ 0 & k_{ci}\Phi_c + k_{cc} \end{bmatrix} \begin{Bmatrix} p_n \\ x_c \end{Bmatrix} = \begin{Bmatrix} 0 \\ f_c \end{Bmatrix}
\tag{4.1}
$$

It should be noted that in the above representation all the Fixed Interface normal modes are taken. The procedure of selecting the dynamic important modes Φ_k from the complete set Φ_n is determined from the EIM measure and is explained below.

As we are only concerned in determining the dynamic importance of mode shapes, stiffness terms are neglected in both the upper and lower partitions of Eq. (4.1). The upper partition of Eq. (4.1) can therefore be written as below.

$$
\ddot{p}_n = -\Phi_n^T \left(m_{ii}\,\Phi_c + m_{ic} \right) \ddot{x}_c
\tag{4.2}
$$

The right hand of the above equation represents a forcing function. The above equation represents the excitation of the kept generalized coordinates by the acceleration excitations applied at the interface dofs. The coefficient matrix of $\ddot{x}_c$ represents the multiplication factors of these acceleration excitations applied at the interface dofs. The size of the coefficient matrix is ($n \times n_c$), where n is the total number of Fixed Interface normal modes and n_c is the number of the interface dofs. To determine the significant modes by EIM, unit rigid body acceleration excitations are applied successively at each of the interface dofs in turn while

keeping all other interface dofs as fixed (i.e. $\ddot{x}_c = I_{n_c n_c}$). This gives the Modal participation factors of each mode to the rigid body acceleration excitations applied at each of the interface dofs and is defined as below.

$$P = -\Phi_n^T \, (m_{ii} \, \Phi_c + \, m_{ic} \,) = P_{jm} \qquad (4.3)$$

where $j=(1,2,...n)$ and $m=(1,2,...\,n_c)$, The larger the mth entry of the jth row in P_{jm}, the more the jth Fixed Interface normal mode will be significantly excited by the rigid body acceleration applied at m^{th} interface dofs. Now, each of these interface dofs are fixed in the lower partition of Eq. (4.1), which gives the expression of reaction loads at these interface dofs as below.

$$[(\Phi_n^T \, (m_{ii} \, \Phi_c + \, m_{ic} \,))^T] \, \ddot{p}_n = f_c \qquad (4.4)$$

Substituting the value of $\ddot{p}_n$ from Eq. (4.2) in Eq. (4.4), we get

$$-[(\Phi_n^T \, (m_{ii} \, \Phi_c + \, m_{ic} \,))^T] \, [\Phi_n^T \, (m_{ii} \, \Phi_c + \, m_{ic} \,) \,] \, \ddot{x}_c = f_c \qquad (4.5)$$

$$-\bar{\bar{M}}_{eff} \, \ddot{x}_c = f_c \qquad (4.6)$$

where the size of $\bar{\bar{M}}_{eff}$ is ($n_c x n_c$) and ($-ve$) sign represents the opposite reaction forces. The expression of the reaction loads obtained at these constrained interface dofs is in terms of the mass of the substructure as seen along each of the interface dofs where the acceleration excitation is applied. $\bar{\bar{M}}_{eff}$ is obtained from the contribution of each of the Fixed Interface normal modes as can be seen from the Eq. (4.7), where $\bar{\bar{M}}_j$, of size ($n_c x n_c$), gives the contribution of the jth fixed interface normal mode to the complete Effective Interface mass $\bar{\bar{M}}_{eff}$.

$$\bar{\bar{M}}_{eff} = \sum_{j=1}^{n} P_{jm}^T \, P_{jm} = \sum_{j=1}^{n} \bar{\bar{M}}_j \qquad (4.7)$$

As $\ddot{x}_c = I_{n_c n_c}$, any element $\bar{\bar{M}}_{eff}(u,v)$ of $\bar{\bar{M}}_{eff}$ represents the reaction force along the interface dofs corresponding to the uth row due to the rigid body acceleration excitation applied along the interface dofs corresponding to the vth column. $\bar{\bar{M}}_{eff}$ has the contribution from all the Fixed Interface normal modes. Only the diagonal terms of $\bar{\bar{M}}_{eff}$ will be

significant, as they will represent the reaction force along a particular interface dofs when rigid body acceleration excitation is applied along the same interface dofs. Therefore, to determine the contribution of jth Fixed Interface normal mode, all the diagonal terms of $\bar{\bar{M}}_j$ are compared relative to the diagonal terms of $\bar{\bar{M}}_{eff}$. Thus, the contributions of each mode to the total EIM can be used as a criterion to classify the modes and an indicator of the importance of that mode. If for model reduction only k Fixed Interface normal modes are selected, then the diagonal terms of $\bar{\bar{M}}_k$ (see Eq. (4.8)) will represent the interface loads from the contribution of these k Fixed Interface normal modes. The completeness and accuracy of the reduced model can be determined by comparing the diagonal terms of $\bar{\bar{M}}_k$ with that obtained from the complete set of n modes i.e. $\bar{\bar{M}}_{eff}$.

$$\bar{\bar{M}}_k = \sum_{j=1}^{k} P_{jm}^T P_{jm} = P_{km}^T P_{km} \tag{4.8}$$

The main advantage of EIM is that it is an absolute measure of dynamic importance i.e. the terms in $\bar{\bar{M}}_{eff}$ can be obtained without requiring the eigenvalue solution of all the n modes. The expression of $\bar{\bar{M}}_{eff}$ is derived below which contains only the partition of FEM mass and stiffness matrices. This is achieved from the orthonormal properties of Φ_n, i.e. $\Phi_n \Phi_n^T = m_{ii}^{-1}$.

$$\begin{aligned}\bar{\bar{M}}_{eff} &= (m_{ci} + \Phi_c^T m_{ii})\Phi_n \Phi_n^T (m_{ii} \Phi_c + m_{ic}) \\ &= \Phi_c^T m_{ii} \Phi_c + m_{ci} m_{ii}^{-1} m_{ic} + m_{ci} \Phi_c + \Phi_c^T m_{ic}\end{aligned} \tag{4.9}$$

Also, one can develop assurance criteria for the reduced model to have at least, say, 95% of the interface loads as predicted by the full mode FEM representation. This can be used in numerical algorithms to guarantee that the reduced representation will predict the response accurately. As only the diagonal terms of $\bar{\bar{M}}_k$ are of interest, these can also be obtained by taking term by term square of the matrix P_{km} and then summing each of its column to give the corresponding diagonal term of $\bar{\bar{M}}_k$. This is shown as below.

$$Z = P_{km}^{\wedge 2} \tag{4.10}$$

where the sum of the rows in the mth column of Z will give the mth diagonal term of $\bar{\bar{M}}_k$.

For the cases of large number of interface dofs, the size of the Effective Interface Mass matrix will be very large and assuring that the reduced representation accurately (95%) predicts the interface loads at all the interface dofs can be very computationally costly. It should be noted that comparison of the $trace(\bar{\bar{M}}_k)$ with the $trace(\bar{\bar{M}}_{eff})$ can lead to misleading results as it is usually the case that the diagonal elements don't have the same units, e.g. the rotational inertias and mass for rotational and translational interface dofs respectively. Therefore, diagonal terms are separately added for each of the rigid body directions. This can be done by partitioning $\bar{\bar{M}}_{eff}$ as in Eq. (4.11), in which it is assumed that the structure has 3 rigid body directions viz. translational along Z direction, rotation about X axis and, rotation about Y axis. Similarly, Z can also be partitioned as shown in Eq. (4.12). The columns of Z_{Tz}, Z_{Rx} and Z_{Ry} are summed and compared with $trace(\bar{\bar{M}}_{TzTz})$, $trace(\bar{\bar{M}}_{RxRx})$ and $trace(\bar{\bar{M}}_{RyRy})$ respectively. This will give the dynamic importance of each mode along the three rigid body directions.

$$\bar{\bar{M}}_{eff} = \begin{bmatrix} \bar{\bar{M}}_{TzTz} & \bar{\bar{M}}_{TzRx} & \bar{\bar{M}}_{TzRy} \\ \bar{\bar{M}}_{RxTz} & \bar{\bar{M}}_{RxRx} & \bar{\bar{M}}_{RxRy} \\ \bar{\bar{M}}_{RyTz} & \bar{\bar{M}}_{RyRx} & \bar{\bar{M}}_{RyRy} \end{bmatrix} \tag{4.11}$$

$$Z = [Z_{Tz} \quad Z_{Rx} \quad Z_{Ry}] \tag{4.12}$$

4.1.2 Comparison of EIM and Effective Mass

Effective Mass ranks the dynamic importance of modes based upon their contribution to the resultant forces at the substructure's fixed interface when the rigid body input is applied simultaneously at all the interface nodes and successively along each of the rigid body directions in turn. EIM ranks the modes based upon their contributions to the forces individually at each of the interface dofs when the rigid body input is applied along each of the interface dofs in turn. The modal participation factors in Effective Mass are given as in Eq. (4.13), where it is assumed that there are three rigid body directions.

$$P_{Effective\ Mass} = -\Phi_n^T \left(m_{ii}\ \Phi_c + m_{ic} \right) \begin{matrix} \begin{bmatrix} 1 & 0 & 0 \\ 0 & 1 & 0 \\ 0 & 0 & 1 \\ 1 & 0 & 0 \\ 0 & 1 & 0 \\ 0 & 0 & 1 \\ \vdots & \vdots & \vdots \end{bmatrix} \\ \underbrace{}_{N_c\ x\ 3} \end{matrix} \qquad (4.13)$$

Thus, the relation between the modal participation factors of Effective Interface mass in terms of that in the case of Effective Mass can be written as below.

$$P_{Effective\ Mass} = P\ R \qquad (4.14)$$

where,

$$R = \begin{bmatrix} 1 & 0 & 0 \\ 0 & 1 & 0 \\ 0 & 0 & 1 \\ 1 & 0 & 0 \\ 0 & 1 & 0 \\ 0 & 0 & 1 \\ \vdots & \vdots & \vdots \end{bmatrix}$$

From Eq. (4.13) and Eq. (4.14) it can be noticed that the columns of P are added algebraically to obtain the columns of $P_{Effective\ Mass}$ prior to the term by term square. If the contributions are equal in magnitude but opposite in direction along one of the rigid body directions then they would get cancelled when computing the resultant force at interface along the corresponding rigid body direction [**8**]. This makes EIM a more proper measure for the determination of dominant modes to be chosen in the reduced representation.

4.1.3 EIM for Displacement and Velocity output

Generally, larger number of modes are required to be chosen for the reduced system to completely represent the interface forces. If acceleration response is of interest then the reduced system should accurately represent the interface forces, and the dynamically important modes which achieve this can be determined by EIM. Thus, EIM is also called as EIM Acceleration Output. However, if velocity and displacement response is of interest then the reduced system should accurately represent the modal velocity and modal displacement at the interface, respectively, and even a lesser number of modes than determined by the EIM

Acceleration Output can achieve this. In fact, the representation of modal displacement at the interface requires even lesser number of modes than to represent modal velocity at the interface. Thus, EIM was extended and two more measures for ranking the dynamic importance of modes based upon their contribution to the modal velocity or modal displacement at the substructure's fixed interface were derived by Kammer and Triller [**9**]. These measures are termed as EIM Velocity output and EIM displacement output. All these three measures based on EIM individually provides an effective means of selecting the dominant modes for accurately determining the acceleration, velocity or displacement response respectively, and allows a means for the proper reduction of the model.

The modal participation factors for the derivation of EIM Velocity output and Displacement output are given in Eq. (4.15) and in Eq. (4.16) respectively,

$$P_{vel} = \lambda_{jj}^{-1/2} P_{jm} \tag{4.15}$$

$$P_{disp} = \lambda_{jj}^{-1} P_{jm} \tag{4.16}$$

where, λ_{jj} is the matrix with diagonal elements as the eigenvalues of the Fixed Interface normal modes. It should be noted from Eq. (4.15) and Eq. (4.16) that the participation of higher modes will be less for the velocity output and even lesser for the displacement output (due to inverse terms of λ_{jj}). Thus, very few lower frequency modes may be sufficient for the accurate representation of the displacement response. Accurate representation of velocity response will need some more modes but will be lesser than that required for the accurate representation of acceleration response. Thus, appropriate measure should be chosen based on the required output.

Also, the advantage of EIM of being an absolute measure is also preserved in EIM velocity output and EIM displacement output. These expressions are derived below in Eq. (4.17) and Eq. (4.18) by using the orthonormal properties of Fixed Interface normal modes as $\Phi_n \lambda_{nn}^{-1} \Phi_n^T = K_{ii}^{-1}$ and $\Phi_n \lambda_{nn}^{-2} \Phi_n^T = K_{ii}^{-1} M_{ii} K_{ii}^{-1}$ see (from Eq. (4.19)).

$$\begin{aligned} \bar{\bar{M}}_{eff\_vel} &= P^T \lambda^{-1} P \\ &= (m_{ci} + \Phi_c^T m_{ii}) \Phi_n \lambda_{nn}^{-1} \Phi_n^T (m_{ii} \Phi_c + m_{ic}) \\ &= (m_{ci} + \Phi_c^T m_{ii}) K_{ii}^{-1} (m_{ii} \Phi_c + m_{ic}) \end{aligned} \tag{4.17}$$

$$\bar{\bar{M}}_{eff\_disp} = P^T \lambda^{-2} P$$

$$= (m_{ci} + \Phi_c^T m_{ii})\Phi_n \lambda_{nn}^{-2} \Phi_n^T (m_{ii} \Phi_c + m_{ic}) \qquad (4.18)$$

$$= (m_{ci} + \Phi_c^T m_{ii}) K_{ii}^{-1} M_{ii} K_{ii}^{-1} (m_{ii} \Phi_c + m_{ic})$$

$$\lambda_{ii}^2 = (\Phi_n^T K_{ii} \Phi_n)(\Phi_n^T K_{ii} \Phi_n) = \Phi_n^T (K_{ii} M_{ii}^{-1} K_{ii}) \Phi_n \qquad (4.19)$$

4.1.4 Extension of EIM for appropriate reduction of Interface dofs

As described in Chapter 2, in the Fixed Interface method normal modes of the substructure are calculated by fixing all the interface dofs of the substructure. To make the substructures statically complete and to allow for the coupling of the substructures at the interface while maintaining the displacement compatibility, the Fixed Interface kept normal modes are augmented with Constraint modes (static modes). These constraint modes provide a means of a statically complete coupling of the substructures by retaining all their interface dofs in the final transformed/reduced coordinate set. This makes the size of each of the final reduced substructures obtained by the Craig Brampton method as the sum of the number of selected generalized coordinates for the representation of the interior dofs and the number of interface dofs. For very large assemblies of complex structures or in the cases where substructures are coupled with line or surface connections, the size of interface dofs is usually very large as compared to the number of chosen generalized coordinates and thus further effort is required for the reduction of these interface dofs.

Many methods have been proposed which allows a second level reduction of the interface dofs of each of the substructures by representing them in terms of some basis functions calculated in the second level eigenvalue analysis. It should be noted that the first level eigenvalue analysis is already done for the reduction of the interior dofs. The size of these basis functions is very small as compared to the original number of interface dofs and therefore this second level eigenvalue analysis is justified. In this chapter, Characteristic Constraint (CC) modes [13] are chosen as the basis functions for the reduction of the interface dofs of each of the substructures. CC modes are obtained by performing a second level eigenvalue analysis on the partitions of the transformed stiffness and mass matrices of each of the substructures corresponding to the interface dofs. This choice is made because CC modes have basic orthonormality properties of the eigenvectors of the interface dofs which is exclusively used to derive absolute expressions (independent of any eigenvalue solution) of

EIM. Thus, using CC modes as basic functions allows the use of absolute measures like EIM for the proper selection of the dominant ones so that the final reduced system which contains selected Fixed Interface normal modes and CC modes for the representation of interior and interface dofs respectively accurately represents all displacement, velocity and acceleration responses as compared to the full model FEM solution. However, since in the transformed set of equations for each of the substructures, the interface dofs and the Fixed interface normal modes are uncoupled in stiffness (see Eq. (2.25)), CC modes for the unconstrained substructures will also have rigid body modes and that again precludes the use of EIM. Therefore, these CC modes for a particular interface are instead obtained after the coupling of the first level reduced substructures and then performing an eigenvalue analysis on the partitions of stiffness and mass matrices corresponding to the particular interface keeping all other interfaces and generalized coordinates as fixed. So at the coupled substructure level irrespective of whether the individual substructures are constrained or not, if the complete structure is constrained then eigenvalue analysis of the partition of stiffness and mass matrices corresponding to a particular interface will not give any rigid body modes and EIM can be effectively used. These modes obtained at the coupled substructure level are therefore termed as Coupled CC modes and are more advantageous for the reduction of the interface dofs as against to the use of CC modes. The procedure of the reduction of interface dofs by using Coupled CC modes is explained below.

(a) Coupled Characteristic Constraint (CC) modes

The Coupled CC modes are derived from the equation at the coupled substructure level, which is obtained by coupling each of the substructures after a first level of reduction is performed on each of them. This coupled equation is written below for two substructures α and β from Eq. (2.36), where x_c is the common interface between the two substructures and $p_k^{(\alpha)}$, $p_k^{(\beta)}$ are the kept interior generalized coordinates of each of the substructures. It should be noted that all the coupling forces at the interface sum up to zero because of the force equilibrium.

$$
\begin{bmatrix}
I_{kk}^{(\alpha)} & 0 & \bar{m}_{kc}^{(\alpha)} \\
0 & I_{kk}^{(\beta)} & \bar{m}_{kc}^{(\beta)} \\
\bar{m}_{ck}^{(\alpha)} & \bar{m}_{ck}^{(\beta)} & \bar{m}_{cc}^{(\alpha)} + \bar{m}_{cc}^{(\beta)}
\end{bmatrix}
\begin{bmatrix}
\ddot{p}_k^{(\alpha)} \\
\ddot{p}_k^{(\beta)} \\
\ddot{x}_c
\end{bmatrix}
$$

$$
+ \begin{bmatrix}
\lambda_{kk}^{(\alpha)} & 0 & 0 \\
0 & \lambda_{kk}^{(\beta)} & 0 \\
0 & 0 & \bar{k}_{cc}^{(\alpha)} + \bar{k}_{cc}^{(\beta)}
\end{bmatrix}
\begin{bmatrix}
p_k^{(\alpha)} \\
p_k^{(\beta)} \\
x_c
\end{bmatrix}
= \begin{Bmatrix}
0 \\
0 \\
0
\end{Bmatrix}
\tag{4.20}
$$

Coupled CC modes are obtained from the above equation by performing an eigenvalue analysis corresponding to the partitions at the interface dofs, fixing all other kept generalized coordinates as well as dofs at all other interfaces, if present. The eigenvalue equation is written as below,

$$
\left(-\omega_c^2 \left[\bar{m}_{cc}^{(\alpha)} + \bar{m}_{cc}^{(\beta)} \right] + \left[\bar{k}_{cc}^{(\alpha)} + \bar{k}_{cc}^{(\beta)} \right] \right) \psi_c = 0
\tag{4.21}
$$

where ω_c^2 are the eigenvalues of the interface dofs and ψ_c are the coupled CC modes. Again, all these coupled CC modes may not be important and only significant ones, determined from a particular EIM measure, are kept. These selected Coupled CC modes are used to transform the interface dofs as follows.

$$
x_c = \psi_k p_c
\tag{4.22}
$$

where, ψ_k are the selected coupled CC modes. After performing the second level transformation Eq. (4.20) is written as below.

$$
\begin{bmatrix}
I_{kk}^{(\alpha)} & 0 & \bar{m}_{kc}^{(\alpha)} \psi_k \\
0 & I_{kk}^{(\beta)} & \bar{m}_{kc}^{(\beta)} \psi_k \\
\psi_k^{T} \bar{m}_{ck}^{(\alpha)} & \psi_k^{T} \bar{m}_{ck}^{(\beta)} & I_{kk}^{(c)}
\end{bmatrix}
\begin{bmatrix}
\ddot{p}_k^{(\alpha)} \\
\ddot{p}_k^{(\beta)} \\
\ddot{p}_c
\end{bmatrix}
$$

$$
+ \begin{bmatrix}
\lambda_{kk}^{(\alpha)} & 0 & 0 \\
0 & \lambda_{kk}^{(\beta)} & 0 \\
0 & 0 & \lambda_{kk}^{(c)}
\end{bmatrix}
\begin{bmatrix}
p_k^{(\alpha)} \\
p_k^{(\beta)} \\
p_c
\end{bmatrix}
= \begin{bmatrix}
0 \\
0 \\
0
\end{bmatrix}
\tag{4.23}
$$

where,

$$
\psi_k^{T} \left[\bar{k}_{cc}^{(\alpha)} + \bar{k}_{cc}^{(\beta)} \right] \psi_k = \lambda_{kk}^{(c)}
$$

$$\psi_k{}^T \left[\bar{m}_{cc}^{(\alpha)} + \bar{m}_{cc}^{(\beta)} \right] \psi_k = I_{kk}^{(c)}$$

Eq. (4.23) gives the final reduced system which will accurately determine the displacement, velocity, and acceleration responses, but only if proper selection of coupled CC modes is done. The extension of EIM is proposed in the following section to properly select the Coupled CC modes of an interface.

(b) Selection of Coupled CC modes

In this section the extension of EIM is proposed to effectively rank the dynamic importance of the Coupled CC modes of a particular interface relative to the already selected generalized coordinates of all the substructures coupled to this interface at the coupled substructure level. The procedure of ranking the Coupled CC modes is based on their contribution to the forces individually at each of the already selected generalized coordinates for the interior. Such an extension can also be found in [**14**] but they used EIM for ranking the dynamic importance of CC modes (instead of the Coupled CC modes) of a particular interface relative to the already selected generalized coordinates of only the substructure in which the interface is contained at the substructure level. As explained earlier, this could be applicable in only those cases where the all substructures of the system are constrained. Even the example problem that was used in [**14**] to show the extension of EIM for choosing CC modes assumes that both the substructures are constrained. In contrast to this, our approach uses Coupled CC modes in which EIM can be effectively used irrespective of whether the individual substructures are constrained or not. Also, further extension is done to develop two more measures for the effective selection of Coupled CC modes based on their contribution to modal velocity or modal displacement at the interior generalized coordinates.

The philosophy of derivation of a measure based on EIM for the selection of Coupled CC modes of a particular interface relative to the already selected generalized coordinates of the interior is to determine which Coupled CC modes contribute significantly to the loads at each of the interior generalized coordinates of each of the substructure coupled to this interface when the coupled structure is excited through these interior generalized coordinates and then constrained.

After neglecting the stiffness terms, the lower partition of the Eq. (4.23) is given as below.

$$\ddot{p}_c = -\psi_c{}^T \begin{bmatrix} \overline{m}_{ck}^{(\alpha)} & \overline{m}_{ck}^{(\beta)} \end{bmatrix} \begin{bmatrix} \ddot{p}_k^{(\alpha)} \\ \ddot{p}_k^{(\beta)} \end{bmatrix} \tag{4.24}$$

It should be noted that in the above representation all the coupled CC modes are taken for ranking them based on EIM. The above equation represents the excitation of the coupled CC modes of a particular interface by the acceleration excitations applied at the interior generalized coordinates of each of the substructures coupled to this interface. The coefficient matrix represents the multiplication factors of these acceleration excitations applied at these interior generalized coordinates. The size of the coefficient matrix is $(n_c \, x \, (n_{k\alpha} + n_{k\beta}))$, where n_c is the total number of Coupled CC modes at the interface to be truncated, $n_{k\alpha}$ is the number of the already kept interior generalized coordinates of the substructure α and, $n_{k\beta}$ is the number of already kept interior generalized coordinates of substructure β. It should be noted that these already kept generalized coordinates for each of the substructure are selected in the first level reduction as described in section 4.1.1, based on their contribution to the loads at the substructure's interface dofs. Now, the coupled CC modes will be selected based on their contribution to the loads at these already selected generalized coordinates.

To determine the significant coupled CC modes by EIM, unit rigid body acceleration excitations are applied successively at each of the already kept generalized interior coordinates in turn while keeping all others interior coordinates as fixed. Thus,

$$\begin{bmatrix} \ddot{p}_k^{(\alpha)} \\ \ddot{p}_k^{(\beta)} \end{bmatrix} = I_{(n_{k\alpha}+n_{k\beta})(n_{k\alpha+k\beta})}$$

which gives the Modal participation factors of each of the coupled CC mode to the rigid body acceleration excitations applied at each of these interior coordinates as below,

$$P_{Coupled\_CCEIM} = -\psi_c{}^T \begin{bmatrix} \overline{m}_{ck}^{(\alpha)} & \overline{m}_{ck}^{(\beta)} \end{bmatrix} = P_{lk} \tag{4.25}$$

where, $P_{Coupled\_CCEIM}$ are called as modal participation factors of the coupled CC modes. The larger the kth entry of the lth row in P_{lk}, the more the lth Coupled CC mode will be significantly excited by the rigid body acceleration applied at k^{th} interior coordinate. Now, each of these

interior coordinates are fixed in the upper partition of Eq. (4.23) to determine the expression of reaction loads at these interior coordinates.

$$\begin{bmatrix} \bar{m}_{kc}^{(\alpha)} \\ \bar{m}_{kc}^{(\beta)} \end{bmatrix} \psi_c \, \ddot{p}_c = \begin{bmatrix} f_c^{(\alpha)} \\ f_c^{(\beta)} \end{bmatrix} \tag{4.26}$$

Substituting the value of $\ddot{p}_c$ from Eq. (4.24) in Eq. (4.26), we get

$$-\begin{bmatrix} \bar{m}_{kc}^{(\alpha)} \\ \bar{m}_{kc}^{(\beta)} \end{bmatrix} \psi_c \, \psi_c^T \begin{bmatrix} \bar{m}_{ck}^{(\alpha)} & \bar{m}_{ck}^{(\beta)} \end{bmatrix} \begin{bmatrix} \ddot{p}_k^{(\alpha)} \\ \ddot{p}_k^{(\beta)} \end{bmatrix} = f_c \tag{4.27}$$

$$-\bar{\bar{M}}_{eff\_CoupledCCEIM} \, \ddot{x}_c = f_c \tag{4.28}$$

where size of $\bar{\bar{M}}_{eff\_CoupledCCEIM}$ is $(n_{k\alpha} + n_{k\beta} \; x \; n_{k\alpha} + n_{k\beta})$. Similar to $\bar{\bar{M}}_{eff}$, $\bar{\bar{M}}_{eff\_CoupledCCEIM}$ is also obtained from the contribution of each of the coupled CC modes as can be seen from the Eq. (4.29), where $\bar{\bar{M}}_l^c$ gives the contribution of the lth coupled CC mode to the complete Coupled CC mode Effective Interface mass $\bar{\bar{M}}_{eff\_CoupledCCEIM}$. Also, only diagonal terms will be significant due to the similar reasons already explained in the section 4.1.1. Therefore only diagonal elements of $\bar{\bar{M}}_l^c$ needs to be compared with the diagonal elements of $\bar{\bar{M}}_{eff\_CoupledCCEIM}$ to determine the contribution and importance of the lth coupled CC mode.

$$\bar{\bar{M}}_{eff\_CoupledCCEIM} = \sum_{l=1}^{n_c} P_{lk}^T \, P_{lk} = \sum_{l=1}^{n_c} \bar{\bar{M}}_l^c \tag{4.29}$$

The completeness and accuracy of the model reduced by second level truncation to k_c modes can be determined by comparing the diagonal terms of $\bar{\bar{M}}_l^c$ (see Eq. (4.30)) with that obtained from the complete set of n_c modes i.e. $\bar{\bar{M}}_{eff\_CoupledCCEIM}$. To this end, similar procedure as described from Eq. (4.10) to Eq. (4.12) should be used for determining only the diagonal terms of $\bar{\bar{M}}_l^c$ (by taking term by term square of the matrix P_{lk} and then summing each of its column to give the corresponding diagonal term of $\bar{\bar{M}}_l^c$) and for separately adding these diagonal terms for each of the rigid body directions.

$$\bar{\bar{M}}_l^c = \sum_{l=1}^{k_c} P_{lk}^T P_{lk} \tag{4.30}$$

Following the derivation explained in section 4.1.1, one can derive the absolute expressions for coupled CC EIM and is given as below. Similarly, the derivation of $\bar{\bar{M}}_{eff\_CoupledCCEIM}$ can be extended for the velocity and acceleration output. In Chapter 6, these measures will be assessed by applying them to an example plate with the objective of determining accurately determining acceleration, velocity and displacement response as compared to full model FEM solution.

$$
\begin{aligned}
\bar{\bar{M}}_{eff\_CoupledCCEIM} &= \begin{bmatrix} \bar{m}_{kc}^{(\alpha)} \\ \bar{m}_{kc}^{(\beta)} \end{bmatrix} \psi_c \, \psi_c^T \begin{bmatrix} \bar{m}_{ck}^{(\alpha)} & \bar{m}_{ck}^{(\beta)} \end{bmatrix} \\
&= \begin{bmatrix} \bar{m}_{kc}^{(\alpha)} \\ \bar{m}_{kc}^{(\beta)} \end{bmatrix} \begin{bmatrix} \bar{m}_{cc}^{(\alpha)} + \bar{m}_{cc}^{(\beta)} \end{bmatrix}^{-1} \begin{bmatrix} \bar{m}_{ck}^{(\alpha)} & \bar{m}_{ck}^{(\beta)} \end{bmatrix}
\end{aligned} \tag{4.31}
$$

4.2 Concluding remarks

Effective Mass may neglect a set of modes which though are dominant along a particular rigid body direction but have opposite contribution. EIM being a more generalized measure of Effective Mass avoids neglecting any dominant modes. However, appropriate EIM measure should be chosen based on the required output as lesser modes may be sufficient for the accurate representation of the displacement response than that required for the accurate representation of velocity response, which requires even lesser modes than that required for the accurate representation of acceleration response. Extension of EIM is proposed to properly select the Coupled CC modes of an interface. On the lines of EIM, three measures can be derived for the selection of coupled CC modes based on the required output of acceleration, velocity, or displacement response.

Chapter 5

Numerical Assessment of CMS

5.1   Application to dynamic analysis of frame

In this section, the Fixed Interface and Free Interface methods are assessed with regard to the degree of reduction attainable on one hand, and the accuracy that can be achieved on the other hand. For this, an example Fixed-Free frame, as shown in Figure 5.1, is taken. The physical properties of the material of the frame are as follows: density (ρ) *7800 Kg/ m^3*, Young's modulus (*E*) *210 GPa*. The dimensions are: cross sectional area (*A*) *1e-2m^2,* and length (*l*) *6m*.

Figure 5.1: An example Fixed-Free beam

Model reduction techniques are applied on the Finite Element model of a structure. Therefore, the first step is to obtain a Finite Element model of the given frame structure. The frame is discretesized using 1-dimensional linear frame element, which is the combination of a linear bar and a linear beam element. The linear frame element has two nodes at each of its ends. Each node of the frame element has three dofs viz. translation along *x* axis (T_x), translation along *y* axis (T_y), and rotation about *z* axis (R_z). The elemental stiffness and mass matrices for the frame element can be referred from [**27**]. The frame is discretesized into *24* similar *1*-dimensional linear frame elements and therefore, there are *25* nodes and *75* dofs in the complete Finite Element model of the frame. The elemental stiffness and mass matrices of *24* frame elements are assembled together to get the global stiffness and mass matrices of the complete frame structure. The dynamic equation of motion of the system can be described as in Eq. (2.1), where *M* and *K* represents the global mass and stiffness matrices respectively.

Displacement boundary conditions are applied in this equation by fixing the most right end node in all its dofs and then the eigenvalue problem is formed. The first few natural frequencies obtained from the solution of this eigenvalue problem are compared with the exact natural frequencies, which are obtained from the analytical approach and can be referred from [**28**]. The comparison is shown in Table 5.1. Since, the natural frequencies obtained by FEM are in good agreement with that obtained from the analytical approach; therefore all the model reduction results will be compared with only FEM results as from now. The total number of dofs in the Finite element model of the Fixed-Free frame structure is *72*, as *3* dofs got removed due to the application of the boundary condition.

Table 5.1: Comparison of natural frequencies of Fixed-Free frame obtained by FEM and Analytical approach.

Mode No.	Analytical	Full Model FEM. No. of Coordinates=72	Per. Error (%)
1	2.33	2.33	0.00
2	14.59	14.59	0.00
3	40.86	40.86	0.00
4	80.05	80.06	-0.01
5	132.33	132.36	-0.02
6	197.67	197.74	-0.04
7	216.19	216.24	-0.02

In the section 5.1.1 and 5.1.2, the Finite element model of Fixed-Free frame is reduced by the Fixed Interface and Free Interface method respectively. The reduction is performed with two main objectives. First objective is that the reduced model has accurate natural frequencies as compared to the full model FEM in the desired frequency range. Second objective is that the reduced model accurately represents the displacement responses as compared to the full model FEM for a given loading. For both the objectives the selection of modes in both the reduction methods is based on the frequency range in which the natural frequencies are of interest and temporal as well as spatial variation of the applied loads. The effect of including constraint modes and residual attachment modes in properly representing the response due to the applied loads is also studied.

5.1.1 Application of the Fixed Interface method

The Fixed Interface method, as described in Chapter 2, is used to reduce the Fixed-Free frame problem. As per the general steps of performing reduction using CMS (see Section 1.1.1), the Fixed-Free frame is divided into two equal substructures and the dofs of each substructure are partitioned into Interior and coupling degrees of freedom as shown in Figure 5.2. Here the number of substructures in which the frame is divided into is decided arbitrarily as the objective is only to examine the accuracy of the method for a particular degree of reduction. However, for practical cases this decision is based on the problem at hand and engineering judgment. It should be noted from Figure 5.2 that apart from the dofs which share a connection between the two adjacent substructures, dofs corresponding to the free-end and the fixed-end are also taken as coupling dofs. This is because considering these dofs as coupling dofs makes the two structurally identical substructures completely identical in terms of interior and coupling dofs. This gives two major advantages. First, as the two substructures have similar dofs as interior and coupling dofs, the fixed interface normal modes are same for both the substructures and eigenvalue analysis is required to be performed only once. This saves time and also cut down the memory requirements. Second, it gives an opportunity to develop algorithms for performing automated substructuring of the system into as many number of substructures as desired, and then performing automated coupling of these substructures. This, as we will see later in Table 5.3, gives some interesting conclusions.
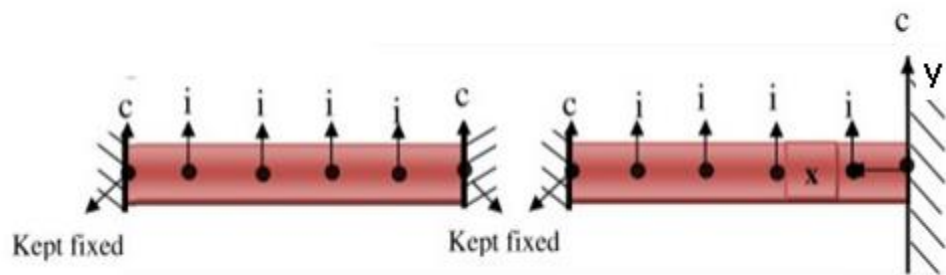
Figure 5.2: Substructuring and partitioning the dofs of Fixed-Free beam in Fixed Interface method

The Fixed Interface normal modes of the substructure are found by fixing the Interface/coupling degrees of freedom, which are represented by *'c'* in Figure 5.2. Then, constraint modes are found corresponding to the coupling dofs of each of the substructure as explained in section 2.1.2. Let's assume that the frequency range of interest is such that it

includes the first five natural frequencies of the complete structure, i.e. *0* to *135 Hz* (see Table 5.1). Since the structure is divided into two completely identical substructures, therefore they have similar Fixed Interface normal modes. The substructure's natural frequencies are given in Table 5.2. As per the thumb rule, the first two modes of each of the substructure are selected as kept modes, as they are the ones which are less than *1.8* times the highest desired frequency of the complete structure i.e. *135* Hz. Finally, the equations of each of the substructure are transformed using these kept mode shapes and the constraint modes shapes and then coupled together to get the reduced order equation of the global system (see Chapter 2 for complete details). The natural frequencies of the reduced order global system are compared with that of the full model FEM in Table 5.2. The total number of coordinates of the reduced system is *10* and the total number of dofs of the full model is *72,* which gives the percentage model reduction as *86.1%*. It can be observed that the natural frequencies of the reduced system are accurate as compared to the full model FEM in the frequency range of interest. It should be noted that in all the following results including this only those natural frequencies are shown of which the corresponding mode shapes correlate well as compared to that of the full model FEM with Model assurance criteria (MAC) [**29**] greater than or equal to *0.95*.

Table 5.2: Comparison of natural frequencies obtained from full model FEM, and Fixed Interface method with 2 substructures.

Mode No.	Full model FEM. Number of dofs =72. Frequency in Hz.	FIXED INTERFACE. No. of Substructures=2		
		Substructures frequencies in Hz. Kept=[1 2]	Coupled Structure frequencies in Hz. No. of Coordinates =10. Percentage model reduction = 86.1%	Per. Error
1	2.33	59.26	2.33	0
2	14.59	163.38	14.59	0
3	40.86	320.4	40.87	-0.02
4	80.06	530.07	80.47	-0.51
5	132.36	793.05	133.26	-0.68
6	197.74	867.26	203.22	-2.7
7	216.24	1110.5	221.79	-2.5

Now, the advantage of similar partitioning of the dofs of each of the substructure is used for developing an algorithm to develop an automated procedure of dividing the structure into as many number of substructures as desired, and then performing an automated coupling of these substructures. Table 5.3 shows comparison of three cases where the Fixed-Free frame is divided into *2*, *3* and *4* identical substructures, and only first mode shape of each of the substructure is kept in all the three cases. Since all the substructures are identical, therefore eigenvalue analysis is required to be performed only once for any one substructure irrespective of the number of substructures in which the structure is divided into. The result shows that by dividing the structure into more number of substructures, more number of natural frequencies of the reduced model are accurate as compared to the full model FEM. However, it should also be noted that by dividing structure into more number of substructures, the size of the reduced system also increases due to increase in the number of coupling dofs, which are retained for the coupling of each of these substructures.

Table 5.3: Comparison of natural frequencies of full model FEM, and model reduced by Fixed Interface method with different number of substructures.

Mode No.	Full Model FEM	CMS- 2 substructures. Kept=1		CMS- 3 substructures. Kept=1		CMS- 4 substructures. Kept=1	
	No. of dofs=72	No. of Coordinates =8		No. of Coordinates =12		No. of Coordinates =16	
		Freq. (Hz)	Per. Error	Freq. (Hz)	Per. Error	Freq. (Hz)	Per. Error
1	2.33	2.33	0.00	2.33	0.00	2.33	0.00
2	14.59	14.61	-0.14	14.59	0.00	14.59	0.00
3	40.86	41.02	-0.39	40.95	-0.22	40.87	-0.02
4	80.06	81.78	-2.15	80.31	-0.31	80.30	-0.30
5	132.36			134.97	-1.97	132.70	-0.26
6	197.74			203.37	-2.85	200.51	-1.40
7	216.24			218.68	-1.13	217.59	-0.62
8	276.23					284.68	-3.06
9	367.86					379.47	-3.16

Thus from the previous paragraph the main objective while performing the model reduction is that the reduced model has accurate natural frequencies in the maximum frequency range with the minimum number of the coordinates in the final reduced system, or maximum percentage reduction. There are mainly two options through which this can be

achieved. First, dividing the complete structure into less number of substructures to keep the size of the final reduced system to minimum, and selecting more number of kept modes for each of these substructures to determine more number of natural frequencies in a larger frequency range. Second, dividing structure into more number of substructures to determine more number of natural frequencies in a larger frequency range, and selecting less number of kept modes for each of these substructures to keep the size of the final reduced system to minimum. To make the comparison that which of the above two options is better, two cases are formed in which the number of coordinates of the final reduced system is kept as same and then it will be determined that which option gives accurate natural frequencies in the maximum frequency range. In the first case, the structure is divided into *2* substructures and first *9* modes of each of the substructure are selected as the kept mode shapes. This case corresponds to the first option mentioned above. In the second case, the structure is divided into *6* substructures and only the first mode of each of the substructure is selected as the kept mode shape. This case corresponds to the second option mentioned above. Both the cases have same number of coordinates in the final reduced system as *24*.
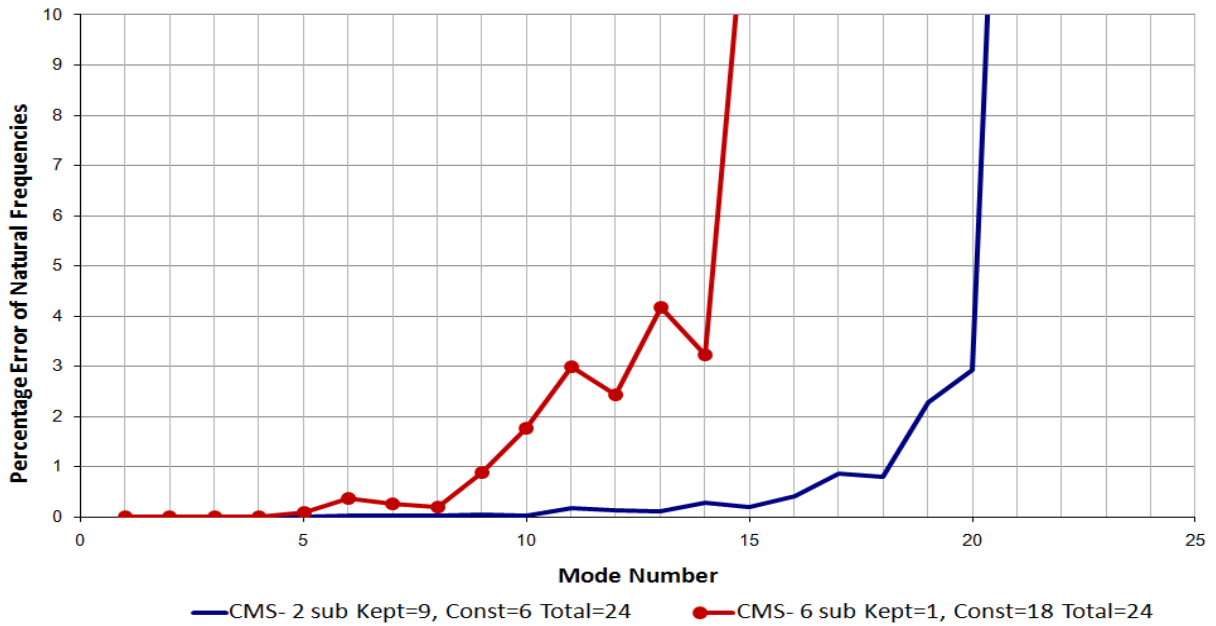
Figure 5.3: Fixed Interface Method: More number of substructures or More number of kept modes.

Figure 5.3 shows the comparison of these two cases. The percentage error of each of the natural frequencies of the reduced model obtained from each case with respect to the natural frequencies of the full model FEM is plotted against their respective mode numbers. It is clear that the first option of dividing the complete structure into less number of

substructures and selecting more number of kept modes for each of these substructures has more number of accurate natural frequencies. This is because in the first case, the final reduced system is mostly populated by the selected normal modes of each of the substructures, where as in the second case, the final reduced system is mostly populated by the static constraint modes. The normal modes perform better as compared to the static modes. However, for very large complex structures, the second option of dividing the structure into more number of substructures is generally better as compared to the first option with regard to the computational time but at the loss of accuracy. This is because it takes less time to perform eigenvalue analysis on several smaller substructures than performing on few larger substructures. Thus, depending on the problem at hand one should make the judgement between the two options.

(a) Effect of Constraint modes:

As described in section 2.1.4, for the case of Forced vibration problem, the mode shapes in the reduced representation should represent both the spatial and the temporal variation of the applied force. The mode shapes are modulated by a time varying function. Consider the reduced system which is obtained by dividing the frame into two substructures, dofs partitioned as shown in Figure 5.2, and having *10* coordinates in the final reduced system. From Table 5.2, it is seen that the natural frequencies of the reduced structure are accurate in the frequency range *0* to *135* Hz. For cases when the system is subjected to a steady-state harmonic excitation it is forced to vibrate or respond at the same frequency as that of the excitation. The response of the linear system can be sufficiently determined by the superposition of its mode shapes. Since for the given reduced system, these mode shapes are accurately determined in the range *0* to *135* Hz, any response varying with frequency in this range can be sufficiently determined by the superposition of the mode shapes corresponding to the natural frequencies in this range. Therefore it can be inferred that the displacement response due to a steady state harmonic excitation with any frequency in this range will be sufficiently determined by the superposition of mode shapes corresponding to natural frequencies in this range. Thus, the temporal variation of force is accounted if it's varying sinusoidally with any frequency in this range. Therefore, a sinusoidal time varying force of *1000*N is applied along *x* axis and *y* axis, and moment of *1000*Nm is applied along rotation about *z* axis of all the nodes at the free end of the Fixed-Free frame. The forcing frequency is chosen to be *60* Hz which is in the range *0* to *135* Hz. The constraint modes completely

represent the applied forces at the coupling dofs in the final transformed coordinates (see Eq. (2.25)). Since the constrained modes are already considered corresponding to all the dofs of the node at the free end where force is applied, the spatial variation of the load is accounted. In Figure 5.4, the spatial displacement obtained from the full model FEM is compared with that obtained from the reduced system. The spatial displacement for the another case, in which the constraint modes are not considered corresponding to the dofs at which force is applied, is also plotted to study the effect of constraint modes. Results conclude that the kept normal mode shapes should be augmented by the constraint modes corresponding to the dofs at which force is applied. It should be noted that one can also obtain accurate response for the case when constraint modes are not considered corresponding to the dofs at which force is applied by keeping more number of normal modes. But for practical cases, it will be difficult to determine that which and how many modes will give the accurate response. Constraint modes on the other hand completely represent the spatial variation of the applied forces in the final reduced coordinates.

The accuracy of the spatial displacement obtained from the reduced system at different forcing frequencies is now studied. The forcing frequency of the applied load is varied from *5* Hz to *215* Hz with an increment of *5* Hz after each iteration. To compare the spatial displacement at different forcing frequencies obtained from the reduced system to that obtained from the full Model FEM following correlation equation is used

$$Correlation = \frac{[\{t_1\}^T\{t_2\}]^2}{[\{t_1\}^T\{t_1\}][\{t_2\}^T\{t_2\}]} \qquad (5.1)$$

where, t_1 and t_2 are vectors representing spatial displacement from full model FEM and reduced system respectively at a particular frequency. This gives an idea that how the two vectors correlate with respect to each other. The Correlation value varies from *0* to *1*, where '*0*' represents no correlation and '*1*' represents exact correlation. In Figure 5.5, the correlation of the spatial displacement, at different forcing frequencies, obtained from the reduced system w.r.t to the full model FEM is shown. As expected the displacement response of the reduced system is in accurate correlation with that of the Full model FEM only when the forcing frequency is in the range *0* to *135* Hz.
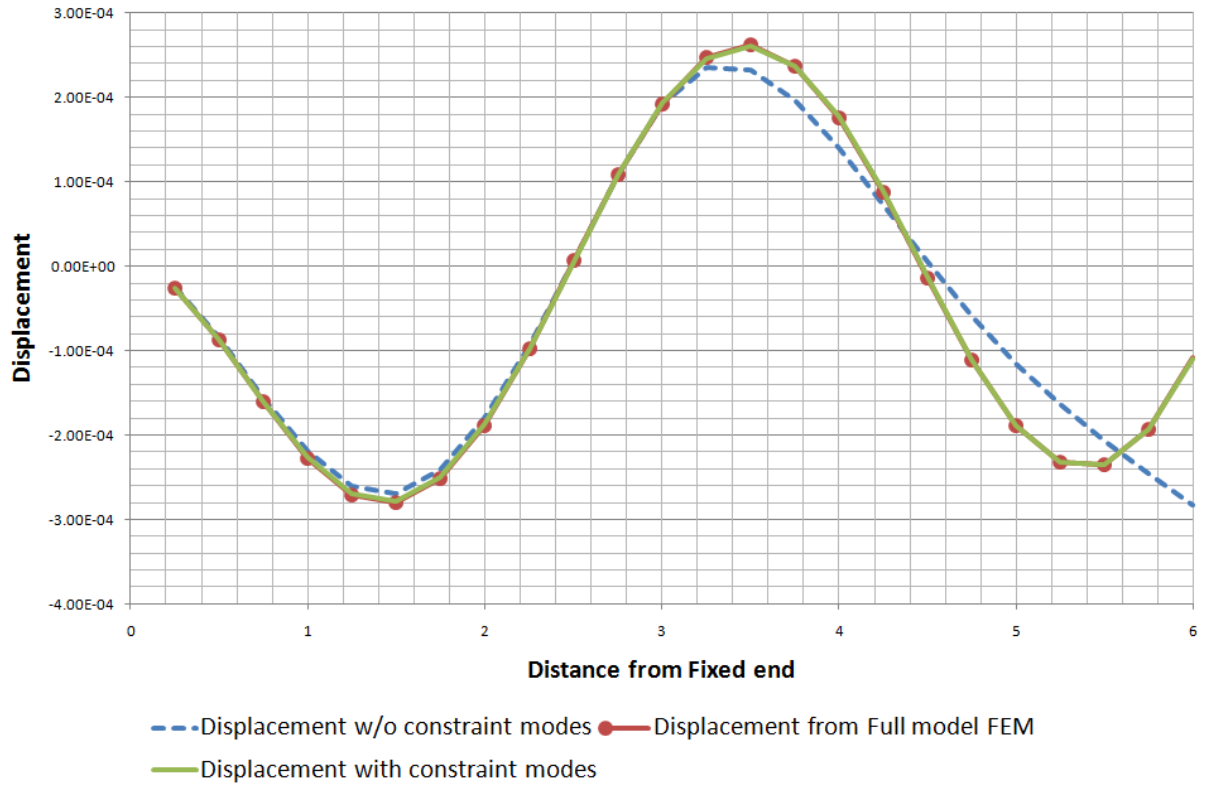
Figure 5.4: Effect of including constraint modes corresponding to the dofs at which force is applied in improving the accuracy of the spatial displacement.

Next, the numerical time integration of the dynamic equation of the motion is performed by using Newmark-beta method with $\beta=1/4$ and $\gamma=1/2$, so that the system is unconditionally stable. Figure 5.6 compares the temporal variation of displacement along direction T_y of the node at free end, obtained from the reduced model with that obtained from the full model FEM, when the forcing frequency is *50* Hz. The time step chosen is *0.002* seconds and total time of simulation is *1* seconds. Result shows that the reduced system performs well as compared to the full model FEM in the given frequency range also in the Transient analysis.
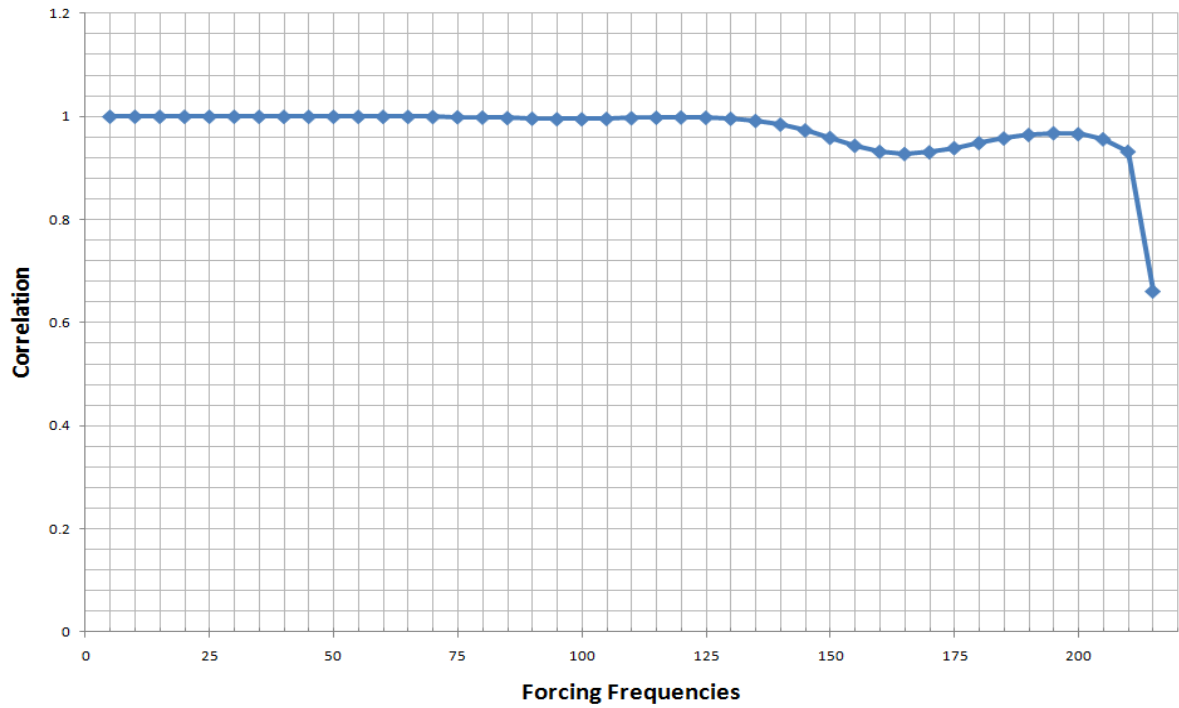
Figure 5.5: Comparison of spatial displacement from Fixed Interface method and FEM at different frequencies.
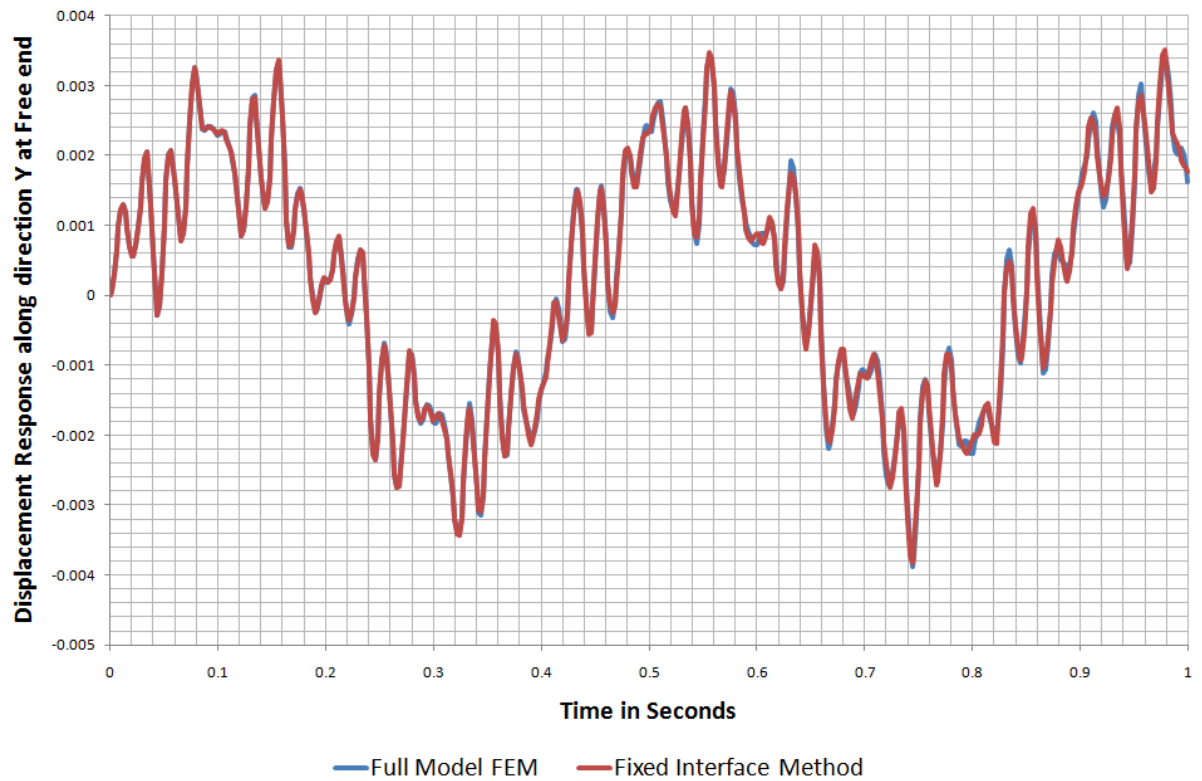
Figure 5.6: Comparison of the temporal variation of response at Free end along Y direction obtained from Fixed Interface method and FEM.

5.1.2 Application of the Free Interface method

The Free Interface method, as described in Chapter 3, is used to reduce the Fixed- Free frame problem. The Fixed-Free frame is divided into two equal substructures and the dofs of each substructure are partitioned into Interior and coupling degrees of freedom as shown in Figure 5.7. As in section 5.1.1 for the case of Fixed Interface method, the dofs are partitioned such that both the substructures are completely identical and similar dofs are chosen as interior and coupling dofs. This again gives an opportunity to develop algorithms for performing automated substructuring of the system into as many number of substructures as desired, and then performing automated coupling of these substructures. Also, eigenvalue analysis need to be performed only once for any one substructure. However partitioning the dofs through this way will make both the substructures unconstrained as shown in Figure 5.7 and therefore, inertia relief residual attachment modes should be calculated corresponding to the coupling dofs for each of the component as described in section 3.1.2(b).
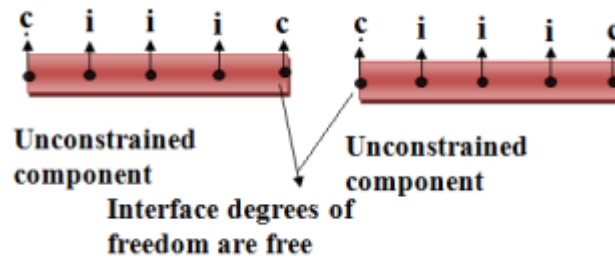
Figure 5.7: Substructuring and partitioning the dofs of Fixed-Free beam in Free Interface method

The Free Interface normal modes of the substructure are found by keeping the Interface/coupling degrees of freedom as free. Let's assume that the frequency range of interest is such that it includes the first eight natural frequencies of the complete structure, i.e. *0 to 285 Hz* (see Table 5.1). The substructure's frequencies obtained are given in Table 5.4. Since each of these substructures is unconstrained, therefore rigid body modes are also present. The first two elastic modes (Mode number 4 & 5) of each of the substructure are selected along with the first three rigid body modes, which are 'must kept modes' for the cases of unconstrained substructures (complete details in section 3.1.2 (b)). Finally, the equations of both the substructure are transformed using these kept mode shapes and the residual modes shapes and then coupled together to get the reduced order equation of global system (see Chapter 3 for complete details). The natural frequencies obtained from this

reduced order global system are compared with FEM in Table 5.4. The total number of coordinates of the reduced system is *16* and the total number of coordinates of the full model is *72,* which gives the percentage model reduction as *77.7%.* The first seven natural frequencies are predicted accurately by the reduced system. Also the 8th natural frequency is fairly accurate. The first five mode shapes which were selected (including rigid body modes) completely fall in the frequency range of interest i.e. *0* to *285* Hz. Therefore, it can be concluded that in the Free Interface method, the substructure's mode shapes only in the frequency range of interest of the complete structure need to be selected, unlike in the Fixed Interface method.

Table 5.4: Comparison of natural frequencies obtained from full model FEM, and Free Interface method with 2 substructures.

Mode No.	Full model FEM. Number of dofs =72.	FREE INTERFACE. No. of Substructures=2		
		Substructures frequencies. Kept=[1 2 3 4 5]	Coupled Structure frequencies. No. of Coordinates =16. Percentage model reduction = 77.7%	Per. Error
1	2.33	0	2.33	0
2	14.59	0	14.591	0
3	40.86	0	40.86	0
4	80.06	59.26	80.06	0
5	132.4	163.38	132.37	0
6	197.7	320.4	197.91	-0.08
7	216.2	530.03	216.29	-0.02
8	276.2	792.88	282.44	-2.24

Table 5.5 shows comparison of three cases where the Fixed-Free frame is divided into *2*, *3* and *4* identical substructures, and only first elastic mode shape of each of the substructure is kept in all the three cases. The result shows that by dividing the structure into more number of substructures, higher natural frequencies can be determined accurately. However, as observed in the case of Fixed Interface method, the size of the reduced system also increases due to increase in the number of coupling dofs, which are retained for the coupling each of these substructures.

Table 5.5: Comparison of natural frequencies obtained from full model FEM, and Free Interface method with different number of substructures.

Mode No.	Full Model FEM	CMS- 2 substructures. Kept=[1 2 3 4]		CMS- 3 substructures. Kept=[1 2 3 4]		CMS- 4 substructures. Kept=[1 2 3 4]	
	Number of dofs =72	No. of Coordinates=14		No. of Coordinates=21		No. of Coordinates=28	
		Freq. (Hz)	Per. Error	Freq. (Hz)	Per. Error	Freq. (Hz)	Per. Error
1	2.33	2.33	0.00	2.33	0.00	2.33	0.00
2	14.59	14.59	0.00	14.59	0.00	14.59	0.00
3	40.86	40.86	0.00	40.86	0.00	40.86	0.00
4	80.06	80.08	-0.02	80.06	0.00	80.06	0.00
5	132.36	133.60	-0.94	132.37	-0.01	132.36	0.00
6	197.74	206.22	-4.29	197.81	-0.04	197.75	-0.01
7	216.24	216.29	-0.02	216.25	0.00	216.24	0.00
8	276.23	287.86	-4.21	278.04	-0.66	276.29	-0.02
9	367.86			373.81	-1.62	368.01	-0.04
10	472.68			496.27	-4.99	475.07	-0.51
11	590.77			611.54	-3.52	596.42	-0.96
12	649.64			651.90	-0.35	650.34	-0.11
13	722.22					736.82	-2.02
14	867.18					910.79	-5.03
15	1025.8					1055.40	-2.89
16	1085.8					1094	-0.76
17	1198.4						
18	1385						
19	1526.7						

As previously done for the Fixed Interface method the effect of number of substructures and kept modes is now examined for the Free Interface method. Two cases are formed in which the number of coordinates of the final reduced system is kept as same. In the first case, the structure is divided into *2* substructures and first *15* elastic modes are selected as the kept mode shapes. In the second case, the structure is divided into *6* substructures and only the first elastic mode is selected as the kept mode shapes. Both the cases have same number of coordinates in the final reduced system as *42*.
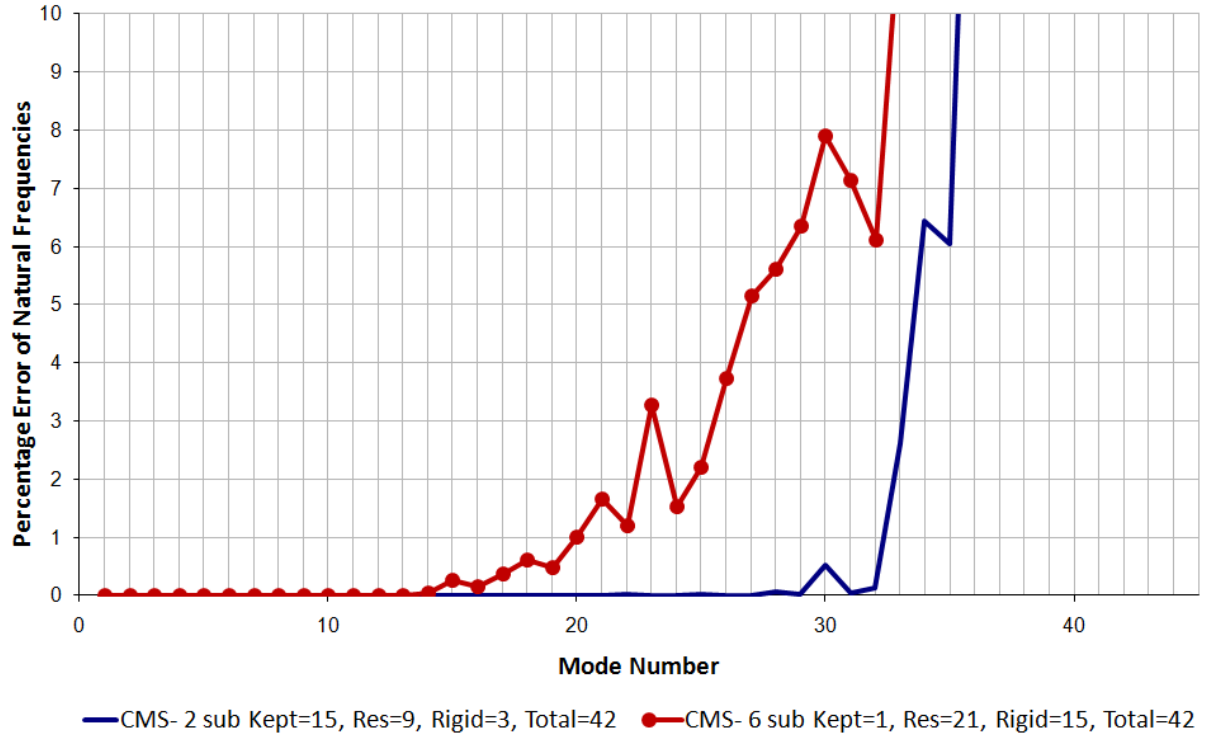
Figure 5.8: Free Interface Method- More number of substructures or More number of kept modes.

Figure 5.8 shows the comparison of these two cases. The percentage error of each of the natural frequencies obtained from each case with respect to the Full model FEM is plotted against their respective mode numbers. As observed in the case of Fixed Interface method, the first option of dividing the complete structure into less number of substructures and selecting more number of kept modes for each of these substructures is better. However, for very large complex structures, the second option of dividing the structure into more number of substructures is generally better as compared to the first option with regard to the computational time.

(a) Effect of Residual modes:

A sinusoidal force of *1000*N is applied along *x* axis and *y* axis, and moment of *1000*Nm is applied along the rotation about *z* axis of all the nodes at the free end of the Fixed-Free frame. Considering the reduced system which is obtained by dividing the frame into two substructures, dofs partitioned as shown in Figure 5.7, and have *16* coordinates in the final reduced system. From Table 5.4, since the reduced structure has accurate natural frequencies in the frequency range *0* to *285* Hz, the temporal variation of force is accounted, if it is varying with time sinusoidally with any frequency or combination of frequencies in the same

range. The spatial variation of the load is also accounted as the residual modes are already considered corresponding to the dofs of the node at the free end, where force is applied. In Figure 5.9, the spatial displacement obtained from the full model FEM is compared with that obtained from the reduced system, when the forcing frequency is *105* Hz, which is in the range *0* to *285* Hz. The spatial displacement for another case, in which the residual modes are not considered corresponding to the dofs at which force is applied, is also plotted to study the effect of residual modes. Results conclude that in the Free Interface method, the kept normal mode shapes should be augmented by the residual modes corresponding to the dofs at which force is applied, as it completely represents the spatial variation of applied forces in the final reduced coordinates. Again, one can also obtain accurate response for the case when residual modes are not considered corresponding to the dofs at which force is applied by keeping more number of normal modes. But for practical cases, it will be difficult to determine that which and how many modes will give the accurate response. Residual modes, like constraint modes, on the other hand completely represent the spatial variation of the applied forces in the final reduced coordinates.

The accuracy of the spatial displacement obtained from the reduced system at different forcing frequencies is now studied. The forcing frequency of the applied load is varied from *5* Hz to *315* Hz with an increment of *5* Hz after each iteration. In Figure 5.10, the modal assurance criteria (MAC) of the spatial displacement, at different forcing frequencies, obtained from the reduced system with respect to the full model FEM is shown. As expected the spatial displacement of the reduced system is in accurate correlation with that of the Full model FEM only when the forcing frequency is in the range *0* to *220* Hz. The response is also fairly correlating with respect to the full model FEM until *285* Hz as expected.

Figure 5.11 compares the temporal variation of displacement along T_y of the node at free end, obtained from the reduced model with that obtained from the full model FEM, when the forcing frequency is *50* Hz. The time step chosen is *0.002* seconds and total time of simulation is *1* seconds. Result shows that the reduced system performs well as compared to the full model FEM in the given frequency range also in the Transient analysis.

Comparing the results of the Fixed and Free Interface method in Table 5.2 and Table 5.4, Free Interface method performs better than Fixed Interface method. It should be noted that in both these cases the structure is divided into same number of substructures and also

same number of elastic modes are considered for each of the substructures. Comparing Figure 5.5 and Figure 5.10 also shows that Free Interface method performs better than Fixed Interface method though the number of substructures and number of elastic modes are same in both cases.
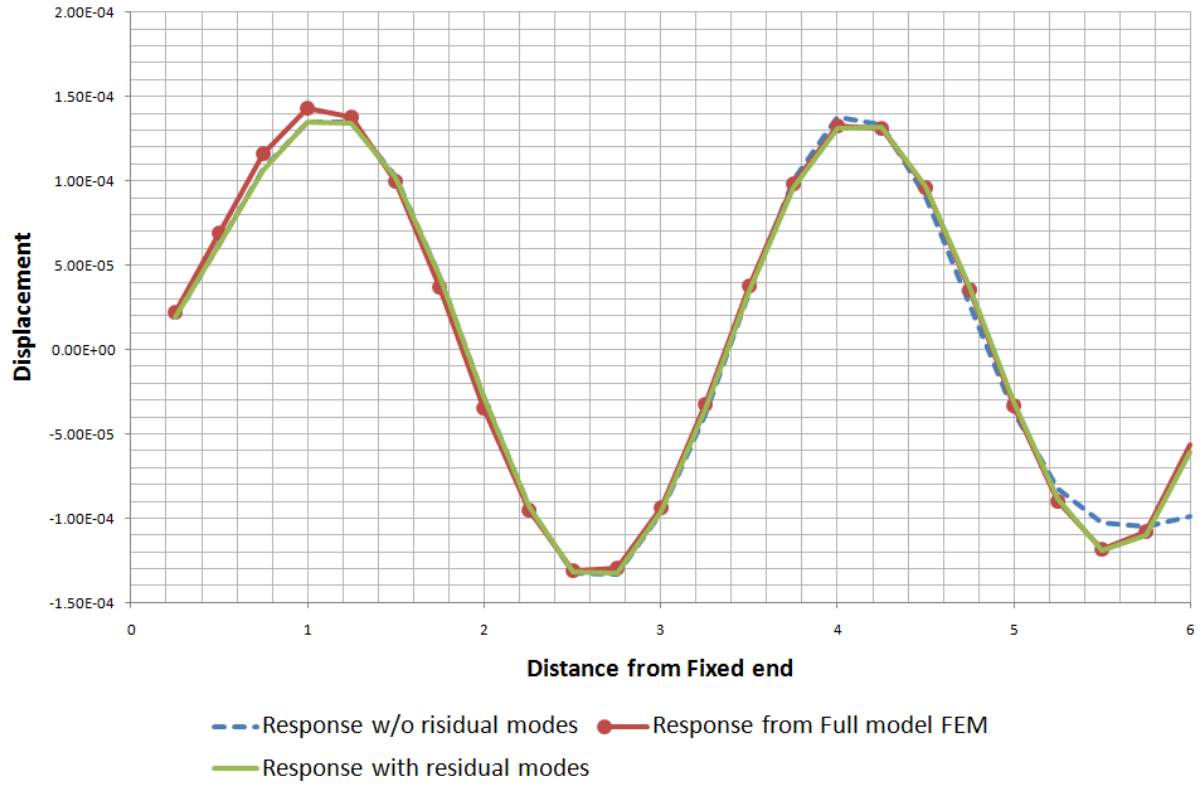
Figure 5.9: Effect of including residual modes corresponding to the dofs at which force is applied in improving the accuracy of the spatial displacement.
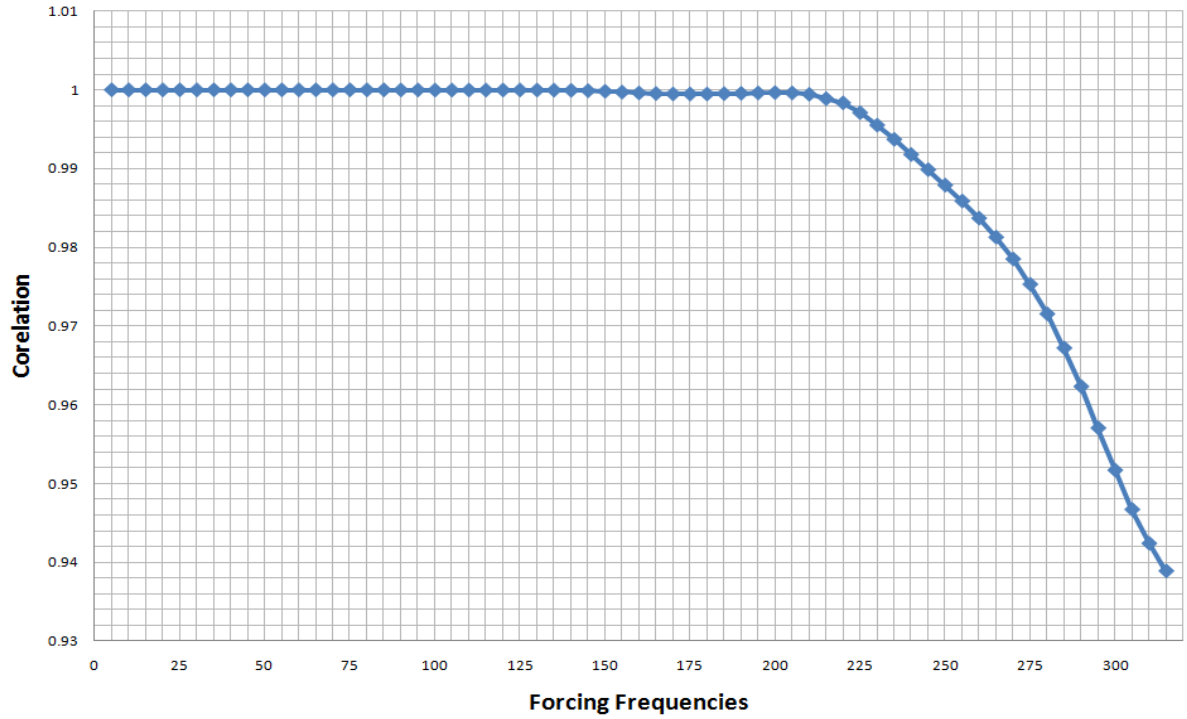
Figure 5.10: Comparison of spatial displacement from Free Interface method and FEM at different frequencies.
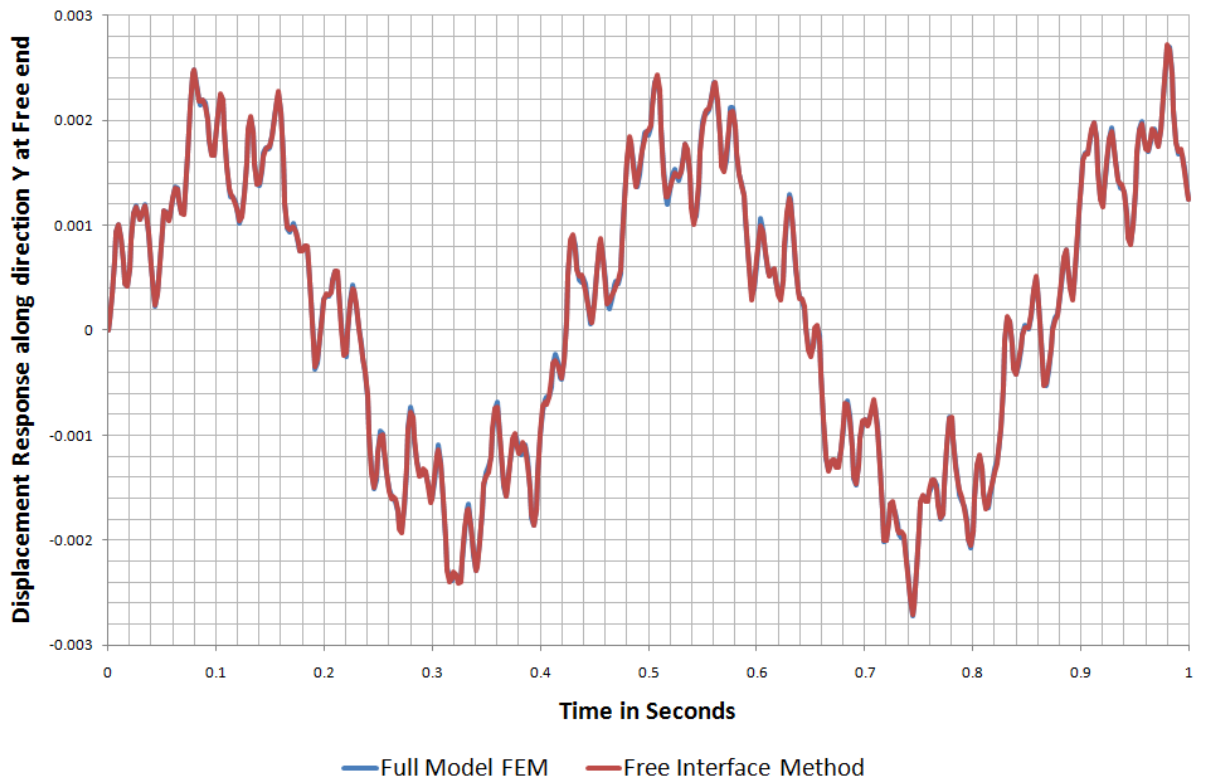
Figure 5.11: Comparison of the temporal variation of response at Free end along direction Z obtained from Free Interface method and FEM.

71

5.2   Application to Dynamic problem of a cracked beam

Structural defects such as cracks are commonly found these days due to long term service of the equipment. These cracks which affect the stiffness and damping properties of the equipment may lead to its structural failure and hence need to be determined. It has been observed that due to presence of crack, natural frequencies of the component gets changed depending upon its location and size. Hence dynamic analysis of these components is a novel method to determine the location and size of cracks.

5.2.1 Motivation for choosing the application

Various researchers have studied the vibration analysis of cracked structures. Gounaris and Dimarogonas [**30**] suggested a finite element method for dynamic analysis of edge cracked beam. Qian *et. al.* [**31**] derived a finite element method of an edged cracked beam and derived the stiffness matrices for a cracked beam element by energy method. Kisa *et al.* [**32**] presented a method of utilizing substructure normal modes to predict the vibration properties of a cracked cantilever beam. They observed that the location and size of crack can be determined by the pattern in which the first few natural frequencies are being affected. Therefore full eigenvalue solution of the structure is not required for this particular application as only the first few natural frequencies are required to be determined to locate the crack in the structure. We have studied in section 5.1.1 and 5.1.2 that Fixed and Free Interface method are techniques which can reduce a system such that it has accurate natural frequencies in the desired frequency range of interest. Thus these methods can be used to accurately determine the first few natural frequencies of the complete model, which are only required to locate the crack in the structure. This can lead to large savings in the computational time. This was the main motivation of solving this problem by both the Fixed and Free Interface method and then comparing them with the full model FEM. This has yet not been done explicitly to the best of our knowledge. Hence we define the problem as follows.

(a) Problem defined:

A cracked cantilever beam of density (*ρ*) *7800* Kg/ m^3, Young's modulus (E) *210* GPa, radius of circular cross (R) *0.1*m and length (l) *1*m is taken and shown in Figure 5.12.

First, the method proposed by Kisa et al. [**33**] of splitting the structure into components at the crack section leading to a substructure approach will be explained. The stiffness matrix of crack modelled from its elastic energy is studied. Then the individual components are coupled together to get the finite element model of the structure. Fixed Interface and Free Interface methods are then used to perform model reduction of the Finite Element model of the cracked beam. The objective is to first compare both the methods in obtaining the natural frequencies of the cracked cantilever beam with regard to the degree of reduction obtainable on one hand and the level of accuracy achieved on the other hand. Later, the natural frequencies of the cracked cantilever beam are calculated while varying the crack location along the length of the beam, and the effect of crack location on its natural frequencies is studied.
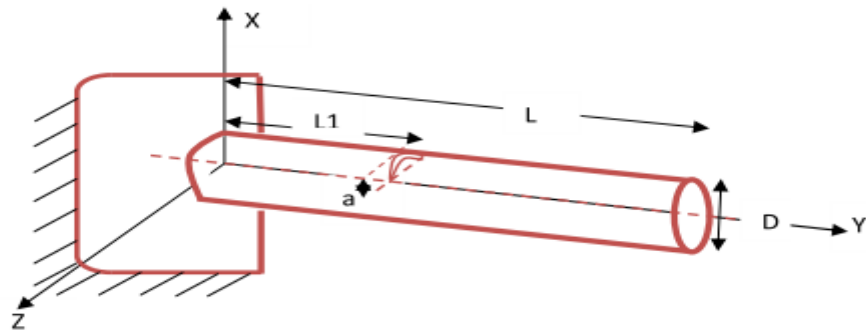
Figure 5.12: A cracked cantilever beam

5.2.2 Substructuring of Cracked beam

The cracked beam is split into substructures as shown in Figure 5.13 where the crack is represented by a mass-less spring. The stiffness of this spring is derived in next section. Each node on the substructure has three degrees of freedom. Substructuring of cracked beam as shown in Figure 5.13 is performed for two basic reasons. First, it provides an opportunity of applying model reduction techniques like Fixed Interface and Free Interface method and thereby reduces the order of the system. Second, the initial non linear system with local non linearity in stiffness at the crack section gets decomposed into linear substructures by splitting the components at the crack section.
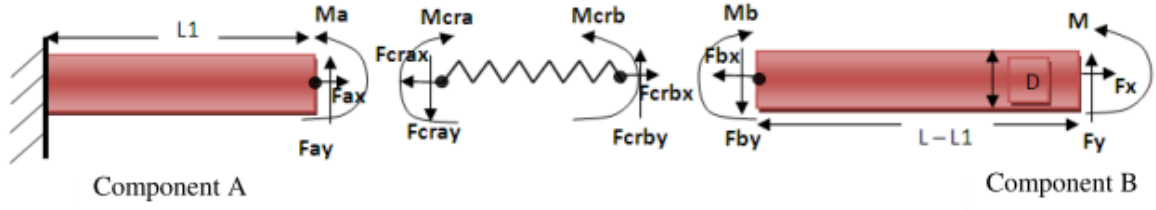
Figure 5.13: Substructuring of cracked cantilever beam

5.2.3 Crack as an element

An important characteristic of the model developed by Kisa et al. [**33**] and briefed below is that it allows discontinuity in the displacement field at the crack section when the crack is open. The crack is modeled by finite elements of zero mass and zero thickness. The compliance matrix of the crack is derived in [**32**] and is given as follows.

$$C = \begin{bmatrix} c_{11} & 0 & c_{13} \\ 0 & c_{22} & 0 \\ c_{31} & 0 & c_{33} \end{bmatrix} \tag{5.2}$$

where c_{11}, c_{22}, c_{13}, c_{31}, c_{33} are the compliance coefficients calculated based on the Linear Elastic Fracture Mechanics theory and Castigliano's theorem. These compliance coefficients are calculated from the non dimensional compliance coefficients c_{11}^{*} , c_{12}^{*} , c_{13}^{*} and c_{33}^{*} as given below. The values of non-dimensional coefficients are read from chart shown in Figure 5.14 for a given crack depth ratio.

$$c_{11} = {c_{11}^{*}}/{E\ pi\ R} \tag{5.3}$$

$$c_{22} = {c_{12}^{*}\ k^{*2}}/{E\ pi\ R} \tag{5.4}$$

$$c_{13} = c_{31} = {c_{13}^{*}}/{E\ pi\ R^2} \tag{5.5}$$

$$c_{33} = {c_{13}^{*}}/{E\ pi\ R^3} \tag{5.6}$$

where k^* is a material constant that depends on the geometry of the beam. For a circular beam it is given as below.

$$k^* = \frac{6(1 + v)}{(7 + 6v)} \qquad (5.7)$$

The inverse of compliance matrix is the stiffness matrix of the nodal points and is given as below.

$$K_{cr} = \begin{bmatrix} C^{-1} & C^{-1} \\ C^{-1} & C^{-1} \end{bmatrix} \qquad (5.8)$$
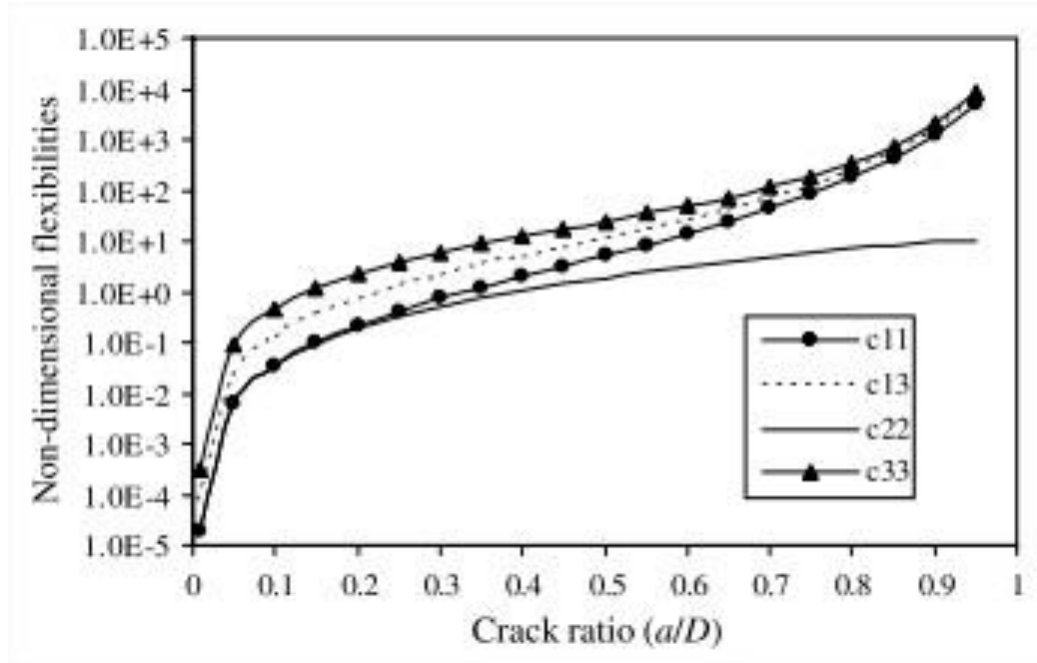
Figure 5.14: Non dimensional compliance coefficients as a function of crack depth ratio a/D [32]

5.2.4 Coupling of Substructures

The combined equation of component A and B with no crack can be written as below.

$$\begin{bmatrix} M_A & 0 \\ 0 & M_B \end{bmatrix} \begin{Bmatrix} \ddot{x}_A \\ \ddot{x}_B \end{Bmatrix} + \begin{bmatrix} K_A & 0 \\ 0 & K_B \end{bmatrix} \begin{Bmatrix} x_A \\ x_B \end{Bmatrix} = \begin{Bmatrix} f_A \\ f_B \end{Bmatrix} \qquad (5.9)$$

where M_A , M_B are the mass matrices, K_A , K_B are the stiffness matrices, f_A , f_B are the force vectors and x_A , x_B are the displacement vectors of component A and B respectively. The

displacement and force vectors are written in terms of their respective values at the crack section.

$$\begin{Bmatrix} x_A \\ x_B \end{Bmatrix} = \begin{Bmatrix} \vdots \\ x_a \\ x_b \\ \vdots \end{Bmatrix}$$

$$\begin{Bmatrix} f_A \\ f_B \end{Bmatrix} = \begin{Bmatrix} \vdots \\ f_a \\ f_b \\ \vdots \end{Bmatrix}$$

(5.10)

where x_a and x_b are displacements of the component A and B respectively, and x_a and x_b are forces of the component A and B respectively at the crack section, The forces exerted on the spring can be written in terms of the stiffness matrix of crack derived in section 5.2.3 and are written as below.

$$f_{cra} = K_{cr} \, (x_{cra} - x_{crb})$$

$$f_{crb} = K_{cr} \, (x_{crb} - x_{cra})$$

(5.11)

where x_{cra} and x_{crb} are displacements at the two nodes A and B of the crack respectively, and f_{cra} and f_{crb} are forces at the two nodes A and B of the crack respectively. Eq. (5.11) can be written in matrix form as below.

$$\begin{Bmatrix} f_{cra} \\ f_{crb} \end{Bmatrix} = \begin{bmatrix} K_{cr} & -K_{cr} \\ -K_{cr} & K_{cr} \end{bmatrix} \begin{Bmatrix} x_{cra} \\ x_{crb} \end{Bmatrix}$$

(5.12)

By invoking compatibility relations at the crack section,

$$\begin{Bmatrix} f_a \\ f_b \end{Bmatrix} = \begin{Bmatrix} -f_{cra} \\ -f_{crb} \end{Bmatrix}$$

(5.13)

$$\begin{Bmatrix} x_a \\ x_b \end{Bmatrix} = \begin{Bmatrix} x_{cra} \\ x_{crb} \end{Bmatrix}$$

(5.14)

From Eq. (5.10) to Eq. (5.14) and applying compatibility equations we get as below.

$$\begin{bmatrix} M_A & 0 \\ 0 & M_B \end{bmatrix} \begin{Bmatrix} \vdots \\ \ddot{x}_{cra} \\ \ddot{x}_{crb} \\ \vdots \end{Bmatrix} + \begin{bmatrix} K_A & 0 \\ 0 & K_B \end{bmatrix} \begin{Bmatrix} \vdots \\ x_{cra} \\ x_{crb} \\ \vdots \end{Bmatrix} = \begin{Bmatrix} \vdots \\ -f_{cra} \\ -f_{crb} \\ \vdots \end{Bmatrix} \tag{5.15}$$

From Eq. (5.15) and Eq. (5.12)

$$\begin{bmatrix} M_A & 0 \\ 0 & M_B \end{bmatrix} \begin{Bmatrix} \vdots \\ \ddot{x}_{cra} \\ \ddot{x}_{crb} \\ \vdots \end{Bmatrix} + \begin{bmatrix} K_A & 0 \\ 0 & K_B \end{bmatrix} \begin{Bmatrix} \vdots \\ x_{cra} \\ x_{crb} \\ \vdots \end{Bmatrix}$$
$$+ \begin{bmatrix} K_{cr} & -K_{cr} \\ -K_{cr} & K_{cr} \end{bmatrix} \begin{Bmatrix} x_{cra} \\ x_{crb} \end{Bmatrix} = \begin{Bmatrix} \vdots \\ 0 \\ 0 \\ \vdots \end{Bmatrix} \tag{5.16}$$

$$\begin{bmatrix} M_A & 0 \\ 0 & M_B \end{bmatrix} \begin{Bmatrix} \vdots \\ \ddot{x}_{cra} \\ \ddot{x}_{crb} \\ \vdots \end{Bmatrix} + \begin{bmatrix} K_{1A} & & 0 & & 0 \\ & 0 & \begin{bmatrix} K_{nA} & 0 \\ 0 & K_{1B} \end{bmatrix} + K_{CR} & 0 \\ & 0 & 0 & K_{nB} \end{bmatrix} \begin{Bmatrix} \vdots \\ x_{cra} \\ x_{crb} \\ \vdots \end{Bmatrix}$$
$$= \begin{Bmatrix} \vdots \\ 0 \\ 0 \\ \vdots \end{Bmatrix} \tag{5.17}$$

where

$$K_{CR} = \begin{bmatrix} K_{cr} & -K_{cr} \\ -K_{cr} & K_{cr} \end{bmatrix} \tag{5.18}$$

$$\begin{bmatrix} M_A & 0 \\ 0 & M_B \end{bmatrix} \begin{Bmatrix} \ddot{x}_A \\ \ddot{x}_B \end{Bmatrix}$$
$$+ \begin{bmatrix} K_{1A} & & 0 & & 0 \\ & \ddots & & & \\ 0 & & K_{nA} + K_{cr} & -K_{cr} & 0 \\ & & -K_{cr} & K_{cr} + K_{1B} & \\ 0 & & 0 & & \ddots \; K_{nB} \end{bmatrix} \begin{Bmatrix} x_A \\ x_B \end{Bmatrix} = \begin{Bmatrix} \vdots \\ 0 \\ 0 \\ \vdots \end{Bmatrix} \tag{5.19}$$

Eq. (5.19) is the coupled equation of the cracked beam and full model FEM solution can be obtained by solving it.

5.2.5 Model reduction

(a) Fixed Interface method

The coupled equation of the component derived in previous section is reduced by Fixed Interface method by transforming the physical degrees of freedom into generalized coordinates as below.

$$\begin{Bmatrix} x_A \\ x_B \end{Bmatrix} = \begin{bmatrix} V_A & 0 \\ 0 & V_B \end{bmatrix} \begin{Bmatrix} p_A \\ p_B \end{Bmatrix} \tag{5.20}$$

where V_A , V_B are the transformation matrices formed by the Fixed Interface method and consist of normal modes as well as constraint modes for substructures A and B respectively. p_A, p_B are the principal reduced coordinates of components A and B respectively. The rest of the procedure of determining natural frequencies is already described in Chapter 2.

(b) Free Interface method

The solution of this problem by Free interface method is more difficult than the Fixed Interface method. Substructuring of the cracked beam problem will lead to constrained components A and unconstrained components C and B as shown in figure Figure 5.15. Residual flexibilities of component A and B can be straight away determined by the procedures described in section 3.1.2. The residual effects in inertia terms are neglected as described in section 3.1.5. This leads to the removal of coupling dofs and achieve even higher level of reduction.
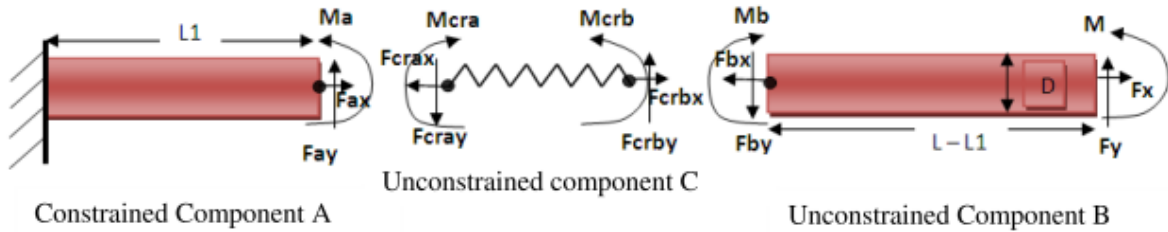
Figure 5.15: Substructuring of the cracked cantilever beam by Free Interface method

5.2.6 Comparison of Fixed and Free Interface results

The full model of cracked beam of length *1*m is discretesized into *10* equal linear beam elements. All the elemental stiffness and mass matrices of the *10* beam elements are assembled together to get the global stiffness and mass matrices of the complete cracked beam structure. There are *11* nodes in the full model and each node has *3* dofs. After application of the boundary condition, there are *30* coordinates in the full model. For solving the problem by Fixed and Free Interface method, the cracked beam is divided at the crack section into two substructures. Each substructure has *5* elements. In both the methods, the dofs at the crack section are only considered as coupling dofs. In each of the method first two modes are selected as kept modes for each of the substructures. In the Fixed Interface method there will be six constraint modes and two normal modes for each substructure in the final reduced system. Thus, the total size of the reduced system in case of Fixed Interface method is *10.* In Free Interface method the rigid body modes corresponding to the unconstrained component B will always be kept, as these are pre removed while calculating the flexibility matrix of the unconstrained component. Since the coupling dofs are further reduced out by neglecting the residual effects in inertia terms (complete details in section 3.1.5), there are two normal modes for each of the substructures and three rigid body modes in the final reduced system. Thus the total size of the reduced system in case of Free Interface method is *7*. The results obtained by solving the cracked beam problem by Fixed and Free Interface method are shown in Table 5.6 and Table 5.7. It can be observed that even though after neglecting the residual effects in inertia terms, the Free Interface method performs equally well with the Fixed Interface method and with a higher level of reduction. Only those modes which correlate well with that of the full model FEM solution are given in both the tables.

Table 5.6: Solution of Cracked beam by Fixed Interface method.

Full model FEM. No. of dofs=30.		Fixed Interface Method. No. of coordinates=10. Percentage model reduction = 66.67%	
No crack	Crack at 0.5m	Crack at 0.5m	
Freq. (Hz)	Freq. (Hz)	Freq. (Hz)	Per error
912.19	886.59	886.65	-0.01
5716.8	5121.3	5146.2	-0.49
8158.8	7948.8	7956	-0.09

Table 5.7: Solution of Cracked beam by Free Interface method and neglecting residual effects in stiffness.

Full model FEM. No. of dofs=30.		Free Interface Method. No. of coordinates=7. Percentage model reduction = 76.67%	
No crack	Crack at 0.5m	Crack at 0.5m	
Freq. (Hz)	Freq. (Hz)	Freq. (Hz)	Per error
912.19	886.59	886.64	-0.01
5716.8	5121.3	5138.8	-0.34
8158.8	7948.8	7957.4	-0.11

Further comparing the Fixed and Free Interface method by keeping the total number of coordinates in the reduced system as same for both cases and then determining that which method performs better. For this, the cracked beam is now discretesized into *20* elements. The total number of coordinates in the full FE model is *60*. The cracked beam is divided at the crack section into two substructures. Each substructure has *10* elements. Total number of coordinates in the final reduced system are kept as constant as *10*. The Fixed Interface method has *6* constraint modes; therefore *4* normal modes can be kept in total for both the substructures so that the size of the reduced system is *10*. The Free Interface method has only *3* rigid body modes and therefore *7* coordinates can be kept in total for both the substructures so that the size of the reduced system is *10*. Thus, the Free Interface method which offers an

advantage of further reducing out the coupling dofs by neglecting the stiffness terms allows selection of more number of normal modes as compared to Fixed Interface method for the same degree of reduction. The results are shown in Table 5.8 for different crack locations. For e.g. when crack is located at *0.1* m from the fixed end then for the case of Fixed Interface method, *6* constraint modes (*'6C'*) appears in the final reduced system, first mode is kept for substructure *A* and first three mode shapes are kept for the substructure *B* to make the size of the final reduced system as *10*. This is represented in short as (*1,6C,3*) for the case of Fixed Interface method. Similarly for the Free Interface method, (*2,3R,5*) represents that first two modes are kept for the substructure *A,* first five modes are kept for substructure *B,* and there are three rigid body modes in the final reduced system. This again makes the size of final reduced system as *10.* It can be observed that even though after neglecting the residual effects in inertia terms, the Free Interface method perform better than the Fixed Interface method for all the different locations of crack. This is because, the Free Interface method offers an advantage of further reducing out the coupling dofs by neglecting the stiffness terms and allows selection of more number of normal modes as compared to Fixed Interface method for the same degree of reduction.

5.2.7 Effect on natural frequencies due to location of crack

Based on the results obtained in Table 5.8, we can observe that the natural frequencies of the cracked beam are lower than those of corresponding full model FEM beam. Because the bending moment is concentrated near the fixed end of the beam, a crack closer to the fixed end will have more effect on the fundamental frequency than a crack closer to the free end. It is evident from Table 5.8 that the first frequency reduction is higher when the cracks are located near the fixed end (at 0.1m). When the crack is located near the midpoint (at 0.5m) then difference is higher in the second natural frequency. The difference in third natural frequency is higher when the crack is near the ¾ of beam length (at 0.7m). When the crack is located near the free end, the first natural frequency is almost unaffected. Thus, by observing the pattern in the variation of natural frequencies, we can get a rough idea of the crack along the beam. However, being given the mode shape of the cracked beam and determining the accurate location of the crack along the length of the beam is the inverse problem.

Table 5.8: Comparison of solution of cracked beam by Fixed and Free interface method

	No crack	Crack at 0.1m					
Mode No.	Full model FEM.	Full model FEM	% difference Full model	Fixed (1,6C,3)	Free(2,3R,5)	% error Fixed Interface	% error Free Interface
1	912.19	778.26	14.68	778.26	778.26	0.00	0.00
2	5716.8	5425.3	5.10	5431.2	5425.3	-0.11	0.00
3	8158.8	7762.3	4.86	7765.4	7767.2	-0.04	-0.06
4	16011	15723	1.80		15727		-0.03
	No crack	Crack at 0.5m					
Mode No.	Full model FEM	Full model FEM	% difference Full model	Fixed (2,6C,2)	Free(4,3R,3)	% error Fixed Interface	% error Free Interface
1	912.19	886.59	2.81	886.65	886.59	-0.01	0.00
2	5716.8	5121.2	10.42	5146.2	5122.1	-0.49	-0.02
3	8158.8	7943	2.64	7951	7945.8	-0.10	-0.04
4	16011	15909	0.64		15918		-0.06
	No crack	Crack at 0.9m					
Mode No.	Full model FEM	Full model FEM	% difference Full model	Fixed (3,6C,1)	Free(6,3R,1)	% error Fixed Interface	% error Free Interface
1	912.19	912.1	0.01	912.14	912.09	0.00	0.00
2	5716.8	5701	0.28	5703.4	5701.1	-0.04	0.00
3	8158.8	8140.4	0.23	8165.2	8140.7	-0.30	0.00
4	16011	15741	1.69	15816	15753	-0.48	-0.08

5.3 Application to dynamic analysis of car axle

In Section 5.1 and 5.2, Fixed and Free Interface methods are extensively studied and it is shown that both the methods give appropriate reduced system which not only has accurate natural frequencies but also gives accurate displacement responses in the desired frequency range of interest as compared to the full model FEM solution. However, yet the reduction in computational time achievable by both of these methods is not highlighted so far. The reduction in computational time can be better examined by applying these techniques for the

reduction of large structures and then assess the reduction in time that can be achieved by these methods in obtaining the solution as compared to full model FEM solution. For this, both of these methods are applied to perform the reduction of car axle.

The finite element model of the axle is already at hand as shown in Figure 5.16 (Courtesy: Volkswagen Gmbh). The axle is modeled by various different types of elements- 4-noded shell elements, 3-noded shell elements, 8-noded solid elements and 6-noded solid elements. Various sets of elements are defined corresponding to different parts of the axle as shown in the Figure 5.16 i.e. axle tap, spring cups, bearing seating, torque tube, weldment and trailing arm. These element sets have different section definitions. The physical properties of the material of axle are: density (ρ) $7.85e^{-9}$ Kg/ mm^3, Young's modulus (E) 210000 N/ mm^2, and Poisson's ratio 0.3. The total number of dofs in the full FE model of car axle is 220971, which is fairly large. This gives an opportunity to appropriately reduce the coordinates of axle such that the reduced model has accurate natural frequencies in the desired frequency range of interest as compared to the full model FEM solution. This reduced model can be used to perform further dynamic or transient analysis and will lead to huge savings in the computational time.
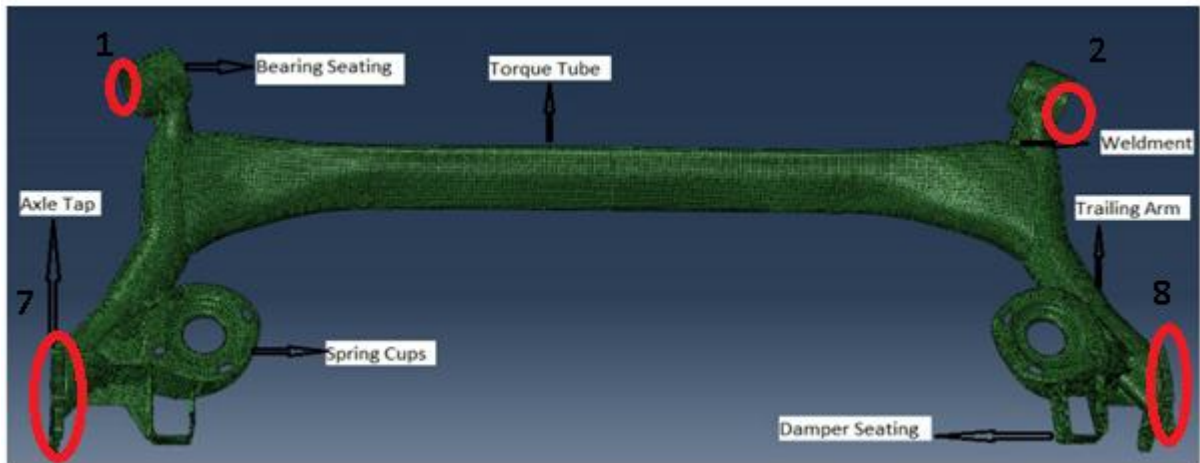
Figure 5.16: Finite Element model of car axle. Courtesy: Volkswagen Gmbh

5.3.1 Model Reduction by Fixed Interface and Free Interface methods

(a) Substructuring:

Many commercial software packages like ABAQUS [34], ANSYS [35], have already implemented the Fixed Interface method as it is widely used in the industry due to its very

simple and effective formulation. ABAQUS is a powerful package which is used widely in the structural dynamics industry for applying advanced methods to the real engineering problems. The version 6.11 of ABAQUS is used in this work. The first step in performing model reduction by Fixed Interface and Free Interface methods is to divide the axle into substructures. In the recent version of ABAQUS, various parts of an assembly can be used as substructures. But it was found that a feature of dividing a single part (as the car axle) into its substructures is not available and therefore substructuring is done manually in MATLAB [36] by partitioning the stiffness and mass matrices corresponding to their substructures. Axle is divided into five substructures as shown in Figure 5.17 and are termed as they appear in figure from left: left trailing arm, left weld, torsion tube, right weld, and right trailing arm. Left weld is a weldment which connects left trailing arm with the torsion tube in the complete car axle model. Similarly, right weld connects the torsion tube and right trailing arm. The weldments are separated as individual substructures for the future objectives of the research group in updating the weldment because of large uncertainty involved in its modeling. This is also an advantage of CMS where those parts which need to be updated can be separated as a substructure and once they are modified using experimental data they can be coupled together with the complete substructure. To partition the stiffness and mass matrix corresponding to the individual substructures all node and element definitions of the complete axle model are written out from ABAQUS on a text file. All node and element numbers corresponding to each of the substructures are separately written. These node and element numbers of each of the substructure are used to find out the node and element definitions of each of the substructures. Similarly, various section and material definitions of different type of element sets in each of the substructures are also found out. All the node, element, section, and material definitions of each of the substructures are given as input to the ABAQUS for generating the stiffness and mass matrix of each of the substructures. MATLAB is used for finding out the node and element definitions of each of the substructures by referring through their respective node and element numbers to the node and element definitions of the complete axle model.
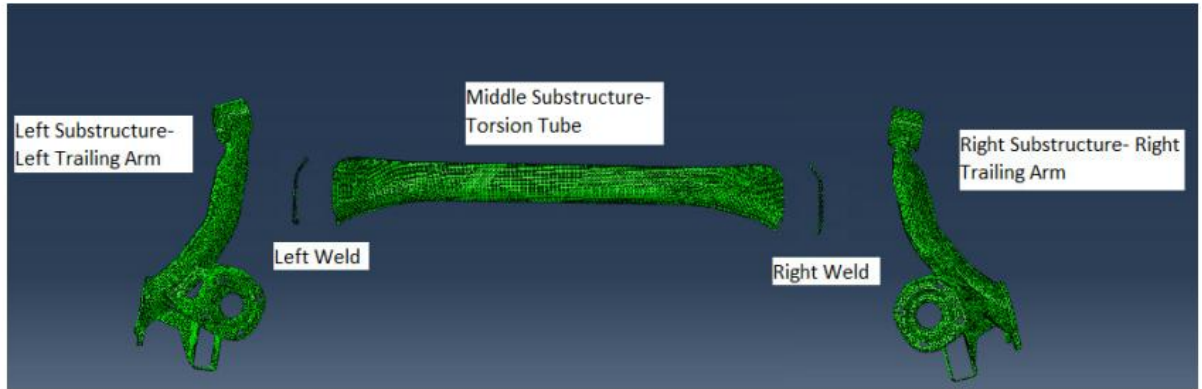
Figure 5.17: Substructuring of car axle

(b) Partitioning the dofs:

The dofs of each of the substructures are partitioned as shown in Figure 5.18. The connections of each of the substructures with the adjacent substructures are taken as coupling dofs and all remaining are taken as interior dofs. The coupling dofs are highlighted as red in the below figure.
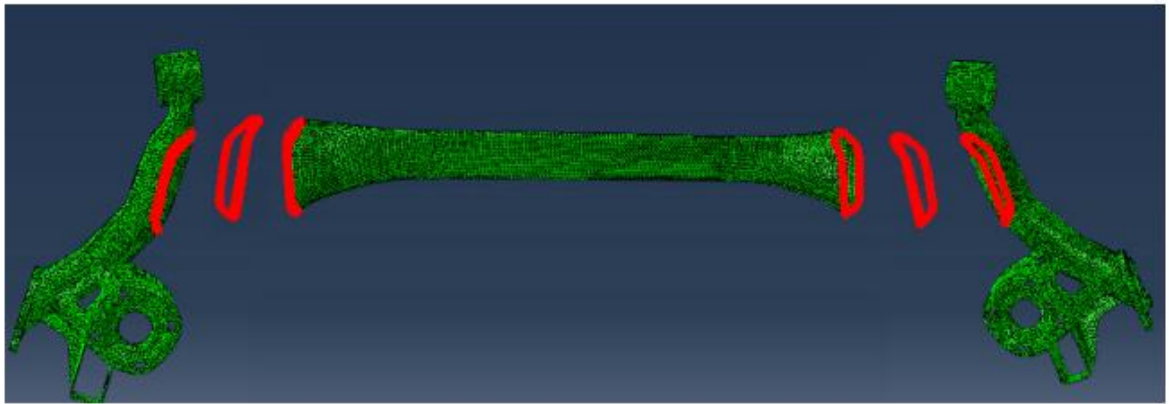
Figure 5.18: Partitioning the dofs of each of the substructures

(c) Application of the Fixed Interface Method:

The Fixed Interface method works well in ABAQUS. The weldments are kept as full model because a large uncertainty is involved in their modeling and they are to be updated in the future objectives of the research group. Therefore only left trailing arm, right trailing arm and torsion tube are reduced. Fixed Interface normal modes and constraint modes are obtained for each of these substructures. For each of the substructures *15* Fixed Interface normal modes

are selected as kept modes. Each of the substructures is reduced through their kept normal and constraint modes and then are coupled together with the full model of weldment to get the reduced system of the axle (complete theoretical details in Chapter 2). The number of coordinates in the full model and the reduced model of each of the substructure are given in Table 5.9. For left trailing arm as well as right trailing arm there are *612* couplings dofs additional to *15* kept normal modes. Similarly for torsion tube there are *612* coupling dofs on each of its end and therefore total *1224* dofs as coupling dofs additional to the *15* kept normal modes. Each of the weldments only has *612* dofs on each of its side for coupling with the trailing arms and torsion tube. After coupling of all the substructures the total number of coordinates in the reduced system is *2493*. The natural frequencies of this reduced system are shown in Table 5.10. It can be observed that the first *24* natural frequencies of the reduced model are in good accordance with respect to the full model FEM results. The first six rigid body modes are not shown in the table.

Table 5.9: Number of coordinates of each of the substructures before and after reduction.

	Right Sub	Middle Sub	Left Sub
Full Model. Number of dofs	80019	140952	80019
After Reduction (15 kept modes). Number of Coordinates	627	1239	627

(d) Application of the Free Interface Method:

It is already shown in the section 5.1 and 5.2 that the Free Interface method performs well as compared to the Fixed Interface method. Therefore it is of interest to perform the reduction of car axle also by the Free Interface method and then compare the results obtained with the Fixed Interface method. However, it was found that algorithms for the determination of the inertia relief residual modes of an unconstrained component in the Free Interface method are inappropriately programmed in ABAQUS. Therefore, the Free Interface method was programmed in MATLAB for performing the reduction of car axle.

The first step is to obtain the stiffness and mass matrices of each of the substructure from ABAQUS. These matrices are written out from ABAQUS on a text file and then imported in MATLAB. But ABAQUS writes the stiffness and mass matrices in its own sparse

format. Also it was important to store these matrices in the sparse format which MATLAB understands to reduce the storage requirements. Therefore, these matrices are converted from the sparse format of ABAQUS to the sparse format of MATLAB. Now these stiffness and mass matrices of each of the substructure are used to find their respective Free Interface normal and residual modes. It should be noted that the procedure of calculating the residual modes involves many arithmetic operations which may lead to "Out of Memory" and "Memory leakage" issues in MATLAB. Therefore such operations should be performed in multiple steps keeping in mind that any operation should not exceed the RAM usage above its limits. The properties of the system which was used to perform the computation is as follows: Processor-Intel Xeon E5450, Processor speed- *3.00* GHz x *8* CPU, RAM- *63.1* GB.

As in Fixed interface method, first *15* modes are kept as the normal modes. As no boundary condition on the axle is considered, all the substructures are unconstrained substructures. Therefore *6* rigid body modes are kept for each of the substructures along with the *15* kept normal modes. The residual modes, rigid body modes and kept normal modes are used to reduce each of the substructures. Each of these substructures are then coupled together to get the reduced system of axle. The natural frequencies of this system reduced by Free Interface method are given in Table 5.10. The percentage error of the natural frequencies of the system reduced by Fixed Interface and Free Interface are obtained with respect to the full model FEM solution and is shown in Table 5.10. As expected, Free Interface method performs better as compared to the Fixed Interface method. The first *32* natural frequencies of the reduced model are in good accordance with respect to the full model FEM results.

Table 5.10: Comparison of natural frequencies obtained from reduction by Fixed Interface and Free Interface method to the full model FEM solution

Mode No.	Full Model No of dofs=220971	Free Interface.15 modes per sub. Reduction=98.86%. No of coordinates=2511		Fixed Interface. 15 modes per sub. Reduction=98.87%. No of coordinates=2493	
		Freq. (Hz)	Per. Error	Freq. (Hz)	Per. Error
7	29.95	29.95	0.00	29.95	0.00
8	124.24	124.24	0.00	124.25	-0.01
9	168.87	168.87	0.00	168.91	-0.02
10	275.79	275.81	-0.01	276.87	-0.39
11	326.61	326.61	0.00	327.32	-0.22
12	377.42	377.42	0.00	377.58	-0.04
13	388.74	388.75	0.00	388.88	-0.04
14	401.63	401.63	0.00	401.63	0.00
15	440.73	440.82	-0.02	444.55	-0.87
16	502.46	502.51	-0.01	503.64	-0.23
17	572.16	572.22	-0.01	573.26	-0.19
18	586.6	586.71	-0.02	588.57	-0.34
19	588.68	588.77	-0.02	589.61	-0.16
20	621.43	621.49	-0.01	623.04	-0.26
21	642.49	642.6	-0.02	644.22	-0.27
22	754.67	758.87	-0.56	757.53	-0.38
23	792.86	793.14	-0.04	793.5	-0.08
24	807.8	808.24	-0.05	822.9	-1.87
25	884.6	889.28	-0.53		
26	919.19	923.77	-0.50		
27	988.67	997.45	-0.89		
28	994.13	997.92	-0.38		
29	995.95	1028.8	-3.30		
30	1041.6	1056	-1.38		
31	1062.5	1075.4	-1.21		
32	1072.7	1085.7	-1.21		

(e) Time considerations:

Table 5.11 shows the time involved in performing the reduction of each of the substructures and in performing the coupling of each of these substructures together to get the global reduced system. These time are CPU-time, which is the time actually required by the processor to complete the operation. The time involved in the reduction involves calculation of the eigenvalues, calculation of residual/constraint modes and finally transforming the equations of each of the substructure in to reduced coordinates. The time as taken by Fixed Interface Method in ABAQUS, Free Interface method in MATLAB are given in the Table 5.11. Fixed Interface method was also programmed in MATLAB to actually compare with the Free Interface method on similar grounds. It can be observed that most of the time is involved in the coupling of each of the substructures together. The time taken for performing the reduction is considerably large for middle substructure as compared to the right and left substructure. This is because of the larger no. of coordinates in the middle substructure as compared to the right and left substructure.

Table 5.11: Time taken in Reduction by Fixed Interface and Free Interface method

Method Type	Time taken			
	Reduction of Right Sub	Reduction of Middle Sub	Reduction of Left Sub	Coupling of Substructures
Fixed Interface ABAQUS	1.44mins	9mins	1.41mins	8.13mins
Free Interface MATLAB	1.37mins	7.08mins	1.37mins	13mins
Fixed Interface MATLAB	1.54mins	7.28mins	1.48mins	12.52mins

A simple static analysis is performed ten times with loads changing in each time. Boundary conditions are applied on the nodes of left and right bearing seating, and left and right axle tap. These locations are shown in Figure 5.16 as *1, 2, 3* and *4*. The boundary conditions are applied such that i) all the nodes at location *1* are fixed along *x*, *y*, and *z* axis ii) all the nodes at location *2* are fixed along *x*, and *z* axis iii) all the nodes at location *7* are fixed along *z* axis. A force of *100*N is applied at location *8* along *z* axis. Ten iterations are performed in which the load is changed by *100*N in each iteration. Static displacement obtained at location *8* along *z* axis at the end of the tenth iteration is noted from the full model FEM and the reduced system, and is found to be same as *42.8* mm. The time taken in

ABAQUS by the system reduced by Fixed Interface method is compared to that obtained from full model FEM solution as shown in Table 5.12. It can be observed that the reduced system completes the simulation in very less computational time as compared to the full model FEM solution. Thus CMS is expected to give even larger reduction in computational times when large number of iterations is involved like transient analysis, modification analysis and optimization.

Table 5.12: Time taken by full model and reduced model in performing multiple static analysis

Static Analysis	Full Model. No. Of Coordinates=220971	Reduced Model. No. Of Coordinates=2493
Time	13 minutes	33 Seconds

Chapter 6

Numerical Assessment of Measures for Selection of Component modes

6.1   Application to Fixed-Free Plate

The key to model reduction is to be able to determine the dynamically important modes that should be kept in the reduced representation so that the reduced system gives accurate responses as compared to the full model FEM solution. Measures based on Thumb rule, Effective Mass and Effective Interface Measure (EIM) are discussed in Chapter 4 for determining the dynamically important modes. In this section, it will be numerically shown that the Thumb rule and Effective Mass measure fails in determining the significant modes as the reduced system obtained by keeping the modes determined as significant by these measures doesn't give accurate responses as compared to the full model FEM solution. It will also be shown that Effective Interface Mass (EIM) measure is the only measure, as compared to Thumb rule and Effective Mass measure, which appropriately determines all the significant modes and the reduced representation obtained by keeping these significant modes give accurate response as compared to the full model FEM solution. EIM generally gives large number of modes which are actually required for accurately determining the acceleration response. For accurate determination of velocity and displacement response such a large number of modes are not required and even a lesser number of modes than determined by the EIM can achieve this. The two extensions of EIM i.e. EIM Velocity output and EIM displacement output (see section 4.1.3 for complete details) for determining the significant modes required in the reduced representation to obtain accurate velocity and displacement response respectively are also shown to perform very well. EIM is also called as EIM acceleration output as it determines modes required for the accurate representation of acceleration response. All these three measures based on EIM viz. EIM acceleration output, EIM velocity output, and EIM displacement output individually provides an effective means of selecting the dominant modes for accurately determining the acceleration, velocity or displacement response respectively and allows a means for the proper reduction of the model.

It should be noted that in this work the Effective Mass measure and EIM are assessed only to rank the dynamically important Fixed Interface normal modes obtained in the Fixed Interface method and they cannot be used to determine the dynamically important Free-Free modes. This is because the Free-Free modes have zero contribution to Effective Mass and also EIM. The use of EIM is further extended to effectively rank the dynamic importance of the Coupled CC modes of a particular interface relative to the already selected significant Fixed Interface normal modes of all the substructures coupled to this interface at the coupled substructure level. The procedure of ranking the Coupled CC modes is based on their contribution to the forces individually at each of the already selected generalized coordinates for the interior.

To assess EIM and Effective Mass measures, an example Fixed-Free plate, as shown in Figure 6.1, is taken. The physical properties of the plate are as follows: density (ρ) *7800 Kg/ m^3*, Young's modulus (*E*) *210 GPa*, length (*l*) *6m*, width (*w*) *3m* and depth (*h*) *0.1m*. The structure is reduced by the Fixed Interface method. In Fixed Interface method, few selected Fixed Interface normal modes and constraint modes are used to transformation the physical dofs into reduced coordinates. The reduced system will give accurate response only if all the dynamically important Fixed Interface normal modes are selected in the reduced representation. The dynamically important Fixed Interface normal modes are determined through three measures Thumb rule, Effective Mass, and Effective Interface Mass Measure. The displacement, veloctiy, and acceleration response obtained from the system reduced by the Fixed Interface kept normal modes selected through each of these measures are compared to the full model FEM solution. It will be shown that Effective Interface Mass is the most appropriate measure as the system reduced by the modes selected through this measure accurately determines the acceleration, velocity, and displacement response as compared to the full model FEM solution.
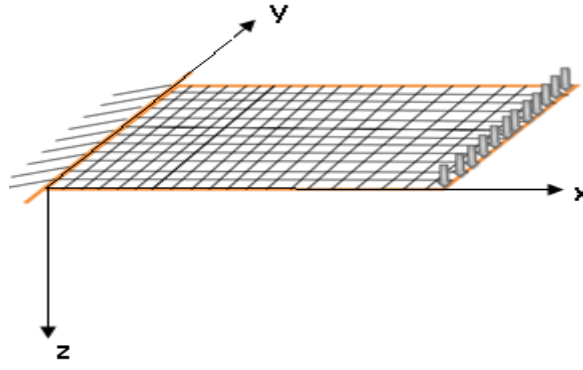
Figure 6.1: A Fixed-Free Plate, with sinusoidal concentrated loads acting at free end.

6.1.1 Application of Fixed Interface Method

To reduce the system by Fixed Interface method, Finite element model of the structure is required. The FE model of the plate is obtained in ABAQUS by discretesizing with *4* node quadrilateral shell elements (Element Type: S4R). The S4R element is based on large strain formulation and also allows transverse shear deformation. Each node of S4R element has *6* dofs, viz. translation along x axis (Tx), translation along y axis (Ty), translation along z axis (Tz), rotation about x axis (Rx), rotation about y axis (Ry), and rotation about z axis (Rz). These notations are used in the tables. The plate is discretesized into *80* elements along the length and *40* elements along the width. The stiffness and mass matrices generated by the ABAQUS solver are imported in MATLAB and are stored in the MATLAB sparse format. Further assessment of the measures and reduction procedures are performed in MATLAB.

Generally in a plate the shear in the *x-y* plane and rotation about the *z* axis are found to have higher frequency of vibration as compared to out-plane modes i.e. rotation about the *x* axis, rotation about the *y* axis, and motion along *z* axis. Therefore, to simplify the analysis and properly assess the effectiveness of the measures, the structure is physically constrained in these directions so that it has only out-plane vibration modes i.e. rotation about the *x* axis, rotation about the *y* axis, and translation along *z* axis. The total number of nodes in full FE model is *3321* and as each node has *3* dofs therefore, total number of dofs is *9963*. The dofs of the left most end nodes are constrained in all the directions. Sinusoidal point loads of amplitude *1000*N are applied on the right most end nodes of the structure along z direction. The structure is divided into two substructures "*substructure-1*" and "*substructure-2*" as shown in Figure 6.2. The nodes which share connection between the two substructures are named as "*Interface-1*". All the right most end nodes on which forces are applied are named

as "*Interface-2*". These nodes are highlighted as black in the below figure. The dofs of the structure are now partitioned. All the dofs of *"Interface-1"* are taken as coupling dofs. Since loads are applied on "*Interface-2*" along z axis, all the dofs of "*Interface-2*" along z axis are also taken as coupling dofs. This is because as already shown and explained in section 5.1.1(a), constraint modes corresponding to these coupling dofs will properly project the applied forces in the final set of transformed coordinates. It should be noted that the dofs of "*Interface-2*" corresponding to the rotation about the x and y axis, and all dofs excluding those along z axis of "*Interface-1*" are taken as interior dofs.

The Fixed Interface normal modes for each of the substructures are obtained by constraining their respective coupling dofs. Since the coupling dofs of each of the substructure are not similar therefore the substructures have different Fixed Interface normal modes. Constraint modes are also determined for each substructure corresponding to their respective coupling dofs. In the following sections, the Fixed Interface normal modes are selected for each of the substructures based on three measures i.e. Thumb rule, Effective Mass measure, and EIM. Each of the substructures is reduced by the constraint modes and these selected Fixed Interface normal modes. The reduced substructures are coupled together and then acceleration, velocity and displacement response are obtained. These responses are compared to that obtained from the full model FEM. The effectiveness of a particular measure in determining the dynamically important Fixed Interface normal modes is assessed based on whether the responses obtained from the system reduced by the Fixed Interface kept normal modes selected through the particular measure gives accurate response as compared to full model FEM soltuion or not.
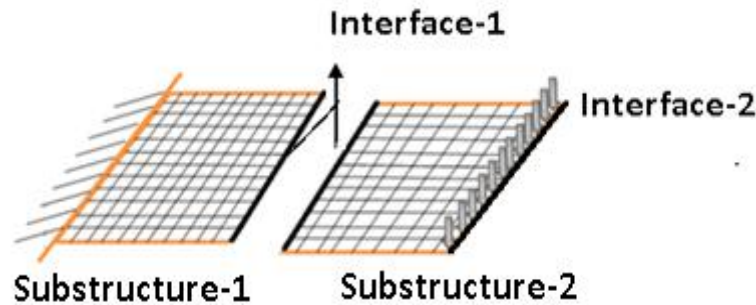
Figure 6.2: Plate divided into two substructures sharing common interface degrees of freedom.

6.1.2 Thumb rule

In Thumb rule, Fixed Interface normal modes are selected depending on the frequency range of interest. All the Fixed Interface normal modes of each of the substructure with the frequency less than *1.8* times the highest desired frequency of the complete structure are chosen. Let's assume that the maximum frequency of interest of the complete structure is *217* Hz. Based on this target frequency, the selected Fixed Interface normal modes of "*substructure-1*" and "*substructure-2*" are given in Table 6.1 and are named as "*FIM1*" and "*FIM2*" respectively. "*substructure-1*" is reduced by transformation matrix consisting of "*FIM1*" and all the constraint modes corresponding to its coupling dofs. Similarly, "*substructure-2*" is reduced by transformation matrix consisting of "*FIM2*" and all the constraint modes corresponding to its coupling dofs. The reduced "*substructure-1*" and "*substructure-2*" are coupled together to get the final reduced global system. The natural frequency of the reduced global system are given in Table 6.1 and as expected all the natural frequencies of the global reduced system in the desired frequency range are accurately determined as compared to full model FE solution. The number of dofs in full FE model of Fixed-Free plate is *9840* and that of the system reduced by Fixed Interface method are *189*.

Now, sinusoidal point loads of amplitude *1000*N are applied at all the nodes of "*Interface-2*" along z axis. The numerical time integration of the dynamic equation of the motion is performed by using Newmark-beta method with *β=1/4* and *γ=1/2*, so that the system is unconditionally stable. Four different nodal locations viz. '*C*', '*M1*', '*M2*', and '*A*' as shown in Figure 6.3 are chosen. The temporal variation of acceleration and displacement is calculated along z axis at these locations. '*M1*' and '*M2*' lies at the centre of each of the substructures, and '*C*' and '*A*' lies at the centre of '*Interface-1*' and '*Interface-2*' respectively.

Table 6.1: Comparison of Natural frequencies of the plate from "full model FEM" and "model reduced by Craig Bampton Method" (Modes Selected as per thumb rule with maximum frequency of interest=217Hz).

Mode No.	Natural Frequencies from Full model FEM. No. of coordinates= 9840	Selected Fixed interface normal modes of Substructure1 (FIM1)	Selected Fixed interface normal modes of Substructure2 (FIM2)	Fixed Interface Method. Kept modes: FIM1&FIM2. No. of coordinates= 189	% error w.r.t full model
1	2.40	61.56	42.258	2.40	0.00
2	10.08	72.52	56.17	10.08	0.00
3	14.91	119.09	108.24	14.91	0.00
4	32.87	168.59	136.87	32.88	-0.03
5	41.77	183.69	154.05	41.77	0.00
6	63.28	218.3	211.45	63.31	-0.05
7	64.70	237.35	212.59	64.71	-0.02
8	81.99	327.81	284.11	82.07	-0.10
9	87.53	334.83	301.69	87.61	-0.09
10	104.64	343.7	315.4	104.78	-0.13
11	122.03	373.46	363.76	122.22	-0.16
12	137.21	401.45	369.01	137.37	-0.12
13	157.6		467.57	157.88	-0.18
14	168.93			169.37	-0.26
15	173.25			174.26	-0.58
16	191.68			192.58	-0.47
17	204.21			207.17	-1.45
18	223.42			225.43	-0.90
19	226.4			226.91	-0.23
20	229.71			232.36	-1.15
21	275.22			282.69	-2.71
22	284.13			291.61	-2.63
23	294.86			301.38	-2.21
24	305.81			315.3	-3.10
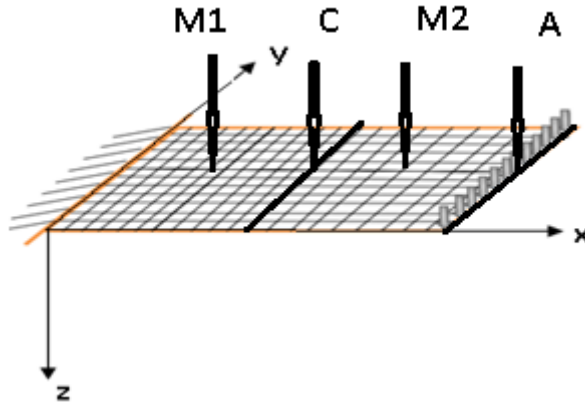
Figure 6.3: Locations at which response are calculated along z axis

These temporal displacement and acceleration responses at the given locations are calculated at different forcing frequencies of the load applied at "*Interface-2*" along *z axis*. The time step chosen for each forcing frequency is *$1/10^{th}$* of its time period so that all the details of the response at that forcing frequency get captured. The total number of time steps is chosen as *200* for each forcing frequency. The responses are calculated from the full FE model and the reduced system. For reduced system, the responses are first obtained in terms of its generalized coordinates and then transformed back to the physical dofs using the same transformation matrix which was originally used to transform the physical dofs into reduced coordinates. For each of the given locations, the temporal displacement and acceleration response of the reduced model obtained at different forcing frequencies are compared to that obtained from the full Model FEM by using Time response assurance criteria (TRAC) [**37**]. The TRAC is a variant of the MAC and gives an idea that how the two time response vectors correlate with respect to each other. Similar to MAC, the value of TRAC varies from *0* to *1*, where *'0'* represents no correlation and *'1'* represents exact correlation. TRAC can be determined from the Eq. (5.1) where t_1 and t_2 are vectors in time in this case. In Table 6.2, the TRAC of the displacement and acceleration response of the reduced system w.r.t full model FEM solution obtained at locations '*C*' and '*M1*' along *z* axis is shown at different forcing frequencies.

Table 6.2: Comparison of displacement and acceleration response at "C" and "M1" in direction Tz from "full model FEM" and "model reduced by Craig Bampton Method" (Modes Selected as per thumb rule with Target Frequency=217Hz).

Forcing Frequency	Response at C in direction Tz		Response at M1 in direction Tz	
	TRAC of displacement response w.r.t Full model	TRAC of acceleration response w.r.t Full model	TRAC of displacement response w.r.t Full model	TRAC of acceleration response w.r.t Full model
20	1	1	1	1
50	0.99	0.84	0.99	0.99
70	0.99	0.95	0.99	0.99
90	0.99	0.98	0.99	0.98
110	0.99	0.79	0.99	0.92
130	0.99	0.88	0.99	0.95
150	0.99	0.6	0.99	0.37

Similarly, Table 6.3 shows the TRAC of the displacement and acceleration response of the reduced system w.r.t full model FEM solution obtained at locations '*M2*' and '*A*' along *z* axis at different forcing frequencies. It can be observed that at all the locations the displacement response of the reduced system is in good correlation w.r.t full model FEM solution at all the forcing frequencies. But the acceleration response is not correlating w.r.t full model FEM solution at many frequencies in the frequency range of interest. Figure 6.4 shows the acceleration response at '*C*' along *z* axis from full model FEM and the reduced system when the forcing frequency is *110* Hz. Figure 6.5 shows the acceleration response at '*M1*' along *z* axis from full model FEM and the reduced system when the forcing frequency is *150* Hz. Both these graphs clearly show that the acceleration response of the reduced system is not accurate as compared to the full model FEM solution.

Table 6.3: Comparison of displacement and acceleration response at "M2" and "A" in direction Tz from "full model FEM" and "model reduced by Craig Bampton Method" (Modes Selected as per thumb rule with Target Frequency=217Hz).

Forcing Frequency	Response at M2 in direction Tz		Response at A in direction Tz	
	TRAC of displacement response w.r.t Full model	TRAC of acceleration response w.r.t Full model	TRAC of displacement response w.r.t Full model	TRAC of acceleration response w.r.t Full model
20	1	0.99	1	1
50	1	0.95	1	0.99
70	0.99	0.97	0.99	0.96
90	0.99	0.98	0.99	0.97
110	0.99	0.79	0.99	0.84
130	0.99	0.97	0.99	0.98
150	0.99	0.87	0.99	0.89
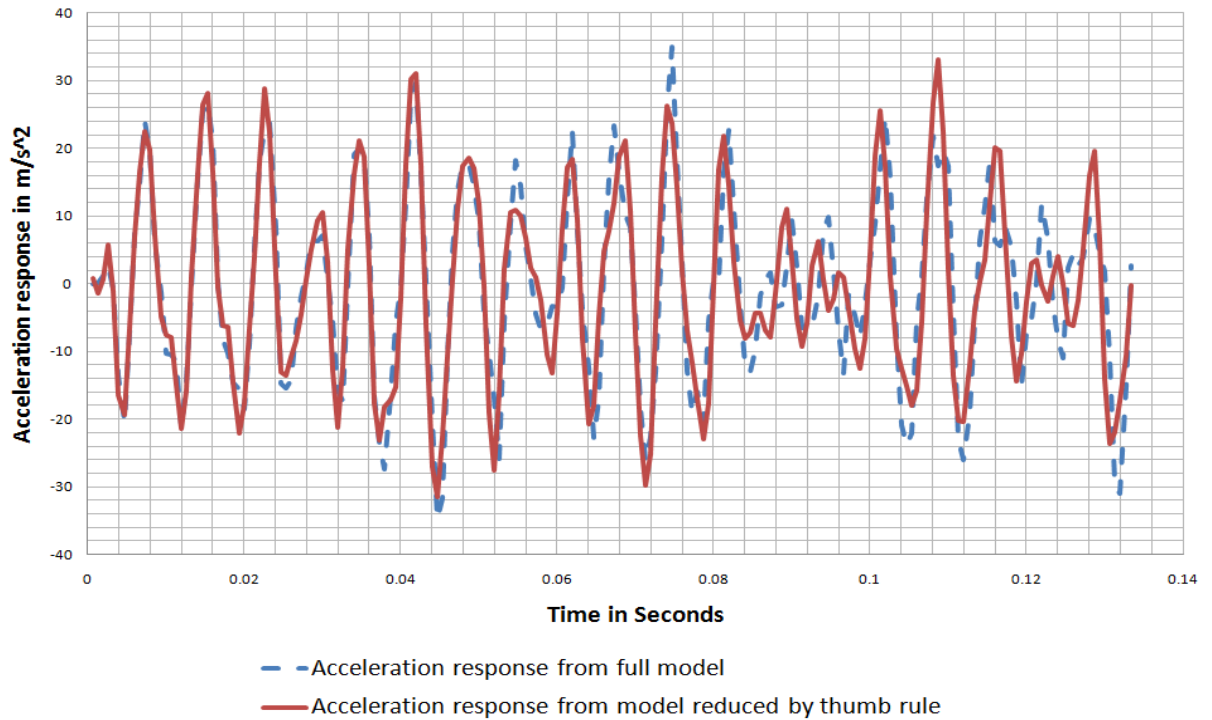
Figure 6.4: Comparison of Acceleration response at "C" in direction Tz from "full model FEM" and "model reduced by Fixed Interface method based on Thumb rule". Force Freq 110 Hz.
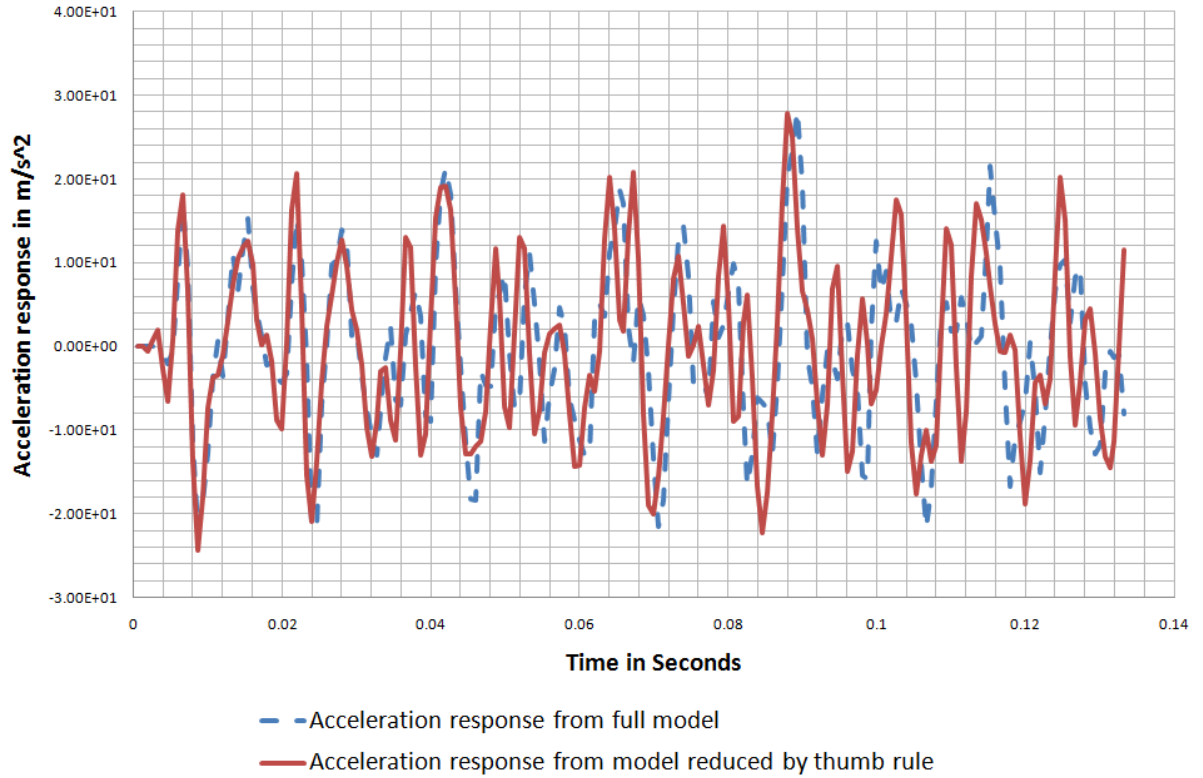
Figure 6.5: Comparison of Acceleration response at "M1" in direction Tz from "full model FEM" and "model reduced by Fixed Interface Method based on Thumb rule". Force Freq 150 Hz.

6.1.3 Effective Mass

As described in section 4.1, the dynamically important modes of each of the substructure are determined based upon their contribution to the total Effective Mass in each of the rigid body directions. Table 6.4 lists the most significant Fixed Interface normal modes of "*substructure-1*" in descending order of their contribution to the total resultant forces at the "*Interface-1*", or in other words to the total Effective Mass, in each of the direction Tz, Rx, and Ry. Similarly, Table 6.5 and Table 6.6 lists the most significant Fixed Interface normal modes of "*substructure-2*" in descending order of their contribution to the total Effective Mass at "*Interface-1*" and "*Interface-2*" respectively in each of the direction. Since only those dofs at "*Interface-2*" which are along *z* axis are considered as coupling dofs, therefore in Table 6.6, Fixed Interface normal modes are ranked based upon their contribution to the total resultant forces only along *z* axis. Only those modes which have more than *3*% contribution to the total Effective Mass are shown in these tables and are considered as most dominating modes. This criteria of considering all the modes with contribution greater than 3% to the total Effective Mass as the most dominating ones is defined in [**38**].

100

Table 6.4: Significant Fixed Interface normal modes of Substructure-1 in direction Tz, Rx and Ry,
having contribution of more than 3% to the total Effective Mass at Interface-1

Tz		Rx		Ry	
Mode Number	Effective Mass %	Mode Number	Effective Mass %	Mode Number	Effective Mass %
1	47.29%	2	64.70%	1	84.04%
4	17.93%	5	11.96%	4	10.99%
8	9.18%	10	3.87%	8	2.83%
15	5.58%	6	3.82%		
22	3.76%	9	3.07%		
32	2.71%	16	1.64%		

Table 6.5: Significant Fixed Interface normal modes of Substructure-2 in direction Tz, Rx and Ry,
having contribution of more than 3% to the total Effective Mass at Interface-1

Tz		Rx		Ry	
Mode Number	Effective Mass %	Mode Number	Effective Mass %	Mode Number	Effective Mass %
1	54.36%	2	70.12%	1	88.54%
4	16.77%	5	11.72%	4	8.30%
8	8.07%	9	3.50%	8	1.88%
15	4.74%	6	2.46%		
22	3.13%				
31	2.22%				

Table 6.6: Significant Fixed Interface normal modes of Substructure-2 in direction Tz, Rx and Ry,
having contribution of more than 3% to the total Effective Mass at Interface-2

Tz	
Mode Number	Effective Mass %
1	53.09%
4	17.41%
8	8.27%
15	4.79%
22	3.10%
31	2.16%

Table 6.7 lists the cumulative sum of the contribution of the most significant Fixed Interface normal modes of *"substructure-1"* to the total Effective Mass at *"Interface-1"* in

each of the direction Tz, Rx, and Ry. It should be noted that the Fixed Interface normal modes are sorted in descending order of their contribution to the total Effective mass before taking the cumulative sum. This will determine the top most significant modes that achieve particular assurance criteria and are to be chosen for the reduced representation. If these modes are not sorted in descending order of their contribution to the total Effective mass before taking the cumulative sum then many more modes would be required to achieve the same assurance criteria. This is illustrated in Figure 6.6.
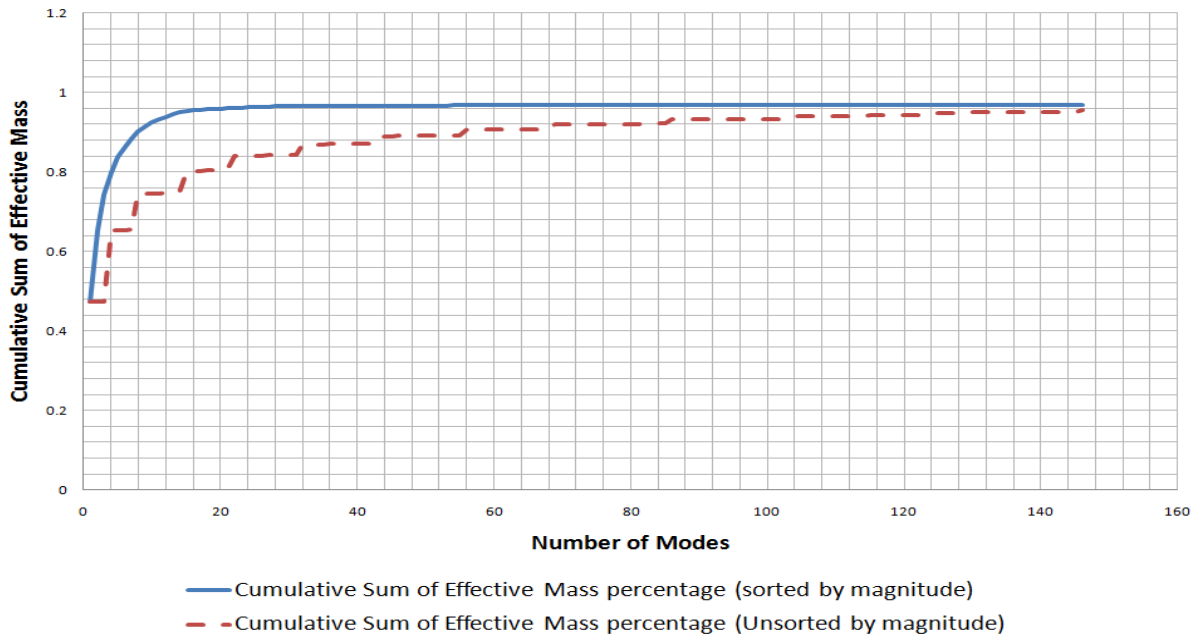
Figure 6.6: Comparison of cumulative sum after the Fixed Interface normal modes sorted and unsorted in descending order of their contribution to the total Effective Mass,.

The assurance criteria of *95%* is chosen so that the reduced model predicts at least 95% of the interface loads as predicted by the full mode FEM representation based upon the Effective mass. Similarly, Table 6.8 and Table 6.9 lists the cumulative sum of the contribution of the Fixed Interface normal modes of *"substructure-2"* to the total Effective Mass at *"Interface-1"* and *"Interface-2"* respectively in each of the direction Tz, Rx, and Ry. These modes achieve *95%* of the total Effective Mass and therefore are selected for the reduced representation. For a particular substructure, the Fixed Interface normal modes to be kept are determined by taking union of all the modes ranked as significant w.r.t to its coupling dofs in each of the directions Tz, Rx, and Ry.

Table 6.7: Cumulative Sum of contribution of the most significant Fixed interface normal modes of Substructure-1 to the total Effective Mass at Interface-1 in direction Tz, Rx and Ry.

Tz		Rx		Ry	
Mode Number	Cumulative sum	Mode Number	Cumulative sum	Mode Number	Cumulative sum
1	0.47	2	0.65	1	0.84
4	0.65	5	0.77	4	0.95
8	0.74	10	0.81		
15	0.80	6	0.84		
22	0.84	9	0.87		
32	0.86	16	0.89		
43	0.88	14	0.91		
56	0.90	23	0.92		
69	0.91	21	0.92		
86	0.92	33	0.93		
104	0.93	29	0.93		
123	0.94	20	0.94		
146	0.94	24	0.94		
169	0.95	30	0.94		
193	0.95	44	0.95		
		38	0.95		
		40	0.95		

Table 6.8: Cumulative Sum of contribution of the most significant Fixed Interface normal modes of Substructure-2 to the total Effective Mass at Interface-1 in direction Tz, Rx and Ry.

Tz		Rx		Ry	
Mode Number	Cumulative sum	Mode Number	Cumulative sum	Mode Number	Cumulative sum
1	0.54	2	0.70	1	0.89
4	0.71	5	0.82	4	0.97
8	0.79	9	0.85		
15	0.84	6	0.88		
22	0.87	10	0.90		
31	0.89	16	0.92		
43	0.91	14	0.93		
54	0.92	20	0.94		
69	0.93	23	0.94		
84	0.94	32	0.95		
104	0.95	28	0.95		
123	0.95				

Table 6.9: Cumulative Sum of contribution of the most significant Fixed Interface normal modes of Substructure-2 to the total Effective Mass at Interface-2 in direction Tz.

Tz	
Mode Number	Cumulative sum
1	0.53
4	0.71
8	0.79
15	0.84
22	0.87
31	0.89
43	0.90
54	0.92
69	0.93
84	0.93
104	0.94
123	0.94

"substructure-1" is reduced by transformation matrix consisting of all the Fixed Interface normal modes determined as most significant based on Effective Mass (from Table 6.7), and all the constraint modes corresponding to its coupling dofs. Similarly, "substructure-2" is reduced by transformation matrix consisting of all the Fixed Interface normal modes determined as most significant based on Effective Mass (from Table 6.8 and Table 6.9), and all the constraint modes corresponding to its coupling dofs. The reduced "*substructure-1*" and "*substructure-2*" are coupled together to get the final reduced global system.

Table 6.10 shows the TRAC of the displacement and acceleration response of the reduced system w.r.t full model FEM solution obtained at locations '*C*' and '*M1*' along z axis at different forcing frequencies. Similarly, Table 6.11 shows the TRAC of the displacement and acceleration response of the reduced system w.r.t full model FEM solution obtained at locations '*M2*' and '*A*' along z axis at different forcing frequencies. It can be observed that both the acceleration and displacement response is not correlating w.r.t full model FE solution at many frequencies in the frequency range of interest. Figure 6.7 shows the acceleration response at '*M2*' along z axis from full model FEM and the reduced system when the forcing frequency is *70* Hz. The graph clearly shows that the acceleration response of the reduced system is completely different to the full model FEM solution. Now, all the coupling dofs at

"*Interface-1*" are fixed and the reaction forces obtained at "*C*" along *z* axis is plotted in Figure 6.8. The reaction forces obtained at "*C*" along *z* axis is also obtained from the full FE model and plotted on the same figure. It can be observed that the reaction forces as predicted by reduced system are completely different than that predicted by full model FE solution. This signifies that the Fixed Interface normal modes selected based on their total contribution of *95*% to the total Effective Mass are not sufficient in predicting the response obtained from the full model FE solution. Thus, results could be misleading if decisions are based on Effective Mass measures. The primary reason of the failure of Effective Mass is explained in section 4.1.2 and its more generalized form i.e. EIM is recommended.

Table 6.10: Comparison of displacement and acceleration response at "C" and "M1" in direction Tz from "full model FEM" and "model reduced by Fixed Interface Method" (Modes Selected as per Cumulative Sum of Effective Mass 0.95).

Forcing Frequency	Response at C in direction Tz		Response at M1 in direction Tz	
	TRAC of displacement response w.r.t Full model	TRAC of acceleration response w.r.t Full model	TRAC of displacement response w.r.t Full model	TRAC of acceleration response w.r.t Full model
20	0.99	0.99	0.99	0.94
50	0.99	0.55	0.99	0.87
70	0.70	0.16	0.83	0.57
90	0.86	0.004	0.75	0.56
110	0.99	0.6	0.93	0.73
130	0.98	0.51	0.83	0.94
150	0.99	0.93	0.97	0.69

Table 6.11: Comparison of displacement and acceleration response at "M2" and "A" in direction Tz from "full model FEM" and "model reduced by Fixed Interface Method" (Modes Selected as per Cumulative Sum of Effective Mass 0.95).

Forcing Frequency	Response at M2 in direction Tz		Response at A in direction Tz	
	TRAC of displacement response w.r.t Full model	TRAC of acceleration response w.r.t Full model	TRAC of displacement response w.r.t Full model	TRAC of acceleration response w.r.t Full model
20	0.99	0.91	0.99	0.98
50	0.99	0.74	0.99	0.93
70	0.96	0.10	0.85	0.04
90	0.97	0.5	0.97	0.66
110	0.99	0.61	0.99	0.7
130	0.99	0.98	0.99	0.99
150	0.99	0.97	0.99	0.97

— — Acceleration response from full model

——— Acceleration response from model reduced by Craig Bampton method with Effective Mass Measure of 0.95
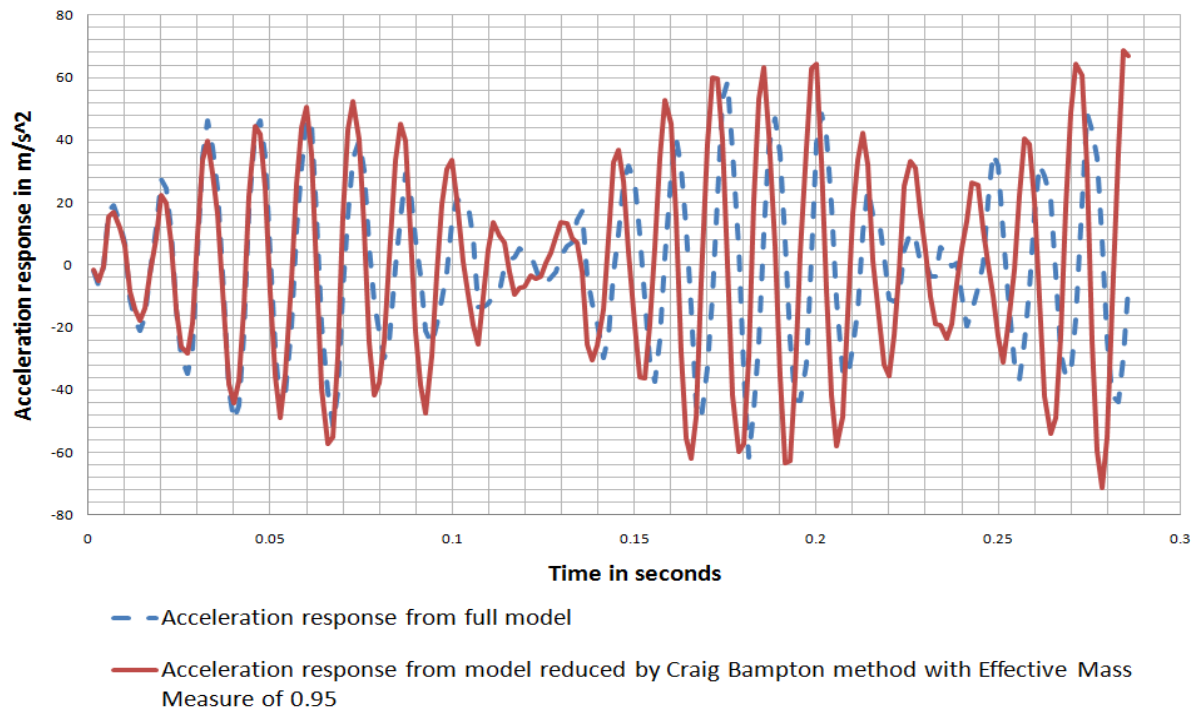
Figure 6.7: Comparison of Acceleration response at "M2" in direction Tz from "full model FEM" and "model reduced by "model reduced by Fixed Interface Method" (Modes Selected as per Cumulative Sum of Effective Mass 0.95). Forcing frequency=70 Hz.
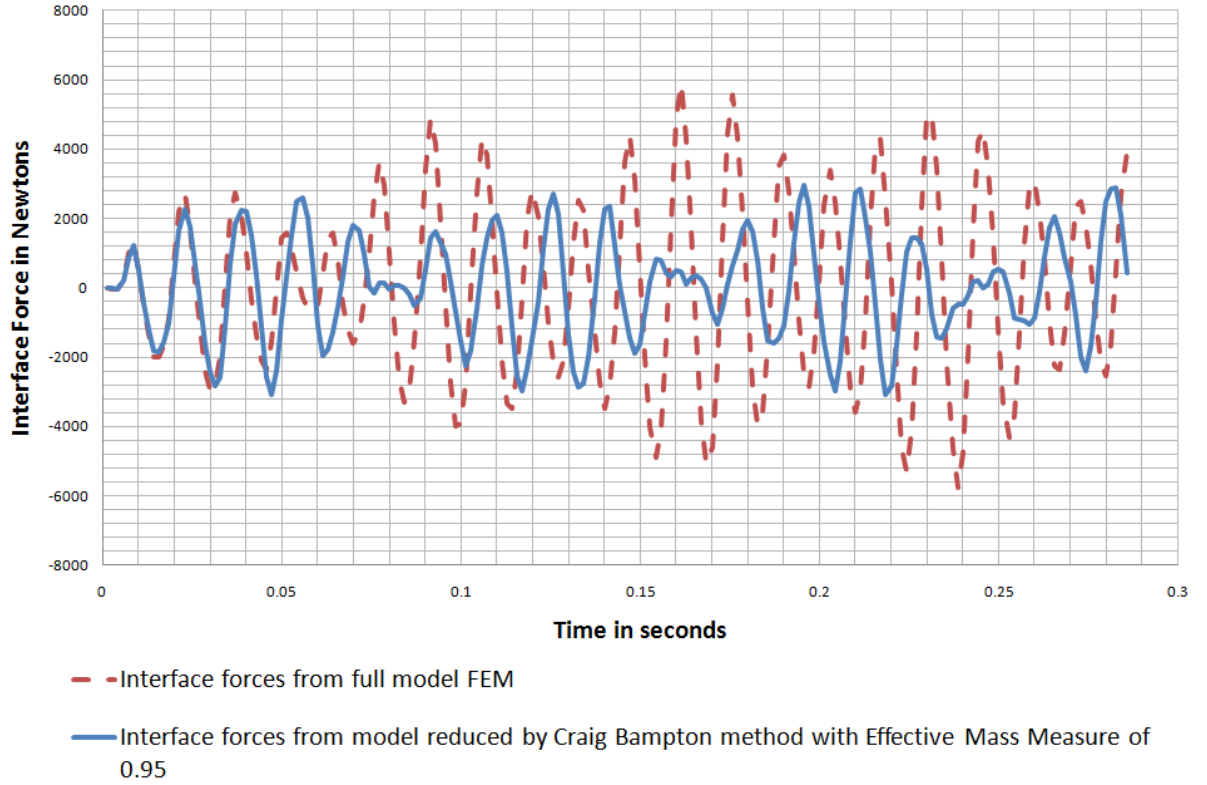
Figure 6.8: Comparison of Reaction Forces at "C" in direction Tz from "full model FEM" and "model reduced by Fixed Interface Method" (Modes Selected as per Cumulative Sum of Effective Mass 0.95). Force frequency=70 Hz.

6.1.4 Effective Interface Mass

As described in section 4.1, EIM is a more generalized form of Effective Mass in which the dynamically important modes of each of the substructure are determined based upon their contribution to the total Effective Interface Mass in each of the rigid body directions. Table 6.12 lists the most significant Fixed Interface normal modes of "*substructure-1*" in descending order of their contribution to the forces individually at each of the dofs of "*Interface-1*". The contributions are separately summed up together corresponding to each of the direction Tz, Rx, and Ry. Similarly, Table 6.13 and Table 6.14 lists the most significant Fixed Interface normal modes of "*substructure-2*" in descending order of their contribution to the forces individually at each of the coupling dofs of "*Interface-1*" and "*Interface-2*" respectively. These contributions are also separately summed up together corresponding to each of the direction Tz, Rx, and Ry.

Table 6.12: Significant Fixed Interface normal modes of Substructure-1 in direction Tz, Rx and Ry, having contribution of more than 3% to the total Effective Interface Mass at Interface-1

Tz		Rx		Ry	
Mode Number	Effective Mass %	Mode Number	Effective Mass %	Mode Number	Effective Mass %
1	13.69%	2	28.12%	1	45.11%
2	13.09%	1	17.67%	2	26.82%
3	5.75%	3	11.51%	4	5.89%
4	4.47%	5	4.06%	3	5.54%
5	4.16%	7	3.81%	5	4.39%
7	2.91%	6	2.92%	7	1.98%

Table 6.13: Significant Fixed Interface normal modes of Substructure-2 in direction Tz, Rx and Ry, having contribution of more than 3% to the total Effective Mass at Interface-1

Tz		Rx		Ry	
Mode Number	Effective Mass %	Mode Number	Effective Mass %	Mode Number	Effective Mass %
1	19.42%	2	30.68%	1	56.03%
2	14.96%	1	28.06%	2	23.75%
4	4.77%	3	8.09%	4	5.24%
3	4.74%	5	4.05%	5	3.55%
5	4.26%	7	3.12%	3	3.23%
7	2.67%	4	2.12%	7	1.33%

Table 6.14: Significant Fixed Interface normal modes of Substructure-2 in direction Tz, having contribution of more than 3% to the total Effective Interface Mass at Interface-1

Tz	
Mode Number	Effective Mass %
2	21.17%
1	12.98%
3	8.24%
5	3.77%
4	3.58%
7	3.04%

It can be observed that the significant modes as listed by Effective Interface Mass (from Table 6.12, Table 6.13, and Table 6.14) are different than those listed by Effective

Mass (from Table 6.4, Table 6.5, and Table 6.6). For e.g. Effective Mass completely misses the modes *2, 3, 5, and 7* of "*substructure-1*" for their contribution to the forces at "*Interface-1*". These modes are determined as significant by Effective Interface Mass measure. Figure 6.9 compares the rankings of Fixed Interface normal modes of "*substructure-1*" as done by their percentage contribution to the total Effective Mass and Effective Interface Mass at "*Interface-1*". It is clearly observed that the rankings done by both the methods are completely different.
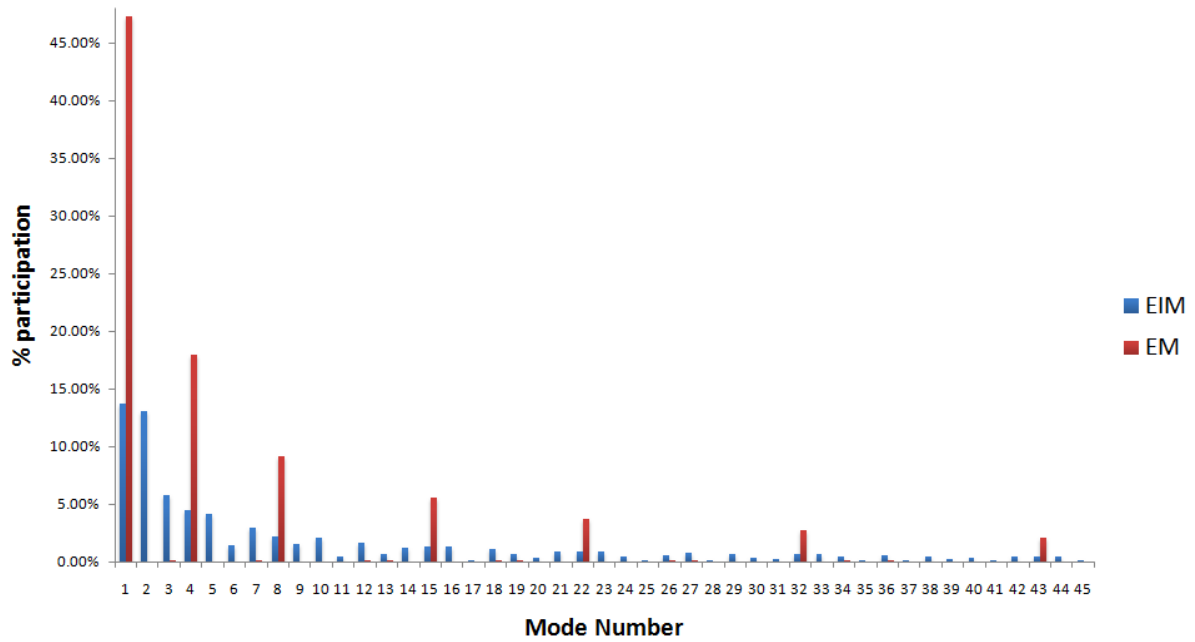
Figure 6.9: Rankings of Fixed Interface normal modes of Substructure-1 by their percentage participation to the total Effective Mass and Effective Interface Mass at Interface-1.

Figure 6.10 shows the number of Fixed Interface normal modes of "*substructure-1*" required to achieve cumulative sum of *95%* of the total Effective Mass at "*Interface-1*" in each of the directions Tz, Rx, and Ry. It should be noted that these Fixed Interface normal modes are sorted in descending order of their contribution to the total Effective Interface mass before taking the cumulative sum. If these modes are not sorted in descending order of their contribution to the total Effective Interface mass before taking the cumulative sum then many more modes would be required to achieve the same assurance criteria. It can be observed that around *307* modes are required for the reduced system to predict at least *95%* of the interface forces obtained by the full model FEM solution along direction *Tz*, as compared to *124* modes along direction Rx and only *12* modes along direction Ry. However, if one is interested only

in the lower frequency range then lower assurance criteria can be chosen which will determine the modes sufficient for predicting the total interface forces at lower frequencies. For e.g. since the Fixed-Interface normal modes have slower convergence rate to total Effective Interface mass along direction Tz, therefore *80%* assurance criteria was chosen instead of *95%*. Table 6.15 shows the comparison of acceleration response obtained from the reduced system to that of full model FEM solution at "*C*", "*M2*", "*M1*", and "*A*" in direction Tz at different forcing frequencies and when modes selected with assurance criteria of *80%* along direction Tz and 95% for direction Rx & Ry.
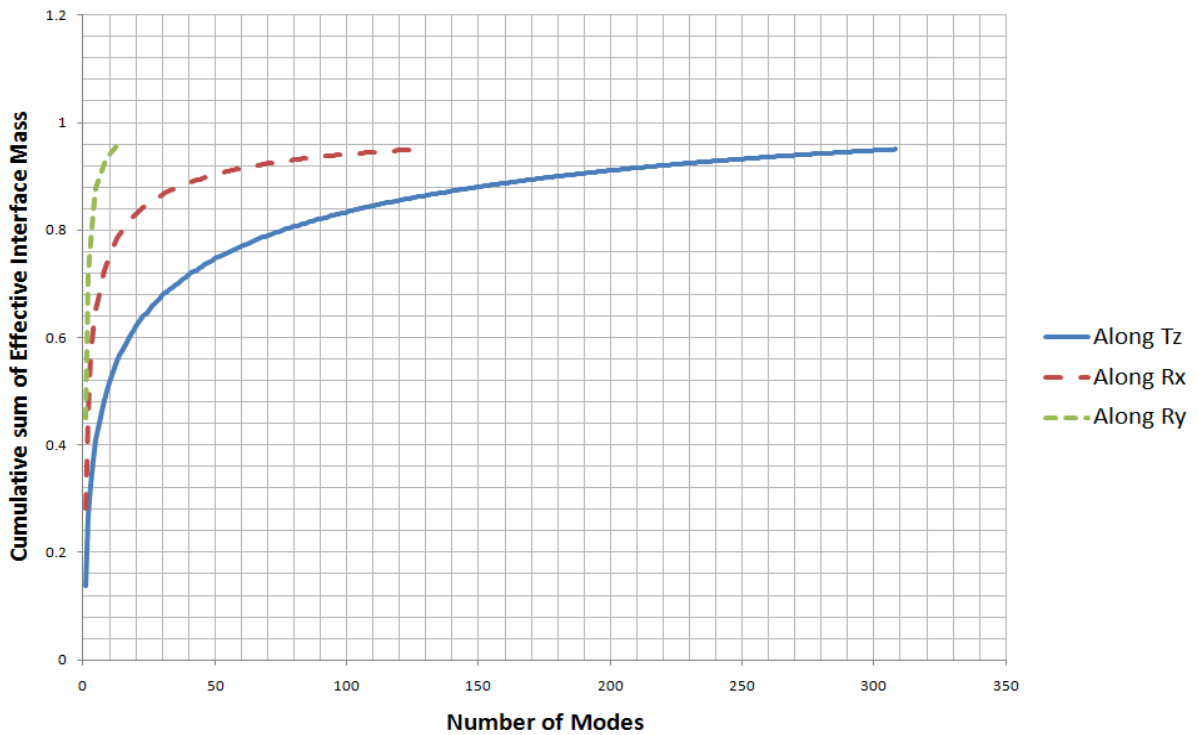
Figure 6.10: Number of modes of Substructure-1 required for obtaining Cumulative Sum of 0.95 of total Effective Interface Mass at Interface-1.

It can be observed that even though by keeping a weak assurance criteria of *80%* along direction Tz which requires only *76* modes, as compared to the assurance criteria *95%* which requires *30*8 modes, all the acceleration responses are matching very well with that obtained from full model FE solution. Thus, this clearly signifies that Effective Interface Mass is a more appropriate measure for determining the dynamically important modes and one can adjust the assurance criteria depending on whether the lower or higher frequency range is of interest. The total number of selected modes of "*substructure-1*" by keeping assurance criteria of 80% along direction Tz, and *95%* along direction Rx and Ry are *142*. The total number of

selected modes of "*substructure-2*" by keeping assurance criteria of *80%* along direction *Tz*, and 95% along direction *Rx* and *Ry* are *92*. The total number of coupling dofs which appear in the final set of reduced equation are *164*. Therefore the total size of the reduced system is *398* which gives 95.95% reduction.

Table 6.15: Comparison of acceleration response at Node C,M2,M1and A in direction Z from "full model FEM" and "model reduced by Fixed Interface Method" (Modes Selected as per Cumulative Sum of Effective Interface Mass of 0.80 along direction Tz and 0.95 for direction Rx & Ry).

Forcing Frequency	Response at C in direction Tz	Response at M1 in direction Tz	Response at M2 in direction Tz	Response at A in direction Tz
	TRAC of acceleration response w.r.t Full model	TRAC of acceleration response w.r.t Full model	TRAC of acceleration response w.r.t Full model	TRAC of acceleration response w.r.t Full model l
20	1	1	0.99	0.99
50	0.99	1	0.99	0.99
70	0.99	1	0.99	0.99
90	0.99	0.99	0.99	0.99
110	0.99	0.99	0.99	0.99
130	0.99	0.99	0.99	0.99
150	0.99	0.99	0.99	0.99

(a) Effective Interface Mass displacement output

As shown in Figure 6.10, EIM requires large number of modes to achieve *95%* of the total interface forces obtained by the full model FEM solution. Generally, larger number of modes is actually required to be chosen for the reduced system to completely represent the interface forces than to completely represent the modal velocity at the interface, which in turn requires even more modes than to completely represent modal displacement at the interface. If acceleration response is of interest then the reduced system should accurately represent the interface forces, and the dynamically important modes which achieve this can be determined by EIM. Thus, EIM is also called as EIM Acceleration Output. However, if velocity and displacement response of interest then the reduced system should accurately represent the modal velocity and modal displacement at the interface, respectively, and even a lesser number of modes than determined by the EIM Acceleration Output can achieve this. Thus, EIM was extended and two more measures for ranking the dynamic importance of modes based upon their contribution to the modal velocity, or modal displacement

at the substructure's fixed interface was proposed. Only EIM displacement output is assessed here and similar extension can be done for EIM velocity output. Table 6.16 lists the cumulative sum of the contribution of the most significant Fixed Interface normal modes of "substructure-1" in descending order of their contribution to the modal displacement individually at each of the dofs of "Interface-1". The contributions are separately summed up together corresponding to each of the rigid body direction Tz, Rx, and Ry. Similarly,

Table 6.17 and Table 6.18 lists the cumulative sum of the contribution of the most significant Fixed Interface normal modes of "*substructure-2*" in descending order of their contribution to the modal displacement individually at each of the coupling dofs of "*Interface-1*" and "*Interface-2*" respectively. It can be observed that many less number of modes are required that quickly converge to the total modal displacement at the interface. Thus, assurance criteria of *99*% is chosen for EIM displacement output. This is because of an inverse frequency term which is also present in the equation of the modal participation factor to the modal displacement excitations at the interface (see Eq. (4.16)). Due to this inverse frequency term, the participation of higher modes, which have higher natural frequencies, is very less. Thus, very few lower frequency modes are sufficient for the accurate representation of the displacement response.

Table 6.16: Cumulative Sum of contribution of the most significant Fixed Interface normal modes of Substructure-1 to the total Effective Interface Mass displacement output at Interface-1 in direction Tz, Rx, and Ry.

Tz		Rx		Ry	
Mode Number	Cumulative sum	Mode Number	Cumulative sum	Mode Number	Cumulative sum
1	0.65	1	0.53	1	0.76
2	0.97	2	0.97	2	0.99
3	0.99	3	0.99		

Table 6.17: Cumulative Sum of contribution of the most significant Fixed Interface normal modes of Substructure-2 to the total Effective Interface Mass displacement output at Interface-1 in direction Tz, Rx, and Ry.

Tz		Rx		Ry	
Mode Number	Cumulative sum	Mode Number	Cumulative sum	Mode Number	Cumulative sum
1	0.80	1	0.74	1	0.88
2	0.99	2	0.99	2	0.99

Table 6.18: Cumulative Sum of contribution of the most significant Fixed Interface normal modes of Substructure-2 to the total Effective Interface Mass displacement output at Interface-2 in direction Tz.

Tz	
Mode Number	Cumulative sum
1	0.65
2	0.99
3	0.99

It should be noted that the expressions for calculation of absolute EIM displacement output (see Eq. (4.18)) involves many mathematical operations and can be very computationally costly for large structures. Figure 6.11 shows the number of Fixed Interface normal modes of *"substructure-1"* required to achieve absolute sum of Effective Interface Mass displacement output at *"Interface-1"* in direction *Tz, Rx,* and *Ry*. It should be noted that here the modes are not sorted in order of their contribution to the total EIM displacement output. It can be observed that only first few Fixed Interface normal modes are required to converge to the absolute sum of EIM displacement output and therefore, for displacement response, the suppositional estimations based on Thumb rule can be used to determine the modes to be retained instead of determining them through more computationally costly EIM displacement output measure. One should take care while making suppositional estimations that first few modes in all the directions should be kept. This is important in the cases when there are high frequency shear modes which although may not fall in the criteria based on thumb rule but still are important to determine accurate response in the in-plane directions. It is quantitatively shown here that first very few modes are dominant for the case of the displacement response. However, these modes will determine accurate response only in a particular frequency range. If a larger frequency range is of interest, these first few significant

modes are kept along with additional modes depending on the target frequency using thumb rule.
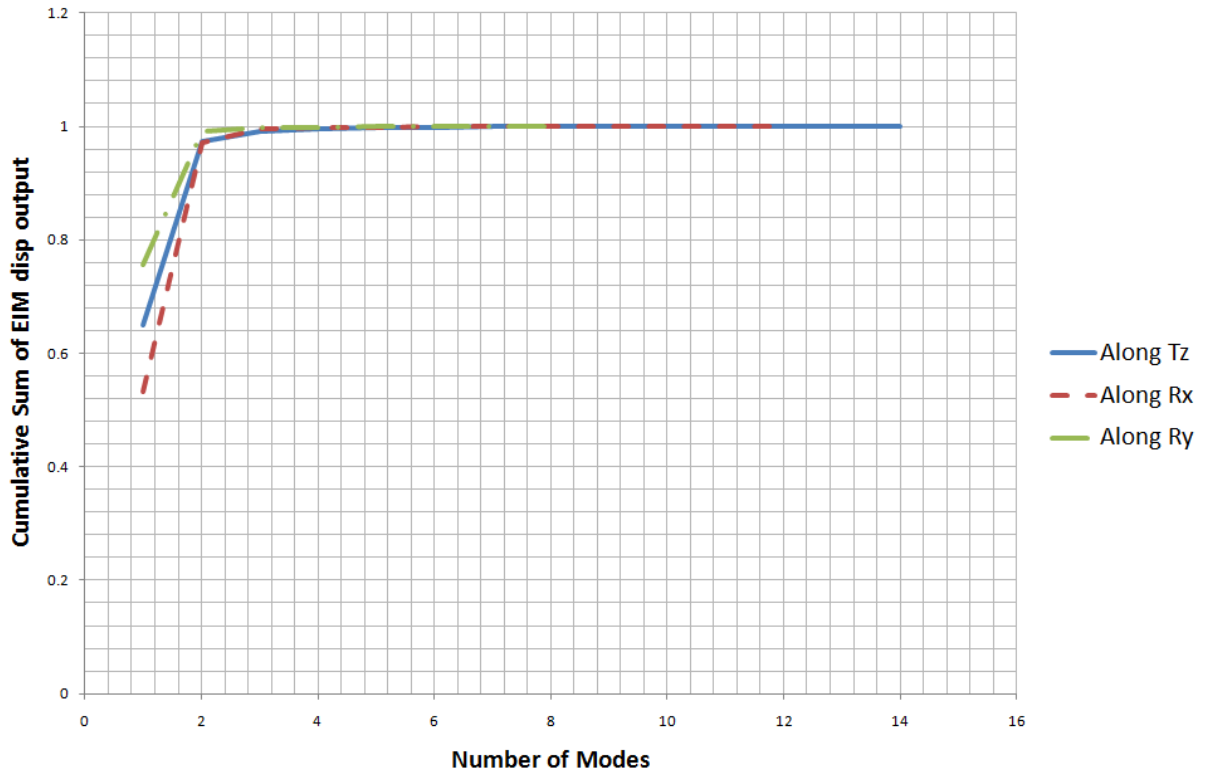
Figure 6.11: Number of Modes of substructure-1 required for obtaining absolute Sum based on Effective Interface Mass displacement output in direction Tz, Rx and Ry.

Assume that the frequency range of interest as *0* to *150*Hz. First eight Fixed Interface normal modes are selected for each of the substructures based on the thumb rule for the maximum frequency of interest *150* HZ. It should be noted that the Fixed Interface normal modes *1*, *2*, and, *3* determined as significant for each of the substructure from EIM displacement output are already contained in this selected set based on thumb rule. Table 6.19 shows the TRAC of the displacement response of the reduced system w.r.t full model FEM solution obtained at locations 'C', 'M1', 'M2', and 'A' in direction *Tz* at different forcing frequencies. It can be observed that all the displacement responses are matching very well with that obtained from full model FE solution.

Table 6.19: Comparison of displacement response at Node C, M1, M2 and A in direction Z from "full model FEM" and "model reduced by Craig Bampton Method" (Modes Selected as per thumb rule with Target Frequency=150Hz).

Forcing Frequency	Response at C in direction Tz	Response at M1 in direction Tz	Response at M2 in direction Tz	Response at A in direction Tz
	TRAC of displacement response w.r.t Full model	TRAC of displacement response w.r.t Full model	TRAC of displacement response w.r.t Full model	TRAC of displacement response w.r.t Full model
20	1	1	1	1
50	1	0.99	1	1
70	0.99	0.99	0.99	0.99
90	0.99	0.99	0.99	0.99
110	0.99	0.99	1	0.99
130	0.99	0.99	0.99	0.99
150	0.99	0.99	0.99	0.99

6.1.5 Selection of Coupled Characteristic Constraint modes using EIM

It has been observed in section 6.1.4 that very large number of interface dofs always appears in the final set of system reduced by Fixed Interface method. Also for very large assemblies of complex structures or in the cases where substructures are coupled with line or surface connections the size of interface dofs is usually very large as compared to the number of chosen generalized coordinates and thus further effort is required for the reduction of these interface dofs.

Once the selection of Fixed Interface normal modes is made for each of the substructures by using a particular EIM measure, each of the substructures is reduced using these normal modes and their respective constraint modes. The reduced substructures are coupled together and then coupled CC modes are obtained corresponding to the particular interface which needs to be reduced (see section 4.1.4 for complete details). The extension of EIM is proposed here to effectively rank the dynamic importance of the Coupled CC modes of a particular interface relative to the already selected generalized coordinates of all the substructures coupled to this interface at the coupled substructure level. The procedure of ranking the Coupled CC modes of the particular interface is based on their contribution to the forces individually at each of the already selected generalized coordinates of the Fixed Interface normal modes of all the substructures coupled to this interface at the coupled

substructure level. Or in other words, the dynamically important Coupled CC modes of a particular interface are determined based upon their contribution to the total Coupled CC EIM (see section 4.1.4 for complete details) at each of the already selected generalized coordinates for the interior. Modes which have greater than *3*% contribution to the total EIM are considered as dominant [**38**] and therefore, ranking of the coupled CC modes is done based on their contribution to the forces only at these significant modes. This is because resources can't be wasted in correlating coupled CC modes w.r.t to less significant ones. From Table 6.12, it can be observed that the most significant (with EIM > *3*%) Fixed Interface normal modes of "*substructure-1*" in all the directions are 1, *2*, *3*, *4*, *5*, *6*, and *7* ('*6*' is also included at lower end). Similarly, from Table 6.13 and Table 6.14, it can be observed that the most significant (with EIM > *3*%) Fixed Interface normal modes of "*substructure-2*" in all the directions are *1*, *2*, *3*, *4*, *5*, and *7*. Table 6.20 lists the cumulative sum of the contribution of the significant Coupled CC modes of "*Interface-1*" to the total coupled CC EIM at significant modes *1*, *2* and *3* of "*substructure-1*". Table 6.21 lists the cumulative sum of the contribution of the significant Coupled CC modes of "*Interface-1*" to the total coupled CC EIM at significant modes *4*, *5*, 6 and *7* of "*substructure-1*".

Table 6.20: Cumulative Sum of contribution of the most significant Coupled CC modes of Interface-1 to the total Coupled CC EIM at most significant coordinates 1, 2, and 3 of Substructure-1.

1		2		3	
Mode No.	Cumulative sum	Mode No.	Cumulative sum	Mode No.	Cumulative sum
3	0.55	4	0.52	6	0.51
1	0.72	2	0.75	5	0.80
14	0.79	16	0.82	38	0.86
11	0.84	19	0.87	35	0.89
17	0.87	13	0.90	32	0.91
21	0.90	22	0.93	40	0.92
18	0.92	25	0.95	30	0.93
8	0.94			21	0.95
24	0.95			24	0.96

Table 6.21: Cumulative Sum of contribution of the most significant Coupled CC modes of Interface-1 to the total Coupled CC EIM at most significant coordinates 4, 5, 6, and 7 of Substructure-1.

4		5		6		7	
Mode No.	Cumulative sum	Mode No.	Cumulative sum	Mode No.	Cumulative sum	Mode No.	Cumulative sum
3	0.50	4	0.50	9.00	0.52	6	0.52
1	0.90	2	0.96	7.00	0.79	5	0.94
18	0.92			41	0.90	38	0.95
23	0.94			42	0.95		
12	0.95			37	0.96		
29	0.96						

Similarly, Table 6.22 lists the cumulative sum of the contribution of the significant Coupled CC modes of "*Interface-1*" to the total coupled CC EIM at significant modes *1*, *2* and *3* of "*substructure-2*". Table 6.23 lists the cumulative sum of the contribution of the significant Coupled CC modes of "*Interface-1*" to the total coupled CC EIM at significant modes *4*, *5* and *7* of "*substructure-2*".

Table 6.22: Cumulative Sum of contribution of the most significant Coupled CC modes of Interface-1 to the total Coupled CC EIM at most significant coordinates 1,2 and 3 of Substructure-2.

1		2		3	
Mode No.	Cumulative sum	Mode No.	Cumulative sum	Mode No.	Cumulative sum
1	0.42	4	0.44	6	0.50
3	0.83	2	0.81	5	0.79
14	0.87	16	0.86	38	0.85
11	0.91	19	0.90	35	0.89
17	0.94	13	0.93	32	0.90
21	0.95	22	0.95	21	0.92
		25	0.96	40	0.93
				27	0.94
				24	0.95

Table 6.23: Cumulative Sum of contribution of the most significant Coupled CC modes of Interface-1 to the total Coupled CC EIM at most significant coordinates 4,5 and 7 of Substructure-2.

4		5		7	
Mode No.	Cumulative sum	Mode No.	Cumulative sum	Mode No.	Cumulative sum
1	0.63	2	0.62	6	0.50
3	0.75	4	0.93	5	0.93
11	0.80	20	0.94	38	0.95
17	0.84	26	0.95	35	0.96
14	0.87	13	0.96	32	
8	0.89			40	
23	0.92			21	
12	0.93			30	
29	0.95			27	
36	0.95				

All these coupled CC modes determined as important w.r.t to the most significant modes of each of the substructures are used to perform the reduction of the "Interface-1". Table 6.24 shows the comparison of acceleration response at "C", "M2", "M1" and "A" in direction Tz when coupled CC modes are selected as per the assurance criteria *95%* of the total Coupled CC EIM at each of the most significant coordinates of "*substructure-1*" and "*substructure-2*". It can be observed that all the acceleration responses of the second level reduced system are matching very well with that obtained from full model FE solution at all the frequencies. Thus by using EIM and Coupled CC EIM we are able to perform an interaction analysis between the significant coordinates of interior and the junction coordinates of a substructure by determining their relative dynamic importance of the one with respect to another. This leads to appropriate reduction of the interface and junction dofs such that the accuracy of the final reduced is not at all compromised.

The total number of CC modes that are found important w.r.t significant coordinates of "*substructure-1*" and "*substructure-2*" by using the assurance criteria of *95%* are *35*. It should be recalled that the total number of significant selected modes of "*substructure-1*" by keeping assurance criteria of *80%* along direction *Tz*, and *95%* along direction *Rx* and *Ry* are *142*; and the total number of significant selected modes of "*substructure-2*" by keeping assurance criteria of *80%* along direction *Tz*, and 95% along direction *Rx* and *Ry* are *92*. The total

number of coordinates of "*Interface-1*" after reduction using these important coupled CC modes is *35*. The unreduced coupling dofs of "*Interface-2*" which appear in the final set of reduced equation are *41*. Therefore, the total size of the reduced system is *310*, which gives 96.84% reduction.

Table 6.24: Comparison of acceleration response at Node C,M2,M1and A in direction Z from "full model FEM" and "model reduced by Craig Bampton Method" (Modes Selected as per Cumulative Sum of Effective Interface Mass of 0.80 along direction Tz and 0.95 for direction Rx & Ry for Interior normal modes and 0.95 for Coupled CC modes.

	Response at C in direction Tz	Response at M1 in direction Tz	Response at M2 in direction Tz	Response at A in direction Tz
Forcing Frequency	TRAC of acceleration response w.r.t Full model	TRAC of acceleration response w.r.t Full model	TRAC of acceleration response w.r.t Full model	TRAC of acceleration response w.r.t Full model
20	1	1	0.99	0.99
50	0.99	1	0.99	0.99
70	0.99	1	0.99	0.99
90	0.99	0.99	0.99	0.99
110	0.99	0.99	0.99	0.99
130	0.99	0.99	0.99	0.99
150	0.99	0.99	0.99	0.99

6.1.6 Selection of Coupled CC modes using EIM displacement output

Similar extension of EIM can be made for selection of important Coupled CC modes for obtaining accurate displacement response by using Coupled CC EIM displacement output (see section 4.1.4 for complete details). It's important to note that Coupled CC modes should be determined w.r.t to all those modes of each of the substructure which one would have considered in the full model of the interface to determine the accurate natural frequencies in a particular frequency range. For e.g. in Table 6.19 it was shown that by selecting first eight Fixed Interface normal modes of each of the substructure and without any interface reduction, all the displacement responses are accurately determined as that obtained from full model FE solution. Now, for the interface reduction problem relative importance of the coupled CC modes should be determined w.r.t all the first eight Fixed Interface normal modes of each of the substructure. This will give a set of significant coupled CC modes which are only required to be kept along with the selected Fixed Interface normal modes to get the same accurate

response. If any of these first eight modes are missed, the Coupled CC mode which is relatively important to that missed mode will not be captured.

Let's assume that the frequency range of interest is *0* to *150* Hz. From Table 6.16, Table 6.17, and Table 6.18 it can be observed that only Fixed Interface normal modes *1, 2 and 3* are significant for "*substructure-1*" and "*substructure-2*" based on EIM displacement output. These modes should always be kept along with additional modes depending on the frequency range of interest. Since the frequency range of interest is *0* to *150* Hz, therefore modes are selected based on thumb rule for each of the substructure, which also include the significant modes determined by EIM displacement output. The relative importance of the coupled CC modes should be determined w.r.t all these selected Fixed Interface normal modes of each of the substructure. Table 6.25 shows that only first *9* Coupled CC modes are required to achieve the total Coupled CC EIM displacement output at each of the selected modes of "*substructure-1*" and "*substructure-2*". These modes are used to reduce the dofs of "*Interface-1*". Table 6.26 shows the comparison of displacement response at "C", "M2", "M1" and "A" in direction Tz when coupled CC modes are selected as *1* to *9* and Fixed Interface normal modes for each of the substructure are selected as per thumb rule with target Frequency *150*Hz. It can be observed that all the displacement responses of the second level reduced system are matching very well with that obtained from full model FE solution at all the frequencies.

Thus by using EIM and Coupled CC EIM we are able to perform an interaction analysis which determines a set of significant interior and junction coordinates of a substructure that are interacting dominantly w.r.t each other. By determining the relative dynamic importance of the one with respect to another leads to appropriate reduction of the interface and junction dofs such that the accuracy of the final reduced model is not at all compromised. Such an interaction analysis can also be very advantageous for use in the applications of power flow analysis [**39**], where it is usually of interest to determine the power levels transferred to a particular substructure due to the excitations applied at the adjacent or connected substructure. This may form the future work.

Table 6.25: Cumulative Sum of contribution of Coupled CC modes of Interface-1 to the total Coupled CC EIM displacement output at the selected coordinates of substructure-1 and substructure-2.

	Mode Numbers	Coupled CC modes of Interface-1								
		1	2	3	4	5	6	7	8	9
Kept modes of Substructure-1	1	0.99	0.99	1.00	1.00	1.00	1.00	1.00	1.00	1.00
	2	0.00	0.98	0.98	1.00	1.00	1.00	1.00	1.00	1.00
	3	0.86	0.86	0.86	0.86	0.99	1.00	1.00	1.00	1.00
	4	1.00	1.00	1.00	1.00	1.00	1.00	1.00	1.00	1.00
	5	0.00	0.99	0.99	1.00	1.00	1.00	1.00	1.00	1.00
	6	0.00	0.59	0.59	0.59	0.59	0.59	0.98	0.98	1.00
	7	0.89	0.89	0.89	0.89	1.00	1.00	1.00	1.00	1.00
	8	1.00	1.00	1.00	1.00	1.00	1.00	1.00	1.00	1.00
Kept modes of Substructure-2	1	1.00	1.00	1.00	1.00	1.00	1.00	1.00	1.00	1.00
	2	0.00	0.99	0.99	1.00	1.00	1.00	1.00	1.00	1.00
	3	0.90	0.90	0.90	0.90	1.00	1.00	1.00	1.00	1.00
	4	1.00	1.00	1.00	1.00	1.00	1.00	1.00	1.00	1.00
	5	0.00	1.00	1.00	1.00	1.00	1.00	1.00	1.00	1.00
	6	0.00	0.66	0.66	0.66	0.66	0.66	0.98	0.98	1.00
	7	0.90	0.90	0.90	0.90	1.00	1.00	1.00	1.00	1.00
	8	1.00	1.00	1.00	1.00	1.00	1.00	1.00	1.00	1.00

Table 6.26: Comparison of displacement response at Node C, M1, M2 and A in direction Tz from "full model FEM" and "model reduced by Craig Bampton Method" (Coupled CC Modes selected as [1to9] for Interface-1 and Fixed Interface normal modes selected as per thumb rule with Target Frequency=150Hz).

Forcing Frequency	Response at C in direction Tz	Response at M1 in direction Tz	Response at M2 in direction Tz	Response at A in direction Tz
	TRAC of displacement response w.r.t Full model	TRAC of displacement response w.r.t Full model	TRAC of displacement response w.r.t Full model	TRAC of displacement response w.r.t Full model
20	0.99	0.99	0.99	0.99
50	0.99	0.99	0.99	0.99
70	0.99	0.99	0.99	0.99
90	0.99	0.99	0.99	0.99
110	0.99	0.99	0.99	0.99
130	0.99	0.99	0.99	0.99
150	0.99	0.99	0.99	0.99

Chapter 7

Closure

7.1   Conclusion

Component mode synthesis provides a methodology through which model equations can be reduced while synthesizing the complete structure into its independent components allowing much independence in the design and analysis of structures. This is especially helpful if structures are designed, fabricated and even tested at different locations and by different organizations.

The key to model reduction is the selection of a particular set of mode shapes or other vectors which completely represent the physics of the problem at hand. Inappropriate selection of mode shapes will drastically affect the accuracy of the results. In Fixed Interface Method, constraint modes plays a very important role in making a statically complete coupling of the substructures and in accurately representing the forces acting at the coupling dofs. Normal modes take care of the time varying response of the structure.

Free Interface method is more advantageous than Fixed Interface method especially for very complex structures which are modeled experimentally. Residual flexibility matrix includes the contribution of deleted modes and its formulation procedure depends on whether the substructure is Constrained or Unconstrained. For Unconstrained substructures, evaluation of flexibility matrix requires pre-removal of rigid body modes and hence these modes are always kept as a dynamic normal mode. In a particular formulation of the Free Interface method, interface or boundary dofs do not appear in equations of motion of the substructure and hence higher degree of model order reduction is attainable as compared to Fixed Interface method. However, this is a less accurate representation as the effects of deleted modes is considered only in quasi-static sense. EIM cannot be used to determine the dynamically important Free-free modes to be chosen in the reduced representation.

Effective Mass may neglect a set of modes which though are individually dominant along a particular direction but have opposite contribution. EIM being a more generalized measure of Effective Mass avoids neglecting of any dominant modes. However, appropriate

EIM measure should be chosen based on the required output as lesser modes may be sufficient for the accurate representation of the displacement response than that required for the accurate representation of velocity response, which requires even lesser modes than that required for the accurate representation of acceleration response. Extension of EIM is proposed to properly select the Coupled CC modes of an interface with relative to the already selected generalized coordinates of all the substructures coupled to this interface at the coupled substructure level. On the lines of EIM, three measures can be derived for the selection of coupled CC modes based on the required output of acceleration, velocity, or displacement response.

Fixed Interface and Free Interface method are assessed by using two academic examples: i) A Fixed-Free beam problem and ii) A Cracked beam problem. The reduction in the computational time achievable by both these methods is also studied by performing the model reduction of a real structure of Car axle. The assessment of Thumb rule, Effective Mass, and Effective Interface measure for the selection of the substructure modes in the Fixed Interface method is done. An example Fixed-Free plate is used and the appropriateness of each of the particular measure is performed by comparing the displacement, velocity, and acceleration response obtained from the system, reduced by the Fixed Interface kept normal modes selected through each of these measures, to the full model FEM solution.

7.2   Scope for future Work

(a) Future investigations can be performed to use EIM in the applications of power flow analysis [39], where it is usually of interest to determine the power levels transferred to a particular substructure due to the excitations applied at the adjacent or connected substructure. EIM can be very effective in such cases by first selecting the junction coordinates dominantly excited by the excitations applied at interior coordinates of one substructure and then selecting the interior coordinates of the adjacent substructure dominantly excited by these selected junction coordinates. Energy levels can be predicted in the adjacent substructure from its selected interior coordinates.

(b) Extension of EIM for the selection of Free-free modes with proper determination of an acceptable level of dynamic completeness that would produce a reduced model of acceptable size and accuracy.

(c) Trends of future research are moving towards the application of CMS to handle geometric and material nonlinearities.

(d) Though CMS has been applied extensively in the field of dynamic analysis, noise reduction, optimal design etc., but not much work has been done in applying this methodology to controls. In particular, not much work has been done to develop a physically realistic and efficient way of modeling of large flexible structures based on substructure models by providing performance robustness to errors or uncertainties, which are inevitable due to modeling errors, and various other factors [40]. So this field requires attention and is also worth investigating.

References

[1] K.J. Bathe, *Finite Element Procedures*. New Jersey: PRENTICE HALL, 1996.

[2] R.R. Craig, *Structural Dynamics, An Introduction to Computer Methods*, 2nd ed.: John Wiley & Sons, 2006.

[3] R.R. Craig and M.C.C. Bampton, "Coupling of substructures for dynamic analysis," *AIAA Journal*, vol. 6, no. 7, pp. 1313-1319, July 1968.

[4] R.R. Craig and Ching-Jone Chang, "Substructure coupling for dynamic analysis and testing," *NASA CR-2781*, 1977.

[5] S.N. Voormeeren, P.L.C. van der Valk, and D.J. Rixen, "A General Mixed Boundary Model Reduction Method for Component Mode Synthesis," *IOP Conf. Series: Materials Science and Engineering 10*, 2010.

[6] L. Hermans, P. Mas, W. Leurs, and N. Boucart, "Estimation and use of residual modes in modal coupling calculations: A case study," in *Proceedings of the 18th International Modal Analysis Conference (IMAC)*, San Antonio, Texas, 2000.

[7] J.C. Chen and J.A. Garba, "Structural Analysis Validation using Modal Test Data," *Joint ASCE/ASME Mechanical Conference*, pp. 109-137, 1985.

[8] D.C. Kammer and M.J. Triller, "Ranking the dynmaic importance of fixed interface modes using a generalization of effective mass," *International Journal of Analytical and Experimental Modal Analysis*, vol. 9, no. 2, pp. 77-98, April 1994.

[9] D.C. Kammer and M.J. Triller, "Selection of Component Modes for Craig-Bampton Substruture Representations," *Journal of Vibration and Acoustics*, vol. 118, pp. 264-270, April 1996.

[10] D.C. Kammer, Joseph Cessna, and Andrew Kostuch, "A Generalization of Effective Mass for selection of Free-Free Target Modes," *Journal of Vibration and Acoustics*, vol. 129, pp. 121-127, February 2007.

[11] S. Donders, B. Pluymers, P. Ragnarsson, R. Hadjit, and W. Desmet, "The wave-based substructuring approach for the efficient description of interface dynamics in dynamic substructuring," *Journal of Sound and Vibration*, vol. 329, pp. 1062-1080, 2010.

[12] P. Cermelj, B. Pluymers, S. Donders, W. Desmet, and M. Boltezar, "Basis Functions and Their Sensitivity in the Wave-Based Substructuring Approach," *PROCEEDINGS OF ISMA*, pp. 1491-1505, 2008.

[13] Matthew P. Castanier, Yung-Chang Tan, and Christophe Pierre, "Characteristic Constraint modes for Component Mode Synthesis," *AIAA Journal*, vol. 39, no. 6, pp. 1182-1187, June 2001.

[14] David M. Simon and Thomas L. Cost, "Selection of Characteristic Constraint Modes for Component Mode Synthesis Using a Modification of Effective Interface Mass," *AIAA Journal*, pp. 2005-2343, April 2005.

[15] Polarit Apiwattanalunggarn, "Model Reduction of Nonlinear Structural Systems using Nonlinear Normal Modes and Component Mode Synthesis," Michigan State University, PhD Thesis 2003.

[16] Jamey T. Bond and Tariq A. Khraishi, "Non-linear Dynamic Modeling using Component Mode Synthesis," *International Journal of Theoretical and Applied Multiscale Mechanics*, vol. 1, no. 2, pp. 150 - 163, 2009.

[17] J. Bond and T. Khraishi, "Transient non-linear simulation with Component Mode Synthesis," *International Journal of Mechanics and Materials in Design*, vol. 5, no. 4, pp. 365–380, 2009.

[18] W.C. Hurty, "Dynamic analysis of structural systems using component modes," *AIAA*, vol. 3, no. 4, pp. 678-685, April 1965.

[19] P. Leger and E.L. Wilson, "Generation of Load dependent Ritz transformation vectors in Structural dynamics," *Engineering Computations*, vol. 4, pp. 309-318, December 1987.

[20] J.M. Dickens, J.M. Nakagawa, and M.J. Wittbrodt, "A Critique of Mode Acceleration and Modal Truncation Augmentation Methods for Modal Response Analysis," *Computers and Structures*, vol. 62, no. 6, pp. 985-998, 1997.

[21] R.L. Goldman, "Vibration Analysis by Dynamic Partitioning," *AIAA Journal*, vol. 7, pp. 1152-1154, 1969.

[22] R.H. Macneal, "A Hybrid Method of Component Mode Synthesis," *Journal of Computers and Structures*, vol. 1, no. 4, pp. 581-601, Dec 1971.

[23] S. Rubin, "Improved Component Mode Representation for Structural Dynamic Analysis," *AIAA Journal*, vol. 13, no. 8, pp. 995-1006, Aug 1975.

[24] R.R. Jr. Craig, "Structural Dynamics: A brief tutorial on substructure analysis and testing," *18th International Modal Analysis Conference*, February 2000.

[25] D.R. Martinez and D.R. Gregory, "A Comparison of Free Component Mode Synthesis Techniques using MSC/NASTRAN," *Sandia National Laboratories*.

[26] Daniel J. Rixen, "A dual Craig–Bampton method for dynamic substructuring," *Journal of Computational and Applied Mathematics*, vol. 168, no. 1-2, pp. 383-391, July 2004.

[27] P. Seshu, *Textbook of Finite Element Analysis*, 4th ed.: Prentice Hall of India Pvt. Ltd., 2006.

[28] S. Graham Kelly, *Fundamentals of Mechanical Vibrations*, 2nd ed.: McGraw-Hill Higher Education.

[29] T. Ting, T.L.C. Chen, and W. Twomey, "Correlating mode shapes based on the modal assurance criterion," *Finite Elements in Analysis and Design*, vol. 14, no. 4, pp. 353-360, November 1993.

[30] G. Gounaris and A. Dimarogonas, "A finite element of a cracked prismatic beam for structural analysis," *Journal of Computers and Structures*, vol. 28, pp. 309-313, 1988.

[31] G.-L. Qian, S.-N. Gu, and J.-S. Jiang, "The dynamic behavior and crack detection of a beam with crack," *Journal of Sound and Vibration*, vol. 138, pp. 233-243, 1990.

[32] M. Kisa and M. Arif Gurel, "Free vibration analysis of uniform and stepped cracked beams with circular cross sections," *International Journal of Engineering Science*, vol. 45, no. 2-8, pp. 364-380, February-August 2007.

[33] M. Kisa and M. Arif Gruel, "Modal analysis of multi-cracked beams with circular cross section," *Engineering Fracture Mechanics*, vol. 73, no. 8, pp. 963-977, May 2006.

[34] ABAQUS. [Online]. http://www.simulia.com/products/abaqus_fea.html

[35] ANSYS. [Online]. http://www.ansys.com/

[36] MATLAB. [Online]. http://www.mathworks.com/products/matlab/

[37] P. Avitabile, T. Van Zandt, N. Wirkkala, B. Birdsong, and L. Craft, "Development of Efficient Reduced Models for Flexible body Dynamic simulation," in *SEM Conference*, 2007 IMAC-XXV.

[38] "Payload verification requirements," NASA, Lyndon B. Johnson Space Center, Houston, TX, NSTS 14046 Revision D, 1997.

[39] Yung-Chang Tan, Matthew P. Castanier, and Christophe Pierre, "Approximation of Power Flow Between Two Coupled Beams Using Statistical Energy Methods," *Journal of Vibration and Acoustics*, vol. 123, no. 4, pp. 510-524, October 2001.

[40] Peiman G. Maghami and Kyong B. Lim, "Synthesis and Control of Flexible Systems with Component level uncertainties," *Journal of Dynamic Systems, Measurement, and*

Control, vol. 131, no. 5, 2009.

Acknowledgements